

ABSTRACT

Title of Document: POLYMER-IONIC LIQUID HYBRID ELECTROLYTES
FOR LITHIUM BATTERIES

Aaron Steven Fisher, Ph.D., 2012

Directed By: Professor Peter Kofinas, Fischell Dept. of Bioengineering

Intellectual Merit:

The goal of this dissertation is to investigate the electrochemical properties and microstructure of thin film polymer electrolytes with enhanced electrochemical performance. Solid electrolyte architectures have been produced by blending novel room temperature ionic liquid (RTIL) chemistries with ionically conductive polymer matrices. A variety of microstructure and electrical characterization tools have been employed to understand the hybrid electrolyte's performance.

Lithium-ion batteries are limited because of the safety of the electrolyte. The current generation of batteries uses organic solvents to conduct lithium between the electrodes. Occasionally, the low boiling point and high combustibility of these solvents lead to pressure build ups and fires within cells. Additionally, there are issues with electrolyte loss and decreased performance that must be accounted for in daily use. Thus, interest in replacing this system with a solid polymer electrolyte that can match the properties of an organic solvent is of great interest in battery research. However, a polymer electrolyte by itself is incapable of meeting the performance characteristics, and thus by adding an RTIL it has met the necessary threshold values.

With the development of the novel sulfur based ionic liquid compounds, improved performance characteristics were realized for the polymer electrolyte. The synthesized RTILs

were blended with ionically conductive polymer matrices (polyethylene oxide (PEO) or block copolymers of PEO) to produce solid electrolytes. Such shape-conforming materials could be lead to unique battery morphologies, but more importantly the safety of these new batteries will greatly exceeds those based on traditional organic carbonate electrolytes.

Broader Impacts:

The broader impact of this research is that it will ultimately help push forward an attractive alternative to carbonate based liquid electrolyte systems. Development of these alternatives has been slow; however bypassing the current commercial options will lead to not only safer and more powerful batteries. The polymer electrolyte system offers flexibility in both mechanical properties and product design. In due course, this will lead to batteries unlike any currently available on the market. RTILs offer quite an attractive option and the electrochemical understanding of novel architectures based upon sulfur will lead to further potential uses for these compounds.

POLYMER-IONIC LIQUID HYBRID ELECTROLYTES FOR
LITHIUM BATTERIES

By

Aaron Steven Fisher

Dissertation submitted to the Faculty of the Graduate School of the
University of Maryland, College Park, in partial fulfillment of the
requirement for the degree of
Doctor of Philosophy
2012

Advisory Committee:

Professor Peter Kofinas, Chair
Professor Robert M. Briber
Professor Sheryl Ehrman
Assistant Professor Liangbing Hu
Associate Professor Chunsheng Wang

© Copyright by
Aaron Steven Fisher
2012

Acknowledgements

I would like to thank all those who helped me accomplish this research both in the laboratory and outside for their patience and support. Firstly, I would like to thank Peter Kofinas. Without his guidance, I would not have been able to do so much so quickly. His insights on funding and collaboration, prompt email responses, proofreading and grammatical skills, the innumerable lunches and of course his unending stream of Apple products, all were integral to my success. As such, I believe I owe you the most thanks.

To Ayan Ghosh, whose patience and knowledge of electrolytes helped me to start my project in second gear. To my undergraduate students, especially Matthew Widstrom and Mian Khalid: Matt, you really got the hang of the synthesis work and I wish you continued success in your endeavors. Mian, you've come a long way; keep your confidence high and you will accomplish what you set your mind to. I have met few people as capable as you.

To the rest of the Kofinas and Briber labs: I apologize for stinking up the lab on many occasions and nearly burning it down on another. Even if everyone didn't contribute scientifically to my project, it was great to have such sociable and outgoing people around all the time.

To my family and friends, especially my fiancée Ashley thank you for your patience with me and my lab work. No experiment ever runs on time. The long hours have paid off and now for the rest of my life I can call myself a doctor. Although not the kind of doctor that Andrea wanted in the family.

Lastly, I would like to give a special thanks to John and Maureen Hendricks, whose donation to University of Maryland and the resulting fellowship have made my graduate school experience truly exceptional. I have travelled to Australia, Boston, Hawaii, Japan, Montreal, Prague, South Korea, and Vancouver to present my research. Never did I think that I would have this kind of experience in graduate school. The contacts formed and the science discussed has been invaluable to completing my PhD.

Table of Contents

I.	Introduction.....	1
II.	Background.....	2
	1. Significance & Innovation.....	2
	2. Lithium-Ion Batteries.....	3
	3. Solid Electrolytes.....	5
	4. Ionic Liquid Electrolytes.....	9
	5. Polymer Electrolytes Containing Ionic Liquids.....	12
III.	Overview of Research Activities.....	15
	1. Electrolyte Component Selection.....	15
	a. Polymer.....	15
	b. Lithium Salt.....	16
	c. Ionic Liquid.....	17
	d. Polymer Electrolyte Synthesis.....	18
	2. Ionic Liquid Analytical Tests.....	19
	a. Differential Scanning Calorimetry (DSC).....	19
	b. Nuclear Magnetic Resonance (NMR).....	19
	c. Mass Spectrometry (MS).....	19
	d. Conductivity.....	20
	3. Analytical Tests of the Polymer Electrolyte.....	21
	a. Differential Scanning Calorimetry.....	21
	b. General Cell Construction.....	21
	c. Conductivity.....	22
	d. Electrochemical Stability Window.....	23
	e. Overvoltage studies.....	24
	f. Transference Number.....	25
	g. Restricted Diffusion.....	26
	h. Cell Cycling.....	26
IV.	S ₂ TFSI in PEO-based Polymer Electrolytes.....	28
	1. Introduction.....	28
	2. Experimental.....	30
	a. Materials.....	30
	b. RTIL preparation.....	30
	c. Electrolyte Preparation.....	30
	d. Electrode Preparation.....	31

e. Electrolyte Characterization.....	31
3. Results and Discussion	32
V. Effect of Anion on PEO-based Polymer Electrolytes.....	56
1. Introduction.....	56
2. Experimental.....	58
a. Materials	58
b. RTIL preparation	58
c. Electrolyte Preparation.....	60
d. Electrolyte Characterization.....	60
3. Results and Discussion	61
VI. Ionic Liquids in Block Copolymer Electrolytes	80
1. Introduction.....	80
2. Experimental.....	82
a. Materials	82
b. Materials Synthesis	82
c. Electrolyte Preparation.....	83
d. Electrolyte Characterization.....	84
3. Results and Discussion	85
4. Conclusions.....	100
VII. Zwitterionic Liquid.....	102
1. Introduction.....	102
2. Experimental.....	104
a. Materials	104
b. RTIL preparation	104
c. Electrolyte Preparation.....	105
d. Electrolyte Characterization.....	105
3. Results and Discussion	106
4. Conclusion	109
VIII. Future Directions	110
IX. Contributions.....	113
X. References.....	115

List of Tables

Table II-1 Nonaqueous electrolytes for Li-Ion batteries ⁷	10
Table IV-1 Resistance and capacitance of equivalent circuit elements from the impedance scans after stated stripping/plating step. The semicircles were modeled as a circuit containing the electrolyte resistance in series to an RC circuit	49
Table V-1 DSC peaks of the neat ionic liquids.....	63
Table V-2 DSC peaks of the electrolyte	65
Table V-3 Volume of anion as determined by molinspiration program. ⁷⁴	69
Table VI-1. Fitting parameters to the Arrhenius for the high temperature region. BCP-IL data is from this paper, the BCP containing no IL data is from Ghosh and Kofinas ²² and the PEO-IL data is from Fisher et al. ⁷⁷ E_a is the activation energy and A is the pre-exponential factor.....	92
Table VI-2 Measured salt diffusion coefficients by the current interrupt method. ^{62,80}	94
Table VI-3 Fraction of full time it took for the overpotential value to reach the specified % of the final overpotential value. For example, during the 100th cycle with negative polarity to the current it took 3.36% of the hour for the measured overpotential to reach 90% of the final overpotential.....	99

List of Figures

Figure III-1 Chemical structures of compounds to be used during the doctoral research	15
Scheme III-2 Sample reaction scheme for synthesis of ionic liquid.....	18
Scheme III-3 Model electrical circuit	21
Figure III-4 Exploded view of the contents of a coin cell used for this research	22
Figure III-5 Common electrode potentials and capacities plotted over the ESW of a carbonate solution ⁷	23
Figure IV-1 Pictures of thin film solid electrolyte in Ar atmosphere. Electrolyte is ~5 cm. x 2cm.....	34
Figure IV-2 Raman spectra of IL-1.0 hybrid polymer electrolyte. Indicated areas are as follows Green: LiTFSI 712-769 cm ⁻¹ Red: PEO 820-886 cm ⁻¹ Blue: S ₂ TFSI 2920-2979 cm ⁻¹	35
Figure IV-3 Confocal Raman Spectroscopy of 50 μm. square. Intensity indicates area under the peak. a) PEO 820-886 cm-1 b) S ₂ TFSI 2920-2979 cm-1 c) LiTFSI 712-769 cm-1 d) component overlay.	36
Figure IV-4 Selected portion of thermograms from indicated electrolyte mixtures. Heating rate was 10 °C/min and cooling rate was 5 °C/min in a heat/cool/heat format with endpoints of -50 °C and 120 °C. Each thermogram is offset 3 W/g, and each tick mark on the y-axis is 1 W/g. Ratio is moles of 20 PEO: 1 LiTFSI : x S ₂ TFSI, where x is indicated in the figure.	38
Figure IV-5 (a) Conductivity over varied temperature for selected electrolyte over the cooling cycle. Ratio is moles of 20 PEO: 1 LiTFSI: x S ₂ TFSI. (b) Effect of thermal history on measured conductivity of IL-1.5 electrolyte.....	40

Figure IV-6 (a) Cyclic voltammetry of Li/IL-1.0/Pt cell. The voltage was cycled from 2.5 to 4.7 V vs. Li/Li⁺ at a rate of 5 mV/s at rt. The current remains relatively constant over the whole voltage range until the upper cathodic limit. Minimal decrease in current is observed from the 1st to 500th cycle. (b) Cyclic voltammetry of a Li/IL-1.0/Al cell. The voltage was cycled from 2.5 to 5.0 V vs. Li/Li⁺ at a rate of 5 mV/s at rt. 43

Figure IV-7 (a) Measurement of IL-1.0 overpotential as a function of time. Cycle number is as indicated in the legend. (b) Value of overpotential of the electrode-electrolyte interface at the end of each 2 hr. cycle (1 hr. charged followed by 1 hr. discharge both at 0.1 mA/cm²) as a function of cycle number. Testing was conducted at 45 °C. 46

Figure IV-8 Nyquist plot of electrolyte during overvoltage study. Frequency range is 1 MHz to 1 Hz. 48

Figure IV-9 a) Selected charge/discharge curves of a Li/electrolyte/ LiFePO₄ cell. Cycling was conducted at 0.01 mA/cm² from 2.5 to 4.0 V. Testing was conducted at 40 °C. b) End capacity of the first 10 cycles for the cell (charge (■) discharge (□)). Capacity values were calculated assuming all active material was available, which given the low values is not expected to be available amount. Coloumbic efficiency (○) was determined by comparing the discharge capacity over the charge capacity for a given cycle. 51

Figure V-1 Ionic conductivity of the solid polymer electrolytes determined by AC impedance spectroscopy upon cooling of the SS/electrolyte/SS cells from 65 °C. 64

Figure V-2 Selected portion of thermograms from the electrolyte based on the indicated anion. The formulation is the molar ratio 20 PEO: 1 LiX : 1 S₂X, where X is indicated in

the legend. The heating rate was 10 °C/min and cooling rate was 5 °C/min in a heat/cool/heat format with endpoints of -50 °C and 120 °C..... 66

Figure V-3 Lithium transference number of the solid polymer electrolytes. T_{Li^+} was determined using the potentiostatic measurement conducted at 40 °C for all anions except ClO_4 , which was run at 50 °C. Molar volume from Table V-3 is overlaid to show relationship between volume and T_{Li^+} 68

Figure V-4 Cathodic stability of the solid polymer electrolytes. Breakdown was determined by first change in the derivative of the potential upon sweeping a SS/electrolyte/Li cell from 2.5 to 6.5 V vs. Li/Li^+ . Cells were run at 25 °C. 71

Figure V-5 Value of overpotential at the end of each 2 h cycle for symmetrical Li/electrolyte/Li cells. b. Overpotential as a function of time during the 25th cycle for the indicated ionic liquid. Each cycle was 1 h negative current followed by 1 h positive current both at 0.1 mA/cm². Testing was conducted at 55 °C. 73

Figure V-6 a. Equivalent circuit used to model the electrolyte during overvoltage cycling b bulk resistance of each anion formulation during the overvoltage cycling c. the resistance of the SEI film d. the resistance due to charge transfer. To highlight the low resistance of the charge transfer there is a gap in the y-axis values. The electrolyte tested had a thickness of 0.0254 cm and a cross sectional area of 0.217 cm²..... 75

Figure VI-1 Compounds used to make the solid polymer electrolyte. All ratios cited in this paper are of the molar formula x PEO : y LiBOB : z S₂BOB..... 83

Figure VI-2 Visual image of the solid block copolymer showing the flexible transparent nature of the as-cast film. The film ratio is 20 PEO of the BCP : 1 LiBOB : 0.1 S₂BOB. 86

Figure VI-3 TEM of the as-cast 20 PEO : 1 LiBOB : 0.1 S₂BOB BCP-IL electrolyte. Dark regions are lithium aggregates that have precipitated from the polymer matrix. 87

Figure VI-4 DSC of the 20 PEO : 1 LiBOB : 0.5 S₂BOB system. A heat/cool/heat cycle was followed between -50 and 120 °C with a cooling rate of 5°C/min and a heating rate of 10°C/min. There were no peaks outside of this range. 88

Figure VI-5 (a) Ionic conductivity of the solid polymer electrolytes determined by AC impedance spectroscopy upon cooling of the SS/electrolyte/SS cells from 65 °C. (b) Enlargement of the previous graph showing the region of high conductivity. Molar ratios are x PEO : y LiBOB : z S₂BOB. 89

Figure VI-6 Measured lithium transference values for the BCP-IL system run at the indicated temperature. Molar ratios are x PEO : y LiBOB : z S₂BOB. 93

Figure VI-7 (a) Overpotential as a function of time for selected cycles of the 20 PEO : 1 LiBOB : 0.1 S₂BOB BCP-IL system. Each cycle consisted of 1 hour of positive and negative current at a rate of 0.1 mA/cm² while at 40 °C. (b) ■ final values of the average overpotential as plotted against cycle. ○ are calculated from the resistance determined by the intermittent AC impedance scans. (c) The resistances as plotted against cycle were determined from fitting the AC impedance scans to a 3 element equivalent circuit. R_S- bulk or series resistance, R_{CT}-charge transfer resistance, R_{SEI}- resistance of the SEI. 96

Figure VII-1 Compounds used to make the solid polymer electrolyte. All ratios cited in this paper are of the molar formula x PEO : y LiBOB : z IL. 105

Figure VII-2 Ionic conductivity of the solid polymer electrolytes determined by AC impedance spectroscopy upon cooling of the SS/electrolyte/SS cells from 65 °C. Ratios are x PEO : y LiBOB : z S₂₂(CH₂COO-Li⁺) TFSI. 107

I. Introduction

The goal of this dissertation was to develop and characterize novel polymer electrolytes for lithium batteries. These novel thin film electrolytes consist of poly(ethylene oxide) (PEO)-based homopolymers and block copolymers blended with sulfur based room temperature ionic liquids (RTIL). In pursuit of this new RTIL compounds have been synthesized and characterized by nuclear magnetic resonance and mass spectrometry. Following this, solution casting of the polymer electrolyte resulted in a flexible material with elevated ionic conductivity and high lithium ion transference (fraction of current due to lithium ion movement). Differential scanning calorimetry was taken to characterize the solid electrolyte's response to variations in operating temperature. For the hybrid solid electrolyte, impedance spectroscopy, galvanostatic and potentiostatic measurements were performed to assess ion conduction, cell stability, and the electrode/electrolyte interface. Additionally charge-discharge curves measurements were undertaken to demonstrate the cycling performance of battery test cells constructed using the solid polymer electrolyte.

II. Background

1. Significance & Innovation

Batteries have become ubiquitous elements in society powering both small and large devices. As portable devices have followed Moore's Law, whereby processing power doubles every two years, batteries have lagged significantly behind this exponential growth increasing at $\sim 1\%$ a year.¹⁻³ This has resulted in a slew of problems whereby devices need to simultaneously become more efficient while improving in performance to maintain current standards of battery life. The demands of greater capacity and power along with the push for smaller devices have exposed the limitations of current battery technology. Besides the need for small scale there is also a large interest in batteries as energy storage elements in the smart grid. Storing energy in the grid and deploying it to match demand is necessary to make inconsistent renewable energy sources viable grid power supplies. The varied demands for energy storage in the near future explains the large growth expected in the battery sector for the foreseeable future.⁴

The focus on higher energy and power densities has driven battery manufacturers to largely neglect the safety of the battery, the device and ultimately the consumer. When considering future device development, it is important to not be limited in design and safety by a component as bulky as the battery. While improvements in the electrode would ultimately make the battery more energy efficient, requiring less active material; safety and shape are still largely controlled by the electrolyte. Current electrolyte technology consists of organic carbonate based liquids, and is limited in terms of operating temperature and voltage. Solid polymer electrolytes have superior voltage,

temperature and mechanical stability, but there is a large trade off with conductivity. It is possible to improve these properties by blending the polymer electrolytes with ionic liquids. Ionic liquids similarly possess good temperature and voltage stability while having appreciable conductivity, but lack mechanical stability. By combining the polymer electrolyte with ionic liquids it is believed that the hybrid system will possess all the desired properties and be conductive enough to be useful as a battery. The current polymer-ionic liquid systems are limited by problems with the ionic liquid, and it is hoped that the development of novel ionic liquids chemistries, based on second period elements, will permit innovation beyond the current systems. Ionic liquid research has largely been artificially limited to nitrogen-based architectures. Sulfur based architectures promise to provide superior electrical properties, which ultimately will allow these hybrid polymer ionic liquid electrolytes to become the next generation of solid electrolytes.

2. Lithium-Ion Batteries

Over the past 150 years the development of rechargeable batteries has progressed at a slow pace relative to other technologies. Since the lead-acid batteries discovery in 1859 (which is still in widespread use because of its low temperature performance), nickel cadmium and nickel metal hydride have become the leading edge of battery chemistry only to be replaced by lithium ion batteries. Lithium ion has supplanted all of these chemistries because it has the highest energy density; lithium has a high electrochemical potential (-3.04 V vs. standard hydrogen electrode, SHE) and is the lightest metal ($\rho = 0.534 \text{ g/cm}^3$)^{2,5} available.

Batteries depend on the exclusive conduction of ions to generate external electrical current. Within the battery, the anode and cathode must be electrically conducting and capable of reversibly intercalating lithium ions, while the electrolyte must be solely ionically conducting. Current Li-ion battery setups consist of a liquid electrolyte containing a plastic separator situated between the electrodes. In previous generations of lithium ion batteries the plastic was a thin electrochemically inert layer meant to prevent dendrite growth. The upcoming generation of lithium-ion batteries has replaced the inert polymers with gelled polymers that provide greater mechanical stability. However, all of these commercialized systems still use organic liquid electrolytes to achieve the required electrical properties.⁶

An electrolyte is a complex material that has many requirements for successful operation in a lithium ion battery. The ideal electrolyte has all of the following properties:⁷

- 1) A large electrochemical stability window. Should an electrode's operating potential exist outside of the kinetic or equilibrium stability it must have the ability to rapidly form a passivating solid electrolyte interphase (SEI).
- 2) Maintenance of the contact between electrode and electrolyte despite volumetric changes that occur during cycling.
- 3) A Li^+ conductivity $\sigma_{\text{Li}} > 10^{-4}$ S/cm at operational temperature.
- 4) An electronic conductivity $\sigma_e < 10^{-10}$ S/cm.
- 5) A lithium transference number (fraction of total current due to Li^+) close to unity.
- 6) Chemical stability over ambient and operational temperatures.

- 7) Safe material, e.g., high flash point preferably non-combustible.
- 8) Low toxicity and low cost.

The low boiling point organic liquids currently use lead to problems with electrolyte loss, and in turn decreased performance over time. Dendrite formation is another problem in liquid electrolytes leading to limited cycling and eventually short circuiting the battery.^{6,8-10} Additionally, each battery must be wrapped in several packaging layers that separate the battery from the user as well as the environment, and limits the internal vapor pressure to safe levels.^{11,12} When considering the scaling down of a battery for miniature devices the packaging layers and precautions do not scale at a similar rate, which ultimately lead to decreases in the battery properties per unit weight and volume.² Such material limitations have driven academic and industrial research in solid electrolytes, whereby the safety profile would be improved allowing for a reduction in safety precautions built into the battery. Another advantage of switching to solid electrolytes, is that future battery architectures would not be limited to simple shapes.² Lastly, solid electrolytes offer a distinct advantage in processing, allowing the assembly to be streamlined.⁹ The ease of processing a polymer electrolyte would allow the production of thin film flexible batteries that could be wound into coils or processed as coatings and sheets.

3. Solid Electrolytes

Among solid electrolytes, polymers offer the advantages of being robust, lightweight, non-combustible, shape conforming and moldable allowing them to meet the requirements of diverse applications. Also due to their solid-like nature, polymer electrolytes are expected to be less reactive than their liquid electrolyte counterparts, and

thus more stable towards lithium.¹³ For polymer electrolytes to be commercially useful, it is necessary that they exhibit appreciable room temperature ionic conductivities while functioning as the separator. In addition, it is also important that the polymer have good cycle life and sufficient mechanical and thermal strength to endure internal pressure and temperature variations during battery performance. A polymer electrolyte exhibiting all of these properties is ideal; however, further research is necessary to develop a system with these properties.

The transition to dry electrolytes has not been smooth. Ionic conductivity becomes a large issue as solids inherently are more resistive than their liquid counterparts. The successful polymer electrolyte or active part of a copolymer exhibits three essential characteristics: atoms or functional groups that can coordinate to cations, a suitable distance between coordinating sites and low barriers to bond rotation and segmental motion.⁹ PEO has been found to be the best lithium ion conductor as a solid electrolyte as it fulfills the criteria outlined above. Its room temperature conductivity is on the order of 10^{-6} S/cm, but varies greatly with the choice of lithium salt.^{14,15} It also has the appropriate chain spacing of 2 carbons between oxygen atoms to be conductive; spacing the oxygen's either 1 or 3 units apart results in lower ionic conductivity.⁹ The limiting factor with PEO though is its semi-crystalline nature at room temperature. As segmental movement is important for ionic conduction, a polymer electrolyte displays its best conductivity above its glass transition temperature, T_g . This remains a large problem with PEO as there is a noticeable increase in conductivity above its T_g . Polyacrylonitrile (PAN) has been cited as a possible alternative to PEO having greater ionic conductivity at

room temperature.¹⁶ However, this comes at the cost of decreased interfacial stability against lithium, which ultimately limits the use of PAN as a lithium electrolyte.¹⁷

Several options have been explored to increase the conductivity of the solid electrolyte system: addition of ceramic components, modifying the PEO to favor the amorphous phase and lowering the T_g by addition of plasticizers.

Forming polymer composites by the addition of ceramic particles (e.g. TiO_2 , fumed silica, zeolites, etc.) increases their measured conductivity by approximately one order of magnitude.¹⁴ Although poorly understood, this increase in conductivity is believed to be a result of the decrease in crystallinity induced by the addition of this second phase.¹⁸ In addition to this, these composite polymer electrolytes have increased mechanical strength¹⁹ and increased interfacial stability²⁰. While composite polymer electrolytes are promising, they still are not sufficient in terms of conductivity to match organic liquids, and the ultimate polymer electrolyte solution may need to incorporate ceramic fillers to be commercially successful.⁷

The formation of copolymers, where one block is PEO, is of great interest because it can alter the morphology of the PEO to favor an amorphous state. Ultimately it is important that this second block provide beneficial properties to the electrolyte. Into this category falls previous research in the Kofinas group whereby PEO is blocked with a lithiated copolymer²¹⁻²³ of PMMA, which has demonstrated moderate lithium ionic conductivity.¹⁴ Work in Balsara's lab and subsequently his startup venture SEEO involves blocking the PEO with polystyrene, which is used to disrupt the crystalline PEO phases, and has demonstrated good conductivity at temperatures between the glass transition temperature of the two blocks.²⁴ Allcock²⁵ has also proposed a phosphazene

polymer, called poly-[bis((methoxyethoxy)ethoxy)phosphazene] (MEEP), which has demonstrated superior conductivity as compared to homopolymer PEO. Its backbone consists of a series of repeating (-P=N-) units, off of which ethylene oxide units of varying length are attached; it can be thought of as an inert scaffold onto which short pendant PEO chains are attached. However, the poor mechanical properties and arduous synthesis process has made this a less attractive option than other solid polymer electrolyte systems.²⁶ While promising, none of the gains begotten alone by these PEO copolymer systems has been sufficient to lead to commercialization.

The addition of plasticizer lowers the T_g , increasing the conductivity while still maintaining the mechanical properties at a given temperature.²⁷ Ideally a plasticizer added to PEO increases the conductivity while not harming the electrochemical or mechanical stability. This has led to a great interest in gel polymer electrolytes where the polymer system is mixed with the carbonate solvents used in commercial systems. These carbonate plasticized systems have demonstrated conductivity $>10^{-3}$ S/cm.²⁸ In these cases the polymer is not viewed as a conductive platform but rather as a matrix (poly(vinylidene fluoride [PVdF] is a common example). Gelled PEO systems have demonstrated elevated conductivity as a solid electrolyte exceeding 10^{-4} S/cm. These systems gains are offset by their lesser mechanical properties and are plagued by many of the same safety issues of the aforementioned organic solvents. Thus it is of great interest to researchers to find polymeric electrolytes that take advantages of the gains by choosing an appropriate plasticizer that does not have the same drawbacks as the organic solvents.

Another type of solid electrolyte fundamentally different from polymer electrolytes are those based upon ceramics and glasses. They are single ion conductors

and have lithium conductivities that are on the order of 10^{-4} S/cm.²⁹ A common choice for solid electrolytes are those based upon lithium phosphorous oxynitrides (LiPON) and Li_2S .³⁰ These systems have demonstrated long life cycles and wide electrochemical stability windows. However, they are limited in their ability to form stable interfaces with the electrodes that do not change volume; this has restricted their use to thin film batteries.⁷ They are also limited as to what temperatures they have appreciable conductivity, with ongoing research aimed at lowering this temperature. A unique way to overcome and also at using 2 electrolyte systems such that the ceramic is only a thin layer protecting the anode.³¹

4. Ionic Liquid Electrolytes

Most salts are solids at room temperature and do not melt until they are at greatly elevated temperatures. ($\text{NaCl} \sim 800$ °C). Room temperature ionic liquids (referred henceforth as RTILs or ionic liquids, ILs) though are a select group of salts whose anion and cation are strongly coordinated but cannot form a crystalline structure due to van der Waals interactions. RTILs are formally defined as a salt that at temperatures below 100°C is a liquid. Common cationic scaffolds for ionic liquids consist of quaternary nitrogen and phosphorous or ternary sulfur. Nitrogen has the most varied architectures available, where imidazolium, pyrrolidinium, pyridinium, piperidinium ring structures are all commonly used ILs besides the tetra-substituted ammonium ion. Instability in charged oxygen species explains their absence from academic literature. The anionic structures are the conjugate Lewis bases of strong acids, common examples are the halides, fluorinated compounds, and sulfonated imides. As compared to the list of common electrolytes (Table 1), ionic liquids possess a number of beneficial

characteristics. They have high conductivity (0.1-20 mS/cm), low to nonexistent vapor pressures, high thermal and electrical stabilities, and are not combustible.³²⁻³⁵ However, they are viscous, air and moisture sensitive, and several IL scaffolds have compatibility issues with lithium and the layers of graphitic carbon.

Table II-1 Nonaqueous electrolytes for Li-Ion batteries⁷

Electrolytes	Example of classical electrolytes	Ionic conductivity ($\times 10^{-3}$ s/cm) at room temp	Electrochemical window (V) vs Li^+/Li^0		Remark
			Reduction	Oxidation	
Liquid organic	1M LiPF_6 in EC:DEC (1:1)	7 ³	1.3 ⁷	4.5 ⁶	Flammable
	1M LiPF_6 in EC:DMC (1:1)	10 ³	1.3 ⁷	> 5.0 ³	
Ionic liquids	1M LiTFSI in EMI-TFSI	2.0 ¹⁵	1.0 ¹⁵	5.3 ¹⁵	Non-flammable
	1M LiBF ₄ in EMI-BF ₄	8.0 ¹⁵	0.9 ¹⁶	5.3 ¹⁶	
Polymer	LiTFSI-P(EO/MEEGE)	0.1 ²⁴	< 0.0 ²⁴	4.7 ²⁴	Flammable
	LiClO ₄ -PEO ₈ + 10 wt % TiO ₂	0.02 ²⁶	< 0.0 ²⁶	5.0 ²⁶	
Inorganic solid	Li _{4-x} Ge _{1-x} P ₅ S ₄ (x = 0.75)	2.2 ²⁸	< 0.0 ²⁸	> 5.0 ²⁸	Non-flammable
	0.05Li ₄ SiO ₄ + 0.57Li ₂ S + 0.38SiS ₂	1.0 ³⁰	< 0.0 ³⁰	> 8.0 ³⁰	
Inorganic liquid	LiAlCl ₄ + SO ₂	70 ²⁰	-	4.4 ²⁰	Non-flammable
Liquid organic + Polymer	0.04LiPF ₆ + 0.2EC + 0.62DMC + 0.14PAN	4.2 ³⁸	-	4.4 ³⁸	Flammable
	LiClO ₄ + EC + PC + PVdF	3.0 ³⁹	-	5.0 ³⁹	
Ionic liquid + Polymer	1M LiTFSI + P ₁₃ TFSI + PVdF-HFP	0.18 ⁴³	< 0.0 ⁴³	5.8 ⁴³	Less flammable
Ionic liquid + Polymer + Liquid organic	56 wt % LiTFSI-Py ₂₄ TFSI + 30 wt % PVdF-HFP + 14 wt % EC/PC	0.81 ⁴⁴	1.5 ⁴⁴	4.2 ⁴⁴	Less flammable
Polymer + Inorganic solid	2 vol % LiClO ₄ -TEC-19 + 98 vol% 95 (0.6Li ₂ S + 0.4Li ₂ S) + 5Li ₄ SiO ₄	0.03 ⁴⁶	< 0.0 ⁴⁶	> 4.5 ⁴⁶	Non-flammable
Ionic liquid + Liquid organic ¹⁹		-	-	-	Non-flammable

Ionic liquids are considered tunable solvents, as the anion and cation can be chosen to control the macro-properties of the electrolyte. Given the drawbacks of ILs discussed above, there have been limitations among the usable anions and cations architectures. With conductivity and electrochemical stability window as the general guiding factors, the most attractive RTIL scaffolds for electrolyte use have been 1-ethyl-3-methyl-imidzaolium³⁶ and either 1-butyl-1-methyl pyrrolidinium or 1-methyl-1-propyl-pyrrolidinium.³⁷ The imidazolium architecture has the highest conductivity and thus makes it an ideal starting point for development of an electrolyte. However, this same scaffold has encountered problems with its stability at low voltages^{38,39} and its

intercalation into the graphite anode resulting in exfoliation and rapid capacity fade.⁴⁰ Both scaffolds continue to be used, but for the electrolyte in lithium ion batteries, pyrrolidinium is preferred.

Among anions the dicyanamide architecture has the highest conductivity, but it is reactive to lithium, which makes it unusable as an anion. Halides do not possess sufficient stability and undergo anodic oxidation at low potentials.³⁴ Other anions with high conductivity values are $[\text{BF}_4]^-$ and $[\text{PF}_6]^-$, however these anions decay at elevated temperatures, are reactive with water, and do not possess sufficient electrochemical stability. Thus the focus of research for the anion has centered around imide⁴¹ and triflate³⁵ architectures. Among these archetypes, the sulfonyl based imide bis(trifluoromethylsulfonyl) imide (TFSI) has demonstrated appropriate thermal and electrical properties. Recent interest though has been on the bis(fluorosulfonyl) imide (FSI) anion, which has demonstrated the ability to reversibly form an SEI film.⁴² However, due to difficulty of FSI production, its footprint in literature is minimal.

Use of ILs as electrolytes in academic settings has shown promising results with the cycled capacity, being close to that delivered by commercialized organic solvents.³⁹ However given its limitations, especially their high cost, IL based systems have not supplanted organic electrolytes in commercial systems. Neat ILs do not contain lithium ions, so for their use as an electrolyte, a lithium salt must be added. However, upon addition of the lithium salt the viscosity increases and the conductivity decreases.³⁵ In the interest of understanding the complex microscale processes occurring in a battery, research has generally matched the anion of the ionic liquid and the salt. Within ionic liquids, conductivity and viscosity have a strong inverse relationship that follows the

Vogel-Tammann-Fulcher equation.^{7,43} While adding lithium salts ultimately reduces conductivity, low salt concentrations in RTIL solutions have adverse effects upon the lithium transference number, inherently limiting the capacity that can be delivered with each cycle.^{44,45} Another problem with ionic liquids is their anodic limit. The highly reducing potential of lithium can itself induce breakdown or cause the graphite planes themselves to demonstrate catalytic properties. To combat this ethylene carbonate, which forms a stable SEI below 1 V vs. Li/Li⁺, can be added. However, this is counterproductive unless significant improvement over the commercialized carbonate solution technology is realized. Given the plethora of attractive properties and the variety of RTILs, great research interest exists in their use as both an additive and the solvent in the electrolyte of a lithium ion battery.

Research into ionic liquids has been largely limited to nitrogen based architectures despite proof of concept with phosphorous, sulfur and even oxygen based anions.⁴⁶ On top of this, recent literature has shown that phosphorous^{47,48} and sulfur^{49,50} based ILs possess superior electrochemical properties (wider ESW and higher conductivities) relative to their nitrogen counterparts. Oxonium cations have proven to be rather unstable and while it would be viewed as the most compatible with the PEO backbone concerns over its chemical stability limit its research promise. As ILs are designable additives it is possible to selectively modify them using knowledge taken from nitrogen ILs and polymer electrolytes to create a better IL.

5. Polymer Electrolytes Containing Ionic Liquids

PEO has conductivity problems at low temperatures because of its semi-crystalline nature. Thus research into PEO has focused on energetically favoring the

amorphous phase by inclusion of a secondary block²², by lower molecular weight polymers, by ceramic particles or by RTILs. Because of the attractive properties of RTILs (incombustible, high electrochemical stability) recent research has focused upon incorporating these additives into polymer electrolyte systems.

Shin et al.⁵¹ have shown that adding RTILs to poly(ethylene oxide) (PEO) results in a marked increase in ionic conductivity. Ranging the concentrations between 0.66-3.24:1 IL: lithium salt (lithium salt used is LiTFSI), the conductivity can be increased between 1 and 2 orders of magnitude (the polymer salt ratio was held constant at 20:1). However the upper limit of conductivity achievable in the polymer electrolyte is still one order less than the conductivity of the neat ionic liquid. It is also apparent that as the temperature is varied for a given electrolyte there is a change in the slope of the conductivity curve occurring at 60°C, which roughly corresponds to the T_g of PEO. Shin states that it is probably due to the melting of the PEO chains, indicating that the Li^+ ions are still interacting with the ether oxygens. This is in agreement with what is seen with polymer electrolytes containing carbonate solvents, where the preferred method of Li^+ conduction is through the polymer chains.^{2,52}

An important part of any electrolyte system is the electrochemical stability window (ESW), which is a measure of the overall stability of the electrolyte. The combination of these two components actually results in an electrolyte that has a breakdown voltage >5.5 V against lithium. This is ideal moving forward as it is functional for not only the current generation of cathodes, but also for the next generation of high voltage cathodes in development now that operate outside of the stability window for the current electrolyte systems.

The large ratio of ionic liquid to polymer in Shin's optimized electrolyte though has adverse effects upon the transference number, inherently limiting the capacity that can be delivered by lithium with each cycle.^{44,45} In the polymer electrolyte without ionic liquid, the experimental value of 0.3 falls short of the expected value of 0.5.⁴⁴ And, Shin³³ attributes the deviation at high IL concentrations to the availability of an alternative lithium conduction pathway. However, their reasoning is a gross generalization of the solid solution kinetics in a solid polymer electrolyte, leading to deviations at most ratios for the electrolyte. This is not surprising as debate exists in the literature among the nature of the transference number and its thermodynamic basis.⁵³

The polymer electrolyte used by Shin has a charge efficiency of ~99.9%. The 0.1% fade per cycle is an intrinsic property of the vanadium oxide cathode used and indicates the electrolyte is working as expected and not causing irreversible changes that diminish the capacity of the battery.⁵⁴ The only disappointing data for the polymer electrolyte/IL system is that a discharge rate of C/10 (C is defined as the current needed to fully charge/discharge a battery in 1 hour, i.e. 2C = 1/2 hour, C/10 = 10 hrs.) draws current too quickly out of the battery. While it is unlikely, it is hoped that a battery can function at high C rates allowing it to generate higher power.

III. Overview of Research Activities

1. Electrolyte Component Selection

Prudent selection of the materials to be used in the electrolyte is nearly as important as the data returned from the testing. In the following section, details will be given about the materials used to prepare the electrolyte. As a reference all chemical structures are pictured in Figure III-1.

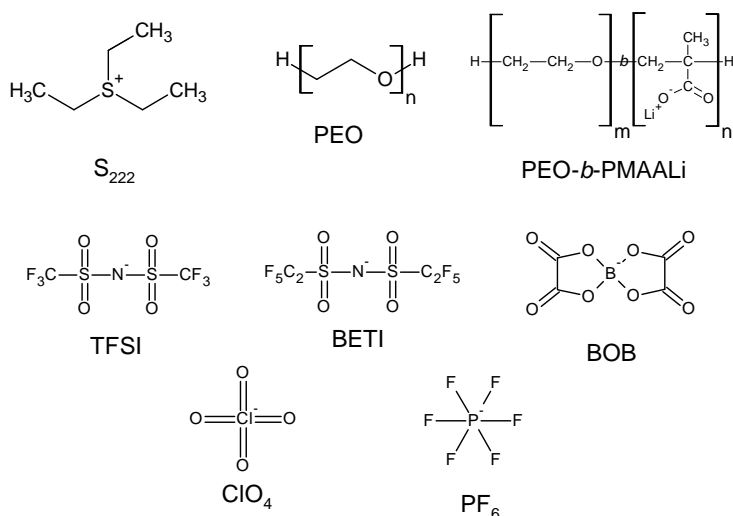


Figure III-1 Chemical structures of compounds to be used during the doctoral research

a. Polymer

Two polymer matrices were chosen to develop the electrolyte: homopolymer PEO and PEO blocked with lithiated PMAA. Because IL and Li salt need to be entrapped in the polymer scaffold while still maintaining mechanical stability high molecular weights were chosen. Given that chain mobility is important for lithium ion conduction⁵⁵, the lower molecular weight PEO may be preferred. There is some concern about the

polymer's polydispersity, but it is believed that its impact upon the observed electrical properties will be minimal. In regards to this Bruce⁵⁶ has shown that higher degrees of polydispersity possess greater conductivity because of the varying lengths of tunnels permitting overlap of the chains. Homopolymer PEO of M_w 300k was chosen for this research.

Ultimately, the polymer scaffold will be changed to look into block copolymer matrices. The motivation of this work comes from the doctoral research of Ayan Ghosh^{21,22,57}, who used lithiated poly(methyl methacrylate) blocked with PEO. His research largely focused on solid block copolymer systems (with a lithium borate based salt) which demonstrated high transference numbers (close to unity). However, insufficient conductivity limited this system and it is believed that the addition of IL to his system could overcome this problem. For this work a block copolymer with an overall M_w of 30k will be used (27k PEO-3k PMAALi). The lithiation is done by reacting PEO-b-PMAA with equimolar LiOH in an appropriate solvent; the Li^+ replaces the H^+ . This is slightly different than Ayan's polymer system as the purchased polymer is methyl acrylic acid and not methyl methacrylate. This change allows for complete lithiation of the minor block without having to first remove the methacrylate group.

b. Lithium Salt

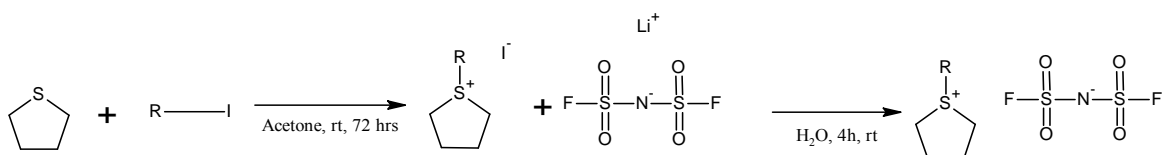
There are two sets of salts of particular interest to the research as the source of lithium ions for the electrolyte. The first salt under consideration is LiTFSI, which has been chosen because of its bulky counterion. It has been extensively studied and will provide a good comparison point to reference literature. The second set of salts to be tested consists of both commercial and experimental anions. The commercial

possibilities are PF_6 and ClO_4 , while the experimental possibilities are bisoxalato borate (BOB) and bis(perfluoroethyl sulfonyl) imide (BETI). Relative to a TFSI based system, the PF_6 anion has both benefits such as its high conductivity and price, but also drawbacks such as its moisture and temperature stability.^{6,58} Numerous other anions exist that exhibit good lithium conductivity in solid polymer electrolytes including bis(perfluoroethyl sulfonyl) imide (BETI) and bis(oxalato) borate (BOB) and ClO_4 .⁵⁹

c. Ionic Liquid

At the outset of the project it was hoped that there would be enough time to investigate both diethyl sulfone and tetrahydrothiophene based architectures. Different length pendant alkyl groups of 1-4 carbons would then be attached to these architectures. While this work was largely successful in creating the TFSI based ILs the sheer number of possibilities limited us to the most readily available triethyl sulfonium based cation. However, because of its simplicity and ability to further this research the synthesis process is disclosed in Scheme III-2. The synthesis begins by mixing the chosen architecture with the appropriate length 1-iodoalkane in dry acetone under inert atmosphere. For BETI and TFSI, the iodine anion is then exchanged for BETI^- or TFSI via an anion exchange with the conjugate alkali cation which then is separated via an organic extraction with dichloromethane (DCM). In the case of ClO_4^- , PF_6^- or BOB the iodide form was first converted to the hydroxide by use of AgNO_3 and NaOH . The appropriate conjugate acid of the anion is then added resulting in the desired IL. BOB which does use the acid first has to be synthesized in-situ and is discussed in further detail in Section V.2.b. For all ILs the absence of iodine was confirmed via qualitative testing of the DCM layer with a 1% solution of AgNO_3 in ethanol. The commonality of

anions between the lithium salt and the ionic liquid was intentional and helped to minimize the number of charged species to be investigated. The ionic liquids were then dried under high vacuum before being transferred for storage in our MBRAUN Labmaster 100 argon glove box.



Scheme III-2 Sample reaction scheme for synthesis of ionic liquid

d. Polymer Electrolyte Synthesis

The polymer electrolytes are synthesized in the glove box under argon. First all of the components are weighed and placed into a PTFE capped glass dram vial (total component weight ~200 mg). Then tetrahydrofuran (THF) or dimethylformamide (DMF) (anion dependent) and a micro sized stir bar were added to allow the solution to become well mixed. During the stirring process the solutions were elevated slightly to ~35°C (THF) or ~60 C to allow all components to go into solution. The solutions were then brought back to room temperature before being cast into shallow depressions on a Bytac sheet. The solutions were allowed to dry, before being heated to ~50-60 °C (THF) or 80 °C (DMF) to turn the electrolytes into melts and ensure all solvent has evaporated. The electrolytes were then brought back to room temperature and stored under argon until they are needed. This process results in electrolytes ~2 cm x 6 cm with a thickness on the order of hundreds of microns. The process can be scaled by using more solution and by enlarging the casting area. Phase separation (due to high salt/IL concentrations), if present within the as-cast hybrid electrolyte film, could be observed with the naked eye.

2. Ionic Liquid Analytical Tests

e. Differential Scanning Calorimetry (DSC)

DSC allows for greater understanding of the phase behaviors of the ILs, which ultimately play into the observed properties. Ionic liquids have a tendency to supercool because of the rapid increase in viscosity that occurs as the temperature is decreased. It is important to understand the location of these metastable regions so that they are kinetically avoided since they can be quite large with these compounds. Hermetically sealed pans, assembled in an argon glove box to avoid contamination with air and moisture, were used. A heat/cool/heat cycle was used to get the thermogram traces as it eliminates the thermal history of the IL.

f. Nuclear Magnetic Resonance (NMR)

NMR of the ^1H , ^{13}C , and ^{19}F nuclei are used to unambiguously identify a compound's connectivity, based upon chemical shifts and splitting patterns. For novel compounds this is necessary for publication, and for previously synthesized compounds it allows comparison to published literature. The solvent used was deuterated methanol, because of its high polarity. ^{19}F spectra were referenced to trifluoroacetic acid.

g. Mass Spectrometry (MS)

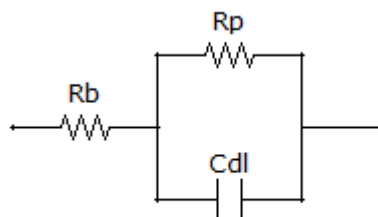
Similar to NMR, MS allows identification of compounds based upon its mass/charge (m/z) ratio. For new compounds this is necessary for publication, and for previously synthesized compounds they are referenced to published literature. The MS was run at the UMD facility in both ESI+ and ESI- mode to see the anion and cation,

respectively. Presence of the peaks at the corresponding m/z ratio will permit identification of a given compound.

h. Conductivity

The general principle behind impedance spectroscopy is that the application of a small perturbation results in an electrochemical response. This response is then fit to a model circuit allowing for determination of its electrical properties. For neat ILs, the equivalent circuit is generally modeled as shown in Scheme III-3, which consists of resistor and capacitor in parallel all of which is in series to another resistor. R_b , bulk resistance, models the diffusion of charged species through the electrolyte, while R_p , polarization resistance, and C_{dl} , double layer capacitance jointly model the interface's electrical properties.

For the ionic liquids systems, a symmetric 2 probe system was used; the AC amplitude for the tests is 10 mV and the frequency is swept from 1 MHz to 1 Hz. The bulk resistance is the high frequency x-intercept, which is then plugged into equation 1. This measurement serves as a baseline for optimal conductivity of the system, as it is expected that the full hybrid electrolyte system will be less conductive than the neat IL. As ILs are very sensitive to water all measurements were conducted under an inert atmosphere in a glove box.



Scheme III-3 Model electrical circuit

3. Analytical Tests of the Polymer Electrolyte

a. Differential Scanning Calorimetry

The principles of the DSC performed on the electrolyte are similar to DSC performed on the pure IL. Assembly of hermetically sealed pans similarly occurred in the argon glove box. The knowledge of the temperature characteristics, specifically the glass transition temperature and melting point, are important for comparison to the observed electrical properties and to understanding the mechanical properties of the electrolyte.

b. General Cell Construction

The cell as depicted in Figure III-4 was assembled in an argon filled glove box devoid of moisture, oxygen and nitrogen. The image depicts a sample cell that is exploded to clearly show the components from one side of the casing to the other. Before being removed for testing the cells will be crimped such that they are air tight and removed for testing on a frequency response analyzer. Prior to testing the cells were annealed at 70 °C for 3-4 hrs. to promote contact between the electrolyte and the electrodes. The composition of the electrode is different depending on the type of test

that is performed. Based upon the construction method of coin cells and the need to keep them airtight, all testing is done with a two probe set-up.

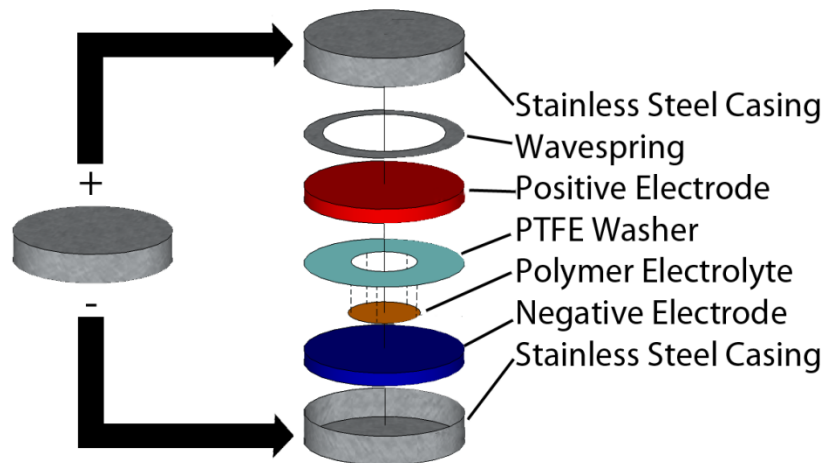


Figure III-4 Exploded view of the contents of a coin cell used for this research

c. Conductivity

The AC impedance of the hybrid polymer electrolyte operates on the same principle as the conductivity measurements of the ionic liquid. The cells are constructed with two symmetric blocking stainless steel electrodes (total electrode thickness 1.5 mm). It is then possible to discern the bulk and interfacial resistance by using a small amplitude AC current (10 mV). A semi-circle is then fit to the high frequency region of the Nyquist plot by the program ZView. The value of the lower frequency intercept is then fit into Equation 1 as the resistance, giving the conductivity value of a given electrolyte. To provide statistical significance to the data, cell compositions are run in triplicate. Debate exists in literature about the minimum ionic conductivity useful for commercial electrolytes, but the accepted threshold ranges between 10^{-3} - 10^{-4} S/cm.

$$\sigma = \frac{t}{R \cdot A}$$

σ - conductivity (S/cm)
 t - thickness (cm)
 R - measured resistance (Ω)
 A - area (cm^2)

(1)

d. Electrochemical Stability Window

The ideal electrolyte will have an ESW that is slightly larger than the theoretical potentials of the electrode. However, the current generation of carbonate electrolytes is stable to ~ 4.3 V and is not stable below 1 V (see Figure III-5⁷). However the selection of certain carbonate electrolytes allows for the formation of an SEI film, which prevents electrolyte breakdown below 1 V. While formation of this film does sacrifice some of the solvent and the cell's deliverable power, it ultimately allows the cell to operate over a wider voltage range. Polymer electrolytes have demonstrated stabilities that exceed 5 volts against Li/Li^+ and ionic liquids, are an ideal additive because they are known to have $\text{ESW} > 6\text{V}$.⁴⁶

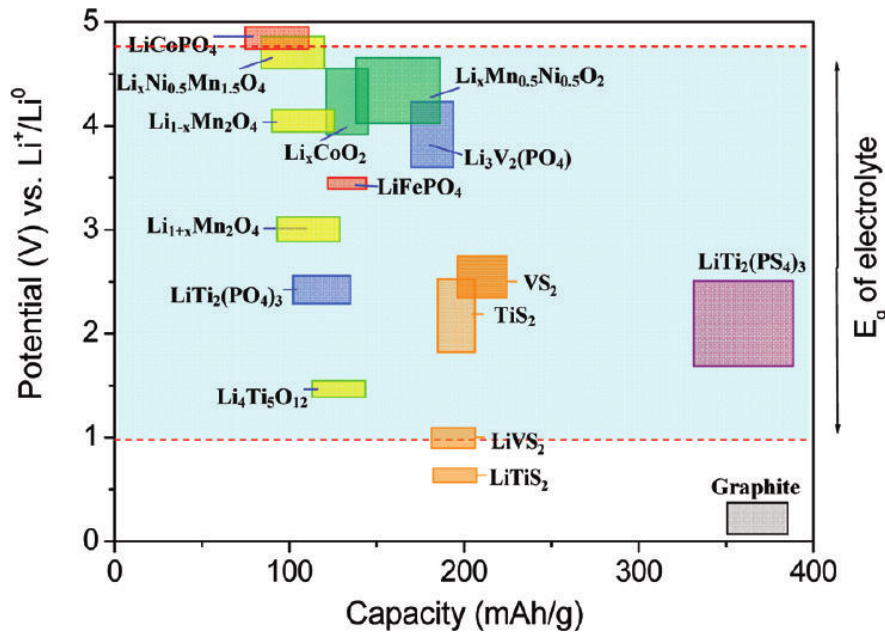


Figure III-5 Common electrode potentials and capacities plotted over the ESW of a carbonate solution⁷

To perform an ESW test (also called linear sweep voltammetry) a coin cell is constructed whereby one electrode is the reference electrode (lithium) and the other is a blocking electrode (stainless steel, platinum or aluminum). Three counter electrodes were investigated because of differing electrochemical stabilities and concerns of this facts impact on the data. For the testing, the voltage is set to 3 V and then stepped at the rate of 1 mV/s to 6.5 V against the Li reference. At the point where the derivative of the current density first changes, the electrolyte is assumed to have begun to break down. To confirm this, the scan was run repeatedly in a cyclic voltammetry experiment involving forward and backward scans to the set points. This allowed for confirmation of electrolyte stability at high voltages.

e. Overvoltage studies

AC impedance and transference generally lead to good understanding of the bulk properties of the electrolyte, but most battery issues occur at the interface between the electrolyte and electrode. Given the extraordinary amount of time to conduct cycling tests and the innumerable side reactions it is more efficient to simply test the overvoltage of an electrolyte. Stability of this interface is important to long cycle life and capacity retention both key metrics of a full battery cell.

Lithium plating and stripping tests are conducted by applying a current of 0.1 mA/cm² and reversing the polarity each hour. The cell's overvoltage at the end of each cycle of current is measured and reported as the overvoltage for that cycle. The ideal voltage profile is constant at a minimal value over each hour time period, and is constant from cycle to cycle. This is ideal as it minimizes the cell potential loss to promoting ionic movement across the interface. This cell is constructed with two lithium electrodes.

Cycling is run at an elevated temperature as long as needed with intermittent breaks for impedance spectroscopy. The impedance scans give great insight into the changes of the resistance of the electrolyte and the interface as lithium is reversibly moved across it.

f. Transference Number

The transference number is a measure of the fraction of total current (σ) that is due to Li^+ ions, wherein each ion's conductivity is multiplied by its charge (q) (Equation 2). It is determined, as per Bruce and Vincent^{53,60}, by potentiostatic measurements of two lithium metal electrodes and obtained by dividing the steady state (superscript e) current by the initial (superscript o) current while accounting for the change in resistance between the steady and initial states (Equation 2). Roughly the transference number corresponds to the ability of each ion to diffuse through the electrolyte membrane and depends on the relative concentration of each ionic species. T_{Li^+} is a good measure of the concentration gradient that develops in the electrolyte system. As this gradient becomes more steep it ultimately harms the delivered capacity as it inhibits the transport of Li^+ ions.⁶¹ The ideal value of T_{Li^+} is unity, but given the complex nature of the solid electrolytes this is expected to be between 0.2 and 0.5. The potentiostatic measurements will be run at 10 mV for 24 hrs, where the system is assumed to be at equilibrium by observing a linear response in I over time.

$$T_{\text{Li}^+} = \frac{\sigma_{\text{Li}^+}}{\sum_{\text{ions}} q_i \sigma_i} = \frac{I^e(\Delta V - I^o R^o)}{I^o(\Delta V - I^e R^e)} \quad (2)$$

g. Restricted Diffusion

The mobility of ions in the electrolyte is essential for conduction of current. However, this generation of current needs to be controlled such that cell discharge occurs in a controlled manner only when connected to an external circuit. Current interrupt tests, as developed by Newman⁶², are able to measure the movement of ions. First, a current density of 0.1 mA/cm² is applied across the symmetrical lithium cell for 15 minutes. Then the current to the cell was turned off and the potential of the cell is monitored as it returned to open circuit. By then fitting a line to the plot in the change of the open circuit potential as in Equation 3 (D_s is the salt diffusion coefficient and L is the distance between the electrodes) the D_s can be determined.

$$\text{slope} = -\frac{\pi D_s^2}{L^2} \quad (3)$$

h. Cell Cycling

It is important to check that the electrolyte does not interfere with the normal capacity fade of the electrode. In a battery system the capacity fade is a result of 2 processes: one, irreversible volume changes that interfere with the physical contact between interfaces and two, the irreversible loss of lithium ions at the interface or in the electrodes themselves. Constant current cycling, whereby the cell is considered fully charged or discharged at a threshold voltage, is limited by the C rate. The C rate which is defined as the time in hours it takes to fully charge or discharge, i.e. C/2 = 2 hours to full charge or 4C = one quarter of an hour to full charge. Lower C rates to a point result in higher capacities, but worse cycle life. A full range of rates will be tested yielding invaluable information on the current limitations of the electrolyte. The cells will be set

up with commercial cathode materials, such as LiCoO_2 or LiFePO_4 , and cycled against lithium showcasing the impact upon capacity of the electrolyte. While graphitic carbon is generally used as an anode material, its edges have catalytic properties which do not allow for intercalation of lithium. However, $\text{Li}_4\text{Ti}_5\text{O}_{12}$ a more stable anode material at 1.5 V was also tested in a half-cell configuration to further showcase the electrolyte.

IV. S₂TFSI in PEO-based Polymer Electrolytes

1. Introduction

Battery technology has been unable to become more powerful, while still remaining safe to the end consumer. To accomplish this a new generation of electrolytes will need to be developed that replaces organic carbonate based electrolytes.⁶ Solid polymer electrolytes are an alternative to liquid combustible systems because they possess superior voltage, temperature and mechanical stability. These benefits though come with a large trade off with conductivity.^{6,8-10,15} Poly(ethylene oxide) (PEO) has conductivity problems at ambient temperatures because of its semi-crystalline nature. Thus, it has become a research focus to energetically favor the amorphous phase by inclusion of a secondary block copolymer²², lower molecular weight polymers⁶³, ceramic particles^{64,65}, carbonate solvents²⁸ or ionic liquids (ILs).^{33,51,66} ILs are attractive additives because they are tunable systems that possess wide temperature and voltage stability while having appreciable conductivity without compromising safety.

ILs are considered tunable solvents, as the anion and cation can be chosen to control the macro-properties of the electrolyte. Of the most commonly used IL architectures, the imidazolium architecture³⁶ has the highest conductivity and thus makes it an ideal starting point for the development of an electrolyte. However, this same scaffold has encountered problems with its stability at low voltages and its intercalation into the graphite anode resulting in exfoliation and rapid capacity fade.^{38,39} Pyrrolidinium architectures³⁷ have been investigated because they possess high native ionic conductivity values. However, because they are poor solvents of lithium they demonstrate limited lithium conductivity values. By combining the polymer electrolyte with ILs, a hybrid

system can be constructed that will meet the performance standards for a battery electrolyte while still maintaining adequate mechanical properties as a solid.⁷

Shin et al.⁵¹ have shown that adding 1-butyl-1-methyl pyrrolidinium TFSI to PEO results in a marked increase in ionic conductivity between 1 and 2 orders of magnitude. However the upper limit of conductivity achievable in the polymer electrolyte is still one order less than the conductivity of the neat ionic liquid. Additionally the large ratio of ionic liquid to polymer in Shin's optimized electrolyte has adverse effects upon the transference number, inherently limiting the capacity that can be delivered by lithium with each cycle.^{44,45} This led to interest in novel IL scaffolds that would overcome these observed limitations while mimicking the preferred method of Li^+ conduction through the polymer chains.^{2,52} Research into sulfur and phosphorous based systems has demonstrated superior electrochemical stability and conductivity values relative to nitrogen based architectures.^{47,49}

Electrolyte research involving ILs has been largely limited to nitrogen based architectures. However, sulfur based architectures promise to provide superior electrical properties, which ultimately will allow these hybrid polymer ionic liquid electrolytes to become the next generation of solid electrolytes. The current polymer-ionic liquid systems are limited by problems with the ionic liquid, and it is hoped that the incorporation of novel ionic liquids chemistries, based on sulfur, will permit innovation beyond the current systems. Our research has focused on the development of hybrid electrolyte structures that blend sulfur based cations with PEO for improved performance as electrolytes in lithium batteries. We report on the mechanical and electrochemical characterization of this system.

2. Experimental

a. Materials

LiTFSI ($\text{LiN}(\text{SO}_2\text{CF}_3)_2$), and lithium, aluminum and platinum foil were purchased from Aldrich and used as received. Poly(ethylene oxide) (M_w 300k) and triethyl sulfide iodide were purchased from Alfa Aesar and used as received.

b. RTIL preparation

S_2TFSI ($\text{S}(\text{CH}_2\text{CH}_3)_3 \text{TFSI}$) was synthesized according to previous literature.⁶⁷ Briefly, S_2I was stirred with LiTFSI (10% stoichiometric excess) in DI H_2O for 4h. The IL was then diluted with dichloromethane and washed 5x with water until no precipitate formed by AgNO_3 . The organic layer was then dried under high vacuum at 60°C for 24h. Characterization was performed by NMR on a Bruker AV-400 high resolution NMR. ^1H , ^{13}C and ^{19}F (TFA capillary reference) were performed in deuterated methanol. Mass spectroscopy measurements were performed on a JEOL AccuTOF-CS ESI-TOF mass spectrometer. ESI+/ESI- modes were looked at over the m/z range of 80-500. ^1H : 3.3341 (q, $J= 7.4$ Hz, 6 H), 1.4694 (t, $J= 7.4$ Hz, 9 H); ^{13}C : 120.213, 32.681, 7.961; ^{19}F : 41.41. ESI⁺: 119.03285, ESI⁻: 279.92384.

c. Electrolyte Preparation

The electrolyte films of different composition were solution cast from tetrahydrofuran onto Bytac molds in an MBRAUN Labmaster 100 argon glove box. The resultant films were dried for several days at 50°C , before being placed into CR2032 coin cell enclosures for electrolyte testing. All constructed cells are annealed for 3 hrs. at 50°C prior to any electrochemical testing.

d. Electrode Preparation

Cathodes were prepared by mixing 80 % LiFePO₄, 10 % carbon black and 10 % PEO by weight in DMF. The paste was ball milled for 30 mins before being spread onto aluminum foil and dried in a 100 °C oven. Discs were punched out and weighed before being placed into a glove box for assembly.

e. Electrolyte Characterization

Differential scanning calorimetry (DSC) measurements were performed on a TA Instruments Q100 differential scanning calorimeter. Samples were hermetically sealed in Al pans under Ar prior to measurements. Samples were run using a heat/cool/heat method to erase thermal history at a heating rate of 10°C/min and a cooling rate of 5°C/min from -50°C to 120°C.

Conductivity measurements for electrolytes were performed in a SS/electrolyte/SS coin cell set up on a Solartron 1287A/1255B platform over the frequency range 1 MHz to 1 Hz. Testing parameters were controlled by the associated CorrWare and ZPlot software, while data analysis was performed using CorrView, ZView and Origins 8. All temperature testing was done in a RevSci IncuFridge with ±0.5°C temperature accuracy.

Raman spectroscopy was performed on a Horiba Yvon LabRam ARAMIS using a 100x objective, a 600 gr/mm grating, a 100 µm hole, a 100 µm slit, a D 0.3 filter and a 633 nm HeNe laser.

Cyclic voltammetry was performed on an Arbin BT2000 to determine the cyclability of the electrolyte. Tested cells were cycled 500 times at room temperature at rate of 5 mV/s. Pt/electrolyte/Li cells were cycled from 2.5 V to 4.7 V vs. Li/Li⁺

reference; Al/electrolyte/Li were cycled from 2.5 V to 5.0 V vs. Li/Li⁺ reference. The half-cell potential for Li/Li⁺ which is used as the reference for all voltammetry measurements, is ~3.04 V relative to the NHE.

Lithium stripping-plating experiments were performed on the Solartron set-up to determine the interfacial stability and reversibility of the electrolyte material. The electrolyte was sandwiched between two lithium electrodes. A current density of 0.1 mA/cm² was applied to the film and was reversed every hour. 100 cycles, each consisting of 1 hr. positive current and 1 hr. negative, were applied to the cell at 45 °C. Impedance spectroscopy was periodically conducted to monitor development of resistance at the interface during the galvanostatic cycling.

The cathode half cells were cycled on an ArbinBT2000 (Arbin Instruments, TX, USA) between 2.5-4.0 V. The applied current for both the charge and discharge was 0.01 mA/cm²; 10 cycles were completed. Cells rested for 1 minute between charging and discharging. Cell temperature was maintained at 40 °C by use of a RevSci Incubator. Cells were equilibrated for 1 hour prior to testing.

3. Results and Discussion

Sulfur based ILs were selected because of their high initial conductivity and wide electrochemical stability. Among possible cation scaffolds triethyl sulfonium was chosen for its structural similarity to PEO, as it possess a thioethylene moiety (C-C-S). As a well-known lithium ion conductor, PEO with its backbone of repetitive oxyethylene (C-C-O) sequences allows lithium to be coordinated to oxygen units as it moves along the voltage gradient. This association between the polymer backbone and IL is believed to favor lithium as the dominant charge carrier in the electrolyte. Additionally, the IL would

plasticize the high molecular weight PEO allowing for increased chain mobility at low temperatures. The anion was selected to allow for elevated temperature applications, and also for the common anion effect with the lithium salt. This led to the widely available TFSI anion, which is only limited because of its instability at high voltages against aluminum. The electrolyte is formed by solution casting to create a homogenous film. Four ratios of ionic liquid were evaluated, with constant ratio of polymer to salt to measure the observed properties. The ratio of PEO to lithium salt was selected from a literature survey, leading us to an O/Li⁺ of 20:1.^{51,68} The IL ratio was selected to give a broad base without compromising the ability to form thin films. The molar ratios tested were 20 PEO : 1 LiTFSI : x S₂TFSI, where $x=0, 0.5, 1.0, \text{ and } 1.5$. Henceforth the electrolytes are referenced by the molar ratio of IL, as IL- x .

Confocal Raman Spectroscopy

After drying, the films formed opaque free standing solid membranes (Figure IV-1), which are strong enough to be rolled and manipulated by hand. Raman spectroscopy was performed on the hybrid solid electrolyte to confirm its homogeneity. Each component's spectrum was individually taken before rastering the laser beam over a 50 μm square. The spectra of IL-1.0 can be seen in Figure IV-2 with the relevant integration areas highlighted (Green: LiTFSI 712-769 cm^{-1} , Red: PEO 820-886 cm^{-1} , Blue: S₂TFSI 2920-2979 cm^{-1}). The color intensity in Figure IV-3(a), (b) and (c) corresponds to the integral of the chosen area (darker=greater) with Figure IV-3(d) corresponding to the overlay of the three color images. The small changes in the depth of color are believed to be largely the result of the imaging of a dimpled surface, which ultimately affected our ability to focus the beam light in a constant xy-plane over the entire sample. The casting

technique results in as-cast films having a variable thickness when observed under a microscope. However, during electrochemical testing this limitation is handled during the annealing process, wherein pressure and temperature are applied to generate uniform contact between the electrode and the electrolyte. Additionally, minor color variations are observed due to the difficulty in selecting peak regions, as there was generally little buffer between peaks of interest and overlapping peaks from other components. The coloring of the overlaid graphs is consistent over the imaged area confirming the homogeneity on the microscale of the electrolyte.



Figure IV-1 Pictures of thin film solid electrolyte in Ar atmosphere. Electrolyte is ~5 cm. x 2cm.

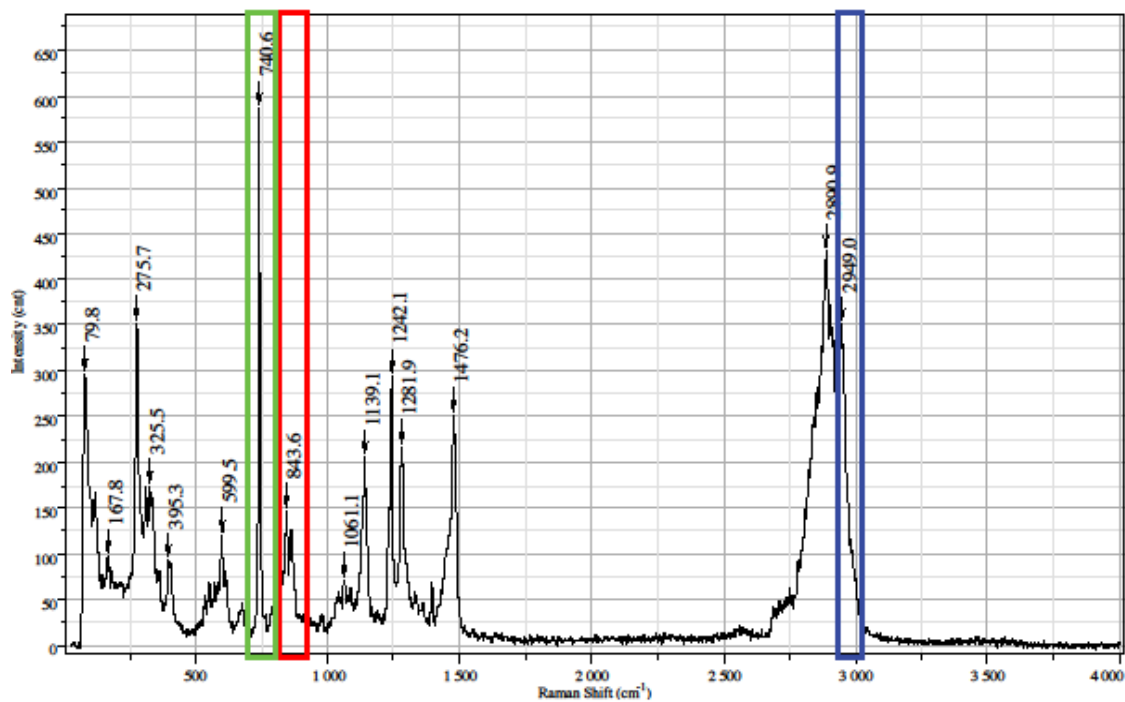


Figure IV-2 Raman spectra of IL-1.0 hybrid polymer electrolyte. Indicated areas are as follows Green: LiTFSI 712-769 cm^{-1} Red: PEO 820-886 cm^{-1} Blue: S_2TFSI 2920-2979 cm^{-1} .

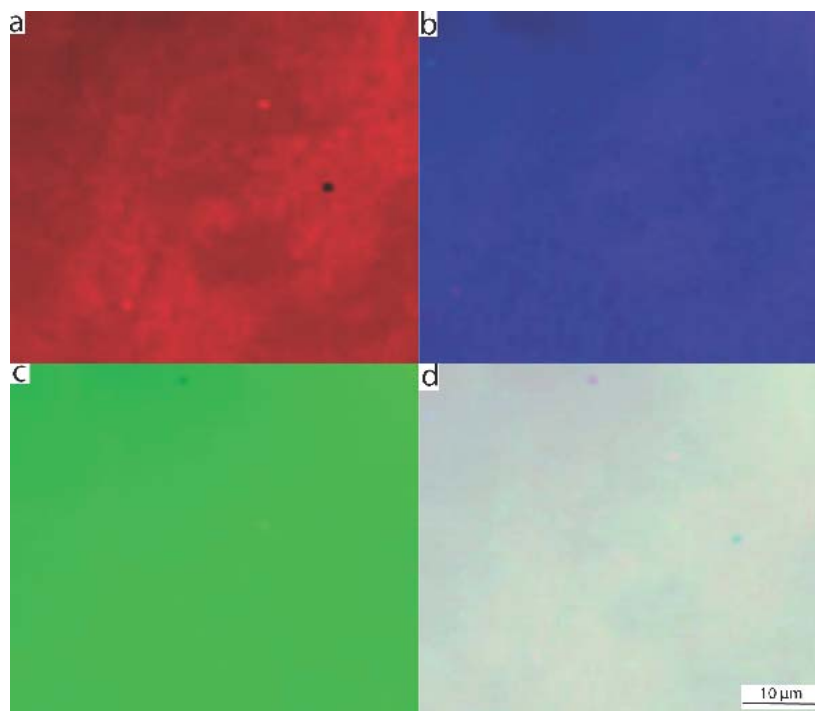


Figure IV-3 Confocal Raman Spectroscopy of 50 μm . square. Intensity indicates area under the peak. a) PEO 820-886 cm^{-1} b) S2TFSI 2920-2979 cm^{-1} c) LiTFSI 712-769 cm^{-1} d) component overlay.

Differential Scanning Calorimetry

Conductivity is a function of temperature, especially in polymer electrolyte wherein chain mobility is largely responsible for conduction of ions. DSC was performed on the electrolyte to observe any thermal hysteresis over operational temperature. Figure IV-4 shows the relevant portion of the cooling and heating cycles of the electrolytes; no peaks were observed outside this region. With increasing concentration of additives, the transition temperatures decrease leading to polymer blends that are amorphous at room temperature. This is preferred because lithium ion conductivity in PEO depends on polymer chain mobility. The large hysteresis can be shown in each of the tested formulations as there is a 20-30 $^{\circ}\text{C}$ difference between the

heating and cooling transition temperatures. These differences remained large despite slower heating and cooling rates. The large superheating and cooling effects is believed to be a result of the ionic liquid as this phenomenon is typically seen in the DSC of neat ILs. It is also of note that the IL-1.0 and IL-1.5 formulation are solid at room temperature, despite the thermograms indicating the hybrid electrolyte is in a region between its freezing point and melting point. Lastly with increasing ionic liquid concentration the transition peaks become broader. The trend in the thermograms confirms the increased presence of the amorphous lithium conducting phase at lower temperature. The dry nature of our electrolyte is further confirmed with the absence of water peaks at either 0 or 100 °C.

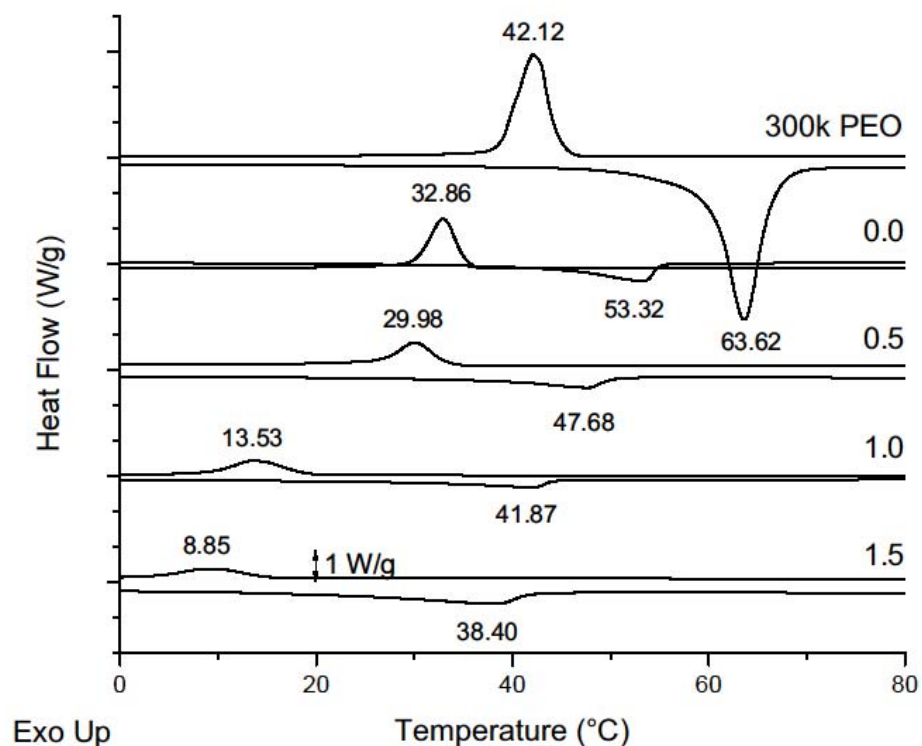


Figure IV-4 Selected portion of thermograms from indicated electrolyte mixtures. Heating rate was 10 °C/min and cooling rate was 5 °C/min in a heat/cool/heat format with endpoints of -50 °C and 120 °C. Each thermogram is offset 3 W/g, and each tick mark on the y-axis is 1 W/g. Ratio is moles of 20 PEO: 1 LiTFSI : x S₂TFSI, where x is indicated in the figure.

Ionic Conductivity

With this difference between heating and cooling cycles we chose to measure the AC impedance while both heating and cooling our samples. The cooling cycle can be seen in Figure IV-5(a) of a SS/electrolyte/SS set-up. At 25°C IL-1.5 has sufficient ionic conductivity (>0.1 mS/cm) to be useful in battery applications. At 35 °C the conductivity

of the optimum system is 0.640 mS/cm. This temperature is of great interest because it is close to the temperature of the human body, wherein the safety of electrolyte systems limits the deployment of medical devices. When comparing the conductivity data to each electrolyte's thermogram, a jump in conductivity is observed at the melting temperature, which corresponds to the transition from semicrystalline to melt in the polymer matrix. On either side of this point the conductivity increases linearly over inverse T , however, at this temperature the value of this slope changes resulting in smaller increases in conductivity over continued temperature increases.

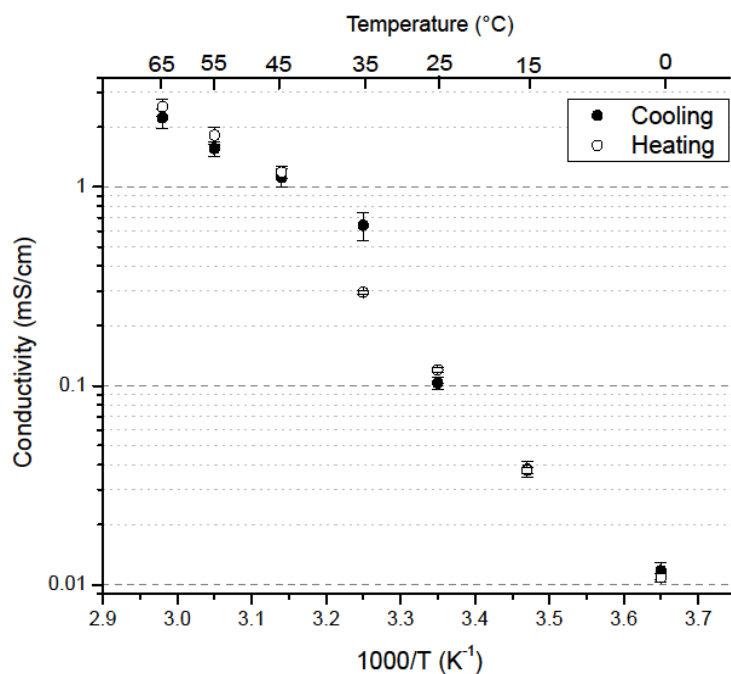
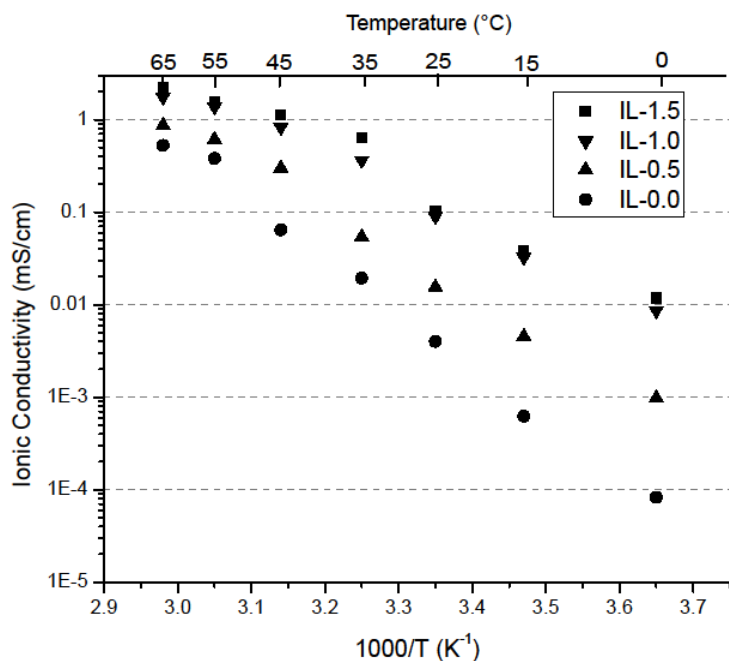


Figure IV-5 (a) Conductivity over varied temperature for selected electrolyte over the cooling cycle. Ratio is moles of 20 PEO: 1 LiTFSI: x S₂TFSI. (b) Effect of thermal history on measured conductivity of IL-1.5 electrolyte.

At low temperatures the addition of IL results in a roughly 3 order of magnitude increase in ionic conductivity, which at higher temperatures diminishes to roughly 1 order of magnitude. This decrease in gain seen by adding IL over increased temperature is believed to be the result of greater reliance on enhanced chain mobility, which leads to greater ionic conductivity in the IL-0 electrolyte. Chain mobility of the PEO systems is largely dependent on the absence of crystalline regions, which occurs above the transition determined from DSC, which is confirmed by the conductivity data. Additionally greater IL concentrations result in diminished increases in conductivity, as seen by the close overlap of IL-1.0 and IL-1.5. This is an agreement with previous hybrid polymer electrolyte systems, whereby the ionic conductivity asymptotically approached that of the pure IL.³³

The observed ionic conductivity values exceeded those of the comparison pyrrolidinium system with significantly less IL. For comparison, the system closest to IL-1.5 ($x=1.73$), reaches 0.1 mS/cm at $\sim 20^{\circ}\text{C}$, a 5°C cooler than our optimal conductivity system³³. At slightly elevated temperatures the difference in conductivity between the pyrrolidinium and triethyl sulfonium is diminished, but the sulfur based system still maintains improved conductivity. Given the numerous constraints applied to selecting an electrolyte system⁷, the confirmation of our hypothesis that triethyl sulfonium based systems mimic the polymer, bodes well for increased performance by using our hybrid solid polymer electrolyte.

Figure IV-5(b) is an isolation of IL-1.5 for the heating and cooling cycles. All data points overlap except for 35°C , which is markedly different (0.640 mS/cm (cooling) to 0.295 mS/cm (heating)). This correlates with the transition temperature determined

from DSC (38.40°C). As expected for the cooling curve which approaches the transition from the melt, the electrolyte is able to supercool until it undergoes a transition prior to the temperature point collected at 25°C. The heating curve peak occurs at a higher temperature and thus the order of magnitude increase in conductivity associated with the transition is not seen until the 45°C temperature point. Considering this, great care was taken to equilibrate cells above room temperature for extended periods of time before cycling.

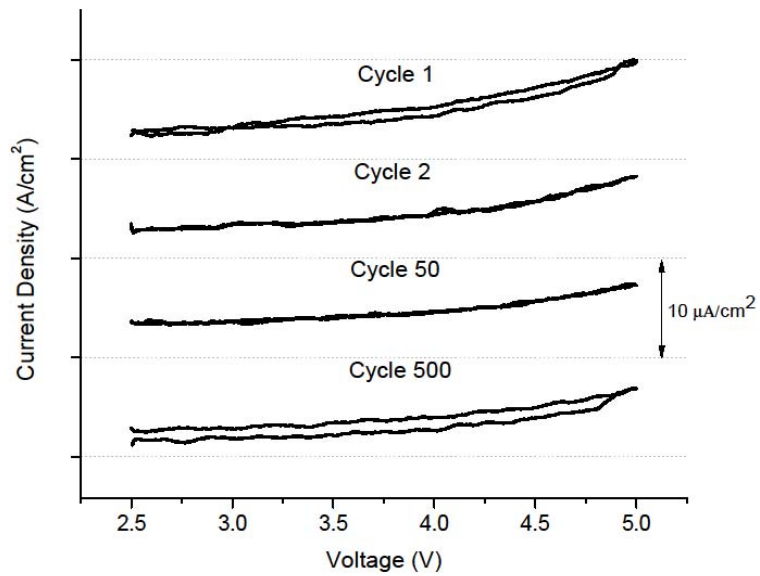
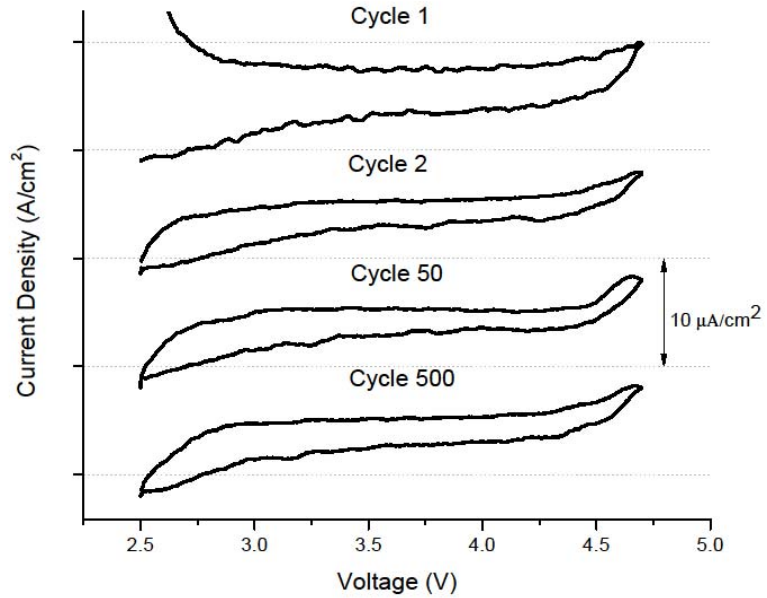
Cathodic Stability

Electrolytes in lithium batteries, besides being thermally stable lithium ion conductors, need to possess sufficiently wide reversible electrochemical stability against Li/Li⁺. Stability to the cathode (cathodic stability) should meet or exceed the potential of current carbonate based electrolytes. Stability to the anode (anodic stability) should allow for the utilization of low voltage anodes by formation of a stable solid-electrolyte interphase (SEI).

Reversible cathodic stability in the IL-1.0 electrolyte was attained using cyclic voltammetry of a Li/electrolyte/Pt cell, cycled from 2.5 to 4.7 vs. Li/Li⁺ for 500 cycles. Platinum was initially used as the counter electrode due to documented concerns in the literature of instability of the TFSI⁻ anion against Al.⁶⁹ In Figure IV-6(a) selected cycles show the reversible stability of the electrolyte that exceeds 4.5 V. In cycle 1 there is a clear breakdown near the upper voltage limit, which diminishes in magnitude with further cycling. After the first forward sweep there is a clear decrease in the current density, which is the result of increased resistance. The ability of the hybrid electrolyte to achieve

high voltages against lithium is confirmed, ultimately presenting further ability for the development of high power lithium batteries that rely on high voltage cathodes.

Figure IV-6 (a) Cyclic voltammetry of Li/IL-1.0/Pt cell. The voltage was cycled from 2.5 to 4.7 V vs. Li/Li⁺ at a rate of 5 mV/s at rt. The current remains relatively constant over the whole voltage range until the upper cathodic limit. Minimal decrease in current is observed from the 1st to 500th cycle. (b) Cyclic voltammetry of a Li/IL-1.0/Al cell. The voltage was cycled from 2.5 to 5.0 V vs. Li/Li⁺ at a rate of 5 mV/s at rt.



In addition to testing our electrolyte system with a Pt counter electrode we decided to investigate its stability against aluminum in the interest of commercial viability. Aluminum is nearly ubiquitously used as the cathodic current collector thus the electrolyte needs to be characterized against it. In Figure IV-6(b) IL-1.0 is cycled from

2.5 to 5 V against Li/Li⁺ for 500 cycles. Over the entire cycling process there was minimal current decay indicating stability against high voltage commercial cathodes. The electrolyte as formulated does in fact appear to have promise for 5 V cathode systems. Further electrolyte testing conducted after completion of this test (not pictured) does indicate electrolyte stability that would provide a buffer zone above cathodes with a 5 V discharge potential.

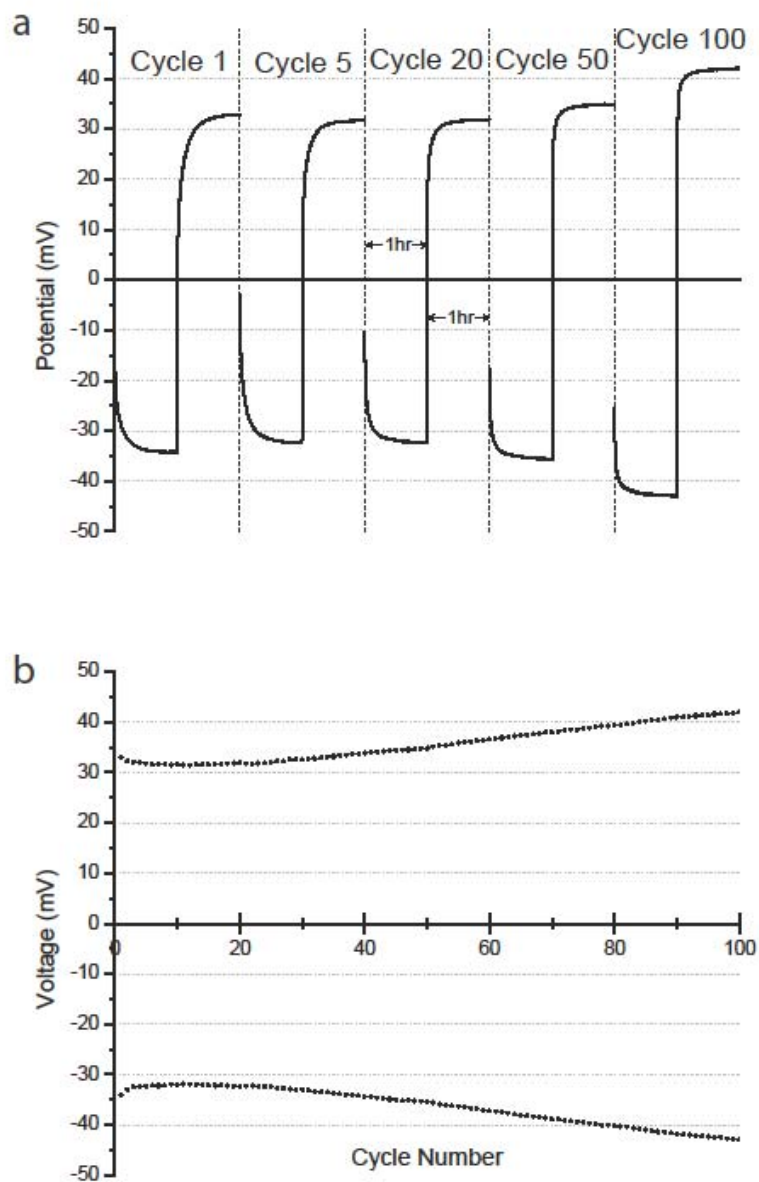
Overvoltage

To document the long term stability of the IL-1.0 electrolyte against lithium, galvanostatic cycling was conducted that involves aggressively stripping and plating lithium. A current density of 0.1 mA/cm² was reversed every hour for 100 cycles at 45 °C with intermittent testing of the conductivity via impedance spectroscopy. Selected cycles can be seen in Figure IV-7(a), which shows that the electrolyte has a delayed response to the current. Initially the plateau region takes over 30 minutes to achieve. Over the first 20 cycles this time reduces by half and the cell is able to reach steady state in ~15 minutes.

The overvoltage at the end of each half-cycle is plotted in Figure IV-7(b). There is an initial decrease in the value followed by a constant value for the succeeding 20 cycles. This constant period is then followed by a steady increase in the overvoltage for each successive cycle, until the completion of the test. This steady growth of the resistance in the electrolyte is attributed to the increase in thickness of the SEI layer as determined by impedance spectroscopy. The Coloumbic efficiency of the plating and stripping cycles were evaluated to determine the reversibility of lithium transport. The first cycle has an efficiency of 91.1%, which is believed to be the result of the

development of SEI layer. In the 2nd cycle this efficiency quickly jumps to 98.3% and remains close to 98% for the remainder of the 100 cycles.

Figure IV-7 (a) Measurement of IL-1.0 overpotential as a function of time. Cycle number is as indicated in the legend. (b) Value of overpotential of the electrode-electrolyte interface at the end of each 2 hr. cycle (1 hr. charged followed by 1 hr. discharge both at 0.1 mA/cm²) as a function of cycle number. Testing was conducted at 45 °C.



The selected impedance scans (Figure IV-8) show a constantly increasing low frequency intercept of the electrolyte. The Nyquist plots from Figure IV-8 were then modeled using an equivalent circuit consisting of the electrolyte resistance (R_e) in series to a parallel circuit element that branches into, the double layer capacitance (C_{dl}) and the

resistance to charge transfer (R_{ct}). The calculated values from using this model circuit are displayed in Table 1. The C_{dl} and the R_e change minimally over the 100 cycles. However, the R_{ct} more than doubles from the fresh cell to the 100th cycle. This is taken to mean the interface layer is gradually increasing in resistance, which is believed to be the result of incomplete dissolution of the interface upon reversal of the current's polarity leading to an SEI of constantly increasing thickness. This is corroborated by the increasing plateau voltage and the compounding of imperfect coulombic efficiency. Given the constant nature of R_e relative to R_{ct} the bulk electrolyte remains largely unaffected by the current decay that is occurring at the electrode-electrolyte interface. Lastly the long term cycling stability of the hybrid electrolyte system confirms suppression of dendrite growth. Although the interface needs to be slightly modified so that it reaches a steady state; the ability to deploy batteries containing metallic lithium would result in a large boost in capacity.

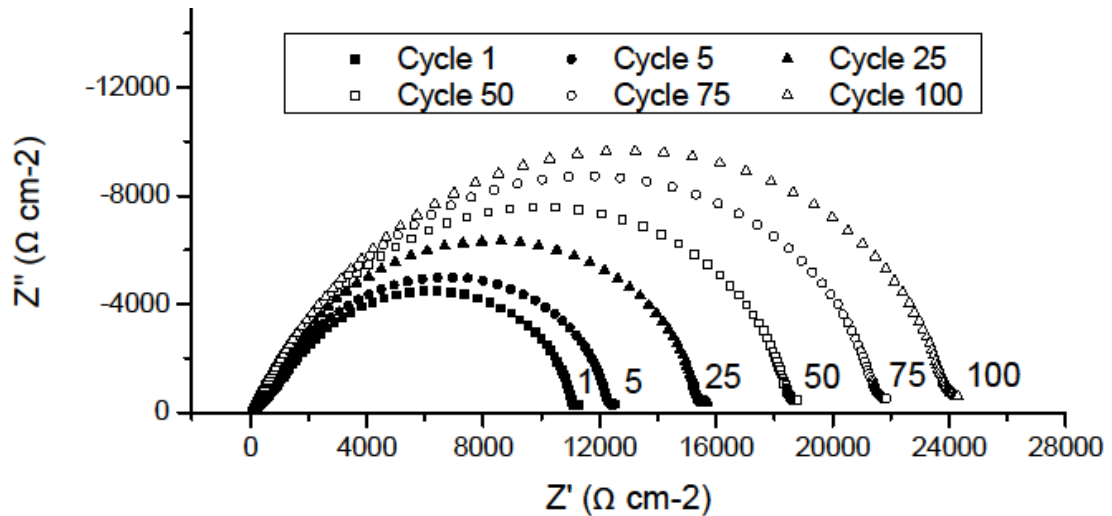


Figure IV-8 Nyquist plot of electrolyte during overvoltage study. Frequency range is 1 MHz to 1 Hz.

Table IV-1 Resistance and capacitance of equivalent circuit elements from the impedance scans after stated stripping/plating step. The semicircles were modeled as a circuit containing the electrolyte resistance in series to an RC circuit

Cycle	0	5	10	25	50	75	100
$R_e (\Omega)$	136.61	118.84	112.71	108.65	115.57	124.13	133
$R_{ct} (\Omega)$	1300.6	1445	1576.6	1812.3	2179	2533.7	2822.2
$C_{dl} (F)$	3.58E-07	3.16E-07	3.08E-07	3.06E-07	3.08E-07	3.07E-07	3.06E-07

Half-Cell Cycling

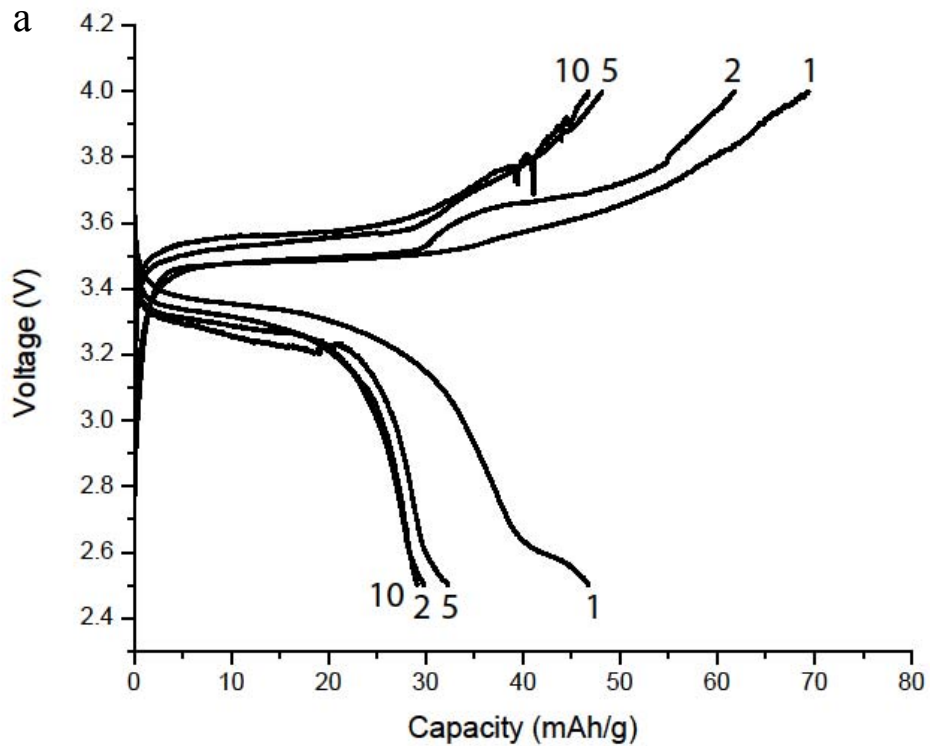
Given the elevated conductivity values and wide electrochemical stability of the electrolyte, research was undertaken to test the electrolyte system against common cathodes and anodes in half-cell based systems. As an early proof of concept the low voltage cathode material LiFePO_4 was investigated. Lithium was used as the anode, as no matching of capacity needs to occur, since its capacity greatly exceeds that of any other active material. Also, there are no intercalation kinetics for the anode because lithium only has to be plated on the surface; making the data easier to interpret. And lastly, if there was long term stability as evidenced by no dendrite growth, the use of lithium could be even considered a full lithium cell as opposed to a half Li-ion cell.

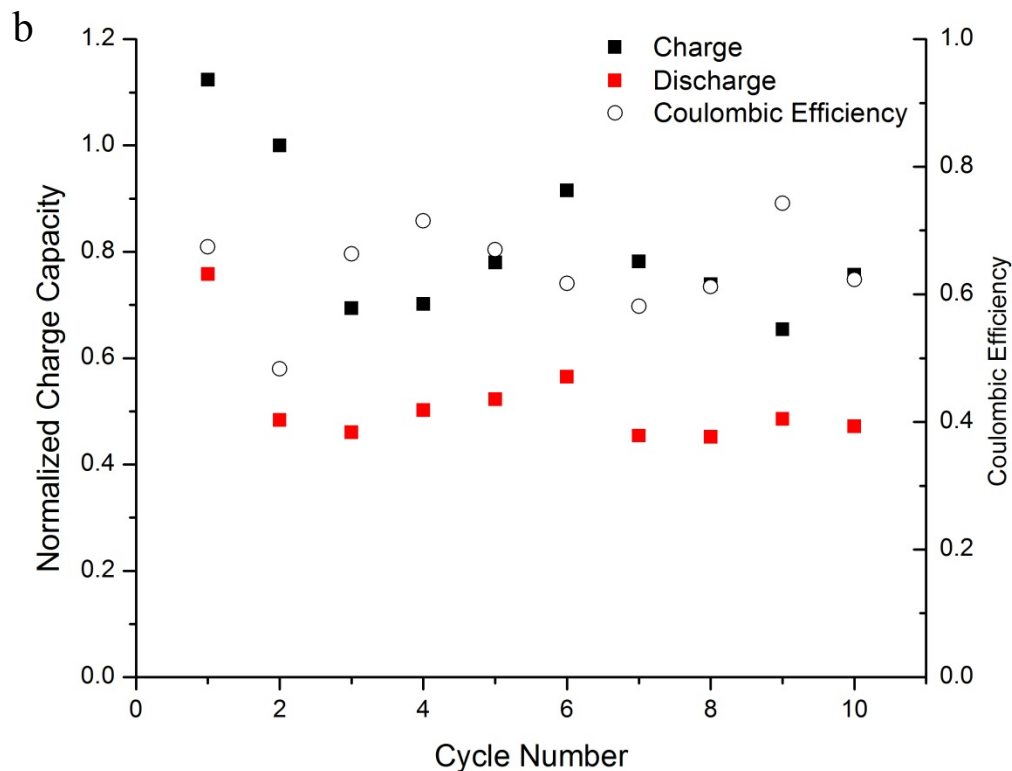
The assembled cathodes were 80 % active material, 10 % carbon black and 10 % PEO binder. PEO was chosen over PVdF or CMC based binders as it is a natural Li^+ conductor and it could anneal with the electrolyte. Ideally the electrolyte itself could be used as a binder and lithium conductor, but dry room facilities were unavailable. This led to some concern over the ability of LiFePO_4 particles to interface with the lithium conducting electrolyte. Additionally the experimental set up with the coin cells limits the amount of cathode material in contact with the electrolyte. Because the PTFE washer

limits the surface area, it is possible that ion path lengths are significantly longer than the cell is thick. This is also believed to negatively affect the observed voltage as intraelectrode ion movement is disfavored. Ongoing incomplete cycling has shown that with elevated temperature, where PEO is a more effective Li^+ conductor, these effects are marginalized. With these two points in mind there was some difficulty in calculating the amount of available active material. A quick calculation is made assuming all active material can be delithiated/lithiated as well as a normalized value. The values are normalized to the second charging process as this accounts for irreversible capacity loss due to formation of the interfaces.

The curves of voltage vs. capacity of a Li/electrolyte/ LiFePO_4 cell can be seen in Figure IV-9a. The numerical values are depicted in Figure IV-3b, along with the coulombic efficiency. The cells were cycled galvanostatically at 0.01 mA/cm^2 between 2.5 and 4.0 V. The first noticeable feature is the large decrease in capacity during the initial cycling. Between the first and second charge and discharges there is capacity retention of 67 % and 48 % respectively. This large decay was unexpected considering the wide electrochemical stability and low current used. If all active material is assumed accessible the first charge capacity is 71.20 mAh/g while the first discharge capacity is 48.03 mAh/g. However, if only the active material in direct contact with the electrolyte is counted the capacity of both the charge and discharge cycles exceeds 140 mAh/g. This factor has led us to also calculate capacity as a relative function of the second cycle.

Figure IV-9 a) Selected charge/discharge curves of a Li/electrolyte/ LiFePO₄ cell. Cycling was conducted at 0.01 mA/cm² from 2.5 to 4.0 V. Testing was conducted at 40 °C. b) End capacity of the first 10 cycles for the cell (charge (■) discharge (■)). Capacity values were calculated assuming all active material was available, which given the low values is not expected to be available amount. Coloumbic efficiency (○) was determined by comparing the discharge capacity over the charge capacity for a given cycle.





The delithiation of the LiFePO_4 during the first cycle occurs in two phases. The first has an overpotential of 50-100 mV relative to the normal plateau region around 3.4 V. However, after it has reached the end of this phase there is a second phase with a gradual increase in voltage until the cut-off at 4 V is reached. This second region is indicative of the additional energy needed to move lithium within the electrode material to the electrode-electrolyte interface where it can then move to the anode. During the first discharging cycle this first phase is nearly the entire observed capacity. The second phase is significantly smaller and may be a function of the greater driving force needed to lithiate active material not in contact with the electrolyte. The plateau similarly occurs at an overpotential of 50-100 mV, which is the energy loss as the Li ions cross the interface. Over increased cycling the overpotential of this plateau region increases relative to the

normal potential of lithiation/delithiation, which has been observed in prior research.⁷⁰ The second phase observed during charging also decreases with cycling as a fraction of the total capacity. Ongoing research shows that this second phase can also be minimized with increased cycling temperature. This is believed to be a result of the net flow of lithium out of LiFePO_4 not in contact with the electrolyte.

The capacity fading seen in Figure IV-9b quickly levels off in the 3rd cycle for both charge and discharge curves. The charge capacity levels off at ~75 % of the second cycle, while the discharge capacity levels off at ~49 %. Plotted out to the 10th cycle a plateau can be seen when looking at the charge and discharge capacities. This is ideal and largely indicates that stability has been achieved between the electrolyte and the electrode, which would be ideal for large number of cycles. Further research of this cycling should be able to show a continuing trend in capacity for this safe electrolyte. Looking closer at the capacities there is greater variation in the charging capacity as opposed to the discharging capacity. The stability of the discharge, wherein Li is put into the FePO_4 , is likely due to the repeated accessing of the most readily available particles closest to the electrolyte-electrode interface. This repeated accessing of a limited number of localized particles can be seen by the close overlaying of the discharge curves. The greater instability of the final values for the charging curves is believed to be the result of progressive delithiation of active material further from the interface with the electrolyte. The sloping nature of the curve does not normally exist for LiFePO_4 ; typically it undergoes a phase transformation whereby most of the capacity is delivered at 3.4 V. However, in these charge curves there is a large sloping region, similar to what is seen in LiCoO_2 , accounting for a good portion of the capacity. This indicates the need for

marginally increasing voltage to promote lithium movement in the electrode. The inconsistency is the result of difficult intraelectrode kinetics and is believed could be diminished with lower current densities or with increased temperature.

In Figure IV-9b the coulombic efficiency is graphically shown. After the initial decay during the first 2 cycles the coulombic efficiency varies widely between 0.58 and 0.74 with an average efficiency of 0.70. However, this loss within a given cycle is not accompanied by an absolute decay in capacity of the cell. This observed phenomenon, called slipping, is believed to be the result of a poorly designed cell set-up. As there is a large amount of active material not in contact with electrolyte the ability of lithium ions to diffuse through the cathode material becomes an issue. Ultimately, access to these regions is easier during delithiation than lithiation and thus resulting in the observed slipping. A redesign of the testing cell is needed to determine whether the slipping is the result of the electrolyte or cell set-up.

4. Conclusions

Polymer electrolyte systems present a unique opportunity for the future of lithium batteries. The solid sulfur based IL hybrid electrolyte system developed maintains many of the pure polymer systems ideal properties while improving its low temperature conductivity over previously investigated IL chemistries. Our casting procedure yields homogenous freestanding films that would ultimately be able to withstand many of the processing steps for a commercial battery system. The hybrid electrolyte has demonstrated sufficient ionic conductivity (0.120 mS/cm) at 25°C, and 1.18 mS/cm at 45°C. At the temperature of the human body, ionic conductivity of the hybrid electrolyte system is ~1 mS/cm, ultimately boding well for the development of a safer battery for

biological purposes. The hybrid electrolyte demonstrated progress towards an electrolyte that will work for higher voltage and higher capacity lithium battery systems. The system possesses reversible cathodic stability exceeding 4.5 V and long term cycling stability against metallic lithium.

Cell testing was undertaken to characterize the cycling performance. A large decay in initial capacity was observed that quickly leveled off. Normalized to the capacity of the second charge cycle the charge capacity stabilized at ~ 0.75 and the discharge capacity at ~ 0.49 , while the coulombic efficiency of a given cell averaged 70% after the initial decay period. Given the stabilization of the cycling data, long term stability for the electrolyte in a battery set-up is predicted. However, current testing setup is insufficient and has led to a number of factors that limits understanding the faults of the electrolyte relative to the experimental protocol. Development of a solid polymer electrolyte for lithium battery applications is still a ways away from commercial deployment. The safety profile of carbonate based electrolyte though is insufficient and merits the continued research of safe solid polymer electrolyte systems.

V. Effect of Anion on PEO-based Polymer Electrolytes

1. Introduction

Lithium is the premier chemistry for high energy and power density batteries. However, its widespread deployment in batteries has been limited due to safety. Complete cells have had a propensity to overheat and combust. The development of a new generation of electrolytes that replaces organic carbonate based electrolytes would ultimately lead to the goal of safer batteries.⁶ The progress in developing polymer electrolytes, which possess superior voltage, temperature and mechanical stability, has been stalled due to low conductivity.^{6,8,9} The commercial focus of polymer electrolytes has been largely relegated to polymer gel electrolytes, which does not avoid the combustible carbonate solutions.²⁸ Although, it is possible to elevate the conductivity of a solid polymer electrolyte while still avoiding the use of combustible components.

Ionic liquids (ILs) have been used successfully to overcome the limited conductivity of polymer matrices because they possess ideal electrochemical properties; namely high conductivity, electrochemical stability, and no volatility. When incorporated into poly(ethylene oxide) (PEO) based polymer matrices they have been shown to elevate the ionic conductivity of the electrolyte several orders of magnitude.^{33,51,66} Of the most commonly used IL architectures for electrochemical purposes, the imidazolium architecture³⁶ has the highest conductivity and thus makes it an ideal starting point for the development of an electrolyte. However, this same scaffold has encountered problems with its stability at low voltages and its intercalation into the graphite anode has resulted in exfoliation and rapid capacity fade.^{38,39} In recognition of this Shin et al.⁵¹ have shown that adding 1-butyl-1-methyl pyrrolidinium

bis(trifluoromethane sulfonyl) imide (TFSI) to PEO leads to a marked increase in ionic conductivity of 2 orders of magnitude for the highest tested concentrations (molar ratio of 20 PEO: 1 LiTFSI: 3.24 IL). However, the large ratio of ionic liquid to polymer in Shin's optimized electrolyte has adverse effects upon the lithium transference number, inherently limiting the capacity that can be delivered by lithium with each cycle.^{44,45}

The success of IL additives spurred interest in novel IL scaffolds that would overcome such observed limitations while mimicking the preferred method of Li^+ conduction through the polymer chains.^{2,52} Prior research into sulfur based IL systems has demonstrated promising electrochemical stability and conductivity values.^{41,49} Motivated by this, our previous work centered on the development of triethyl sulfonium TFSI.⁷⁰ A flexible and mechanically stable electrolyte was characterized. The PEO based solid polymer electrolyte was able to demonstrate ionic conductivity of 0.120 mS/cm at room temperature and ~ 0.7 mS/cm at 40 °C (molar ratio of 20 PEO:1 LiTFSI: 1 IL). This elevated conductivity of the electrolyte was accompanied by reversible stability against both lithium and at voltages exceeding 4.5 V vs. Li/Li^+ .

Lingering concerns about the reactivity of TFSI with aluminum motivated our research to investigate different anions which possess similar electrochemical properties without reactivity to aluminum.⁶ Among all possible anions, those for lithium batteries are chosen for their ability to dissociate completely from the lithium ions allowing for single ion movement. There are several salts that meet this basic criterion, although the prevailing commercial choice has been LiPF_6 due to its combination of stability and conductivity. Relative to a TFSI based system, the PF_6 anion has benefits such as its high conductivity and price and drawbacks such as its moisture and temperature stability.^{6,58}

Numerous other anions exist that exhibit good lithium conductivity in solid polymer electrolytes including bis(perfluoroethyl sulfonyl) imide (BETI) and bis(oxalato) borate (BOB) and ClO_4 .⁵⁹

Since no single anion possesses all the ideal characteristics related to conductivity and stability, we replaced all of the anions in the system with both experimental and commercial anions using the triethyl sulfonium cation as our starting point. This fundamental change in the chemistry of the electrolyte was investigated with the intention of demonstrating an improvement over our previous sulfur based IL polymer electrolyte system, while also adding stability to aluminum current collectors. Herein, we report on the electrochemical characterization of the different formulations of our solid polymer electrolyte systems.

2. Experimental

a. Materials

LiTFSI ($\text{LiN}(\text{SO}_2\text{CF}_3)_2$), lithium foil, AgNO_3 , HClO_4 (70%) HPF_6 (65%), LiTFSI, LiClO_4 , and LiPF_6 were used as received from Aldrich. Poly(ethylene oxide) (M_w 300k), triethyl sulfonium iodide (97%) (S_2I), boric acid (99%), and oxalic acid (10% aqueous solution) were used as received from Alfa-Aesar. LiBOB was used as received from Chemetall. An aqueous solution of LiBETI was prepared with HBETI (Synquest Laboratories) and LiOH.

b. RTIL preparation

S_2OH : Procedure adapted from Golding et al.⁷¹ Equimolar amounts of AgNO_3 (2010 mg, 1.83 mmol) and NaOH (473.1 mg, 11.83 mmol) were mixed in 10 mL of water to form

AgOH. The resulting solution was sonicated and vacuum filtered to obtain AgOH as a brown solid. Quantitative yield was assumed and the silver hydroxide was combined with S₂I (2000mg, 7.89 mmol) in 10 ml of water and allowed to stir for 1h. The solution was then vacuum filtered and dried to produce an orange-brown liquid.

S₂BOB: Procedure adapted from Vijayaraghavan and MacFarlane⁷² A flask was charged with one equivalent each of S₂OH (7.89 mmol, 1074 mg) and of boric acid (487.8 mg, 7.89 mmol) and two equivalents of oxalic acid (1420 mg, 15.78 mmol) and allowed to stir under vacuum for 2h until dry. 80.9% of a white solid was yielded. ¹H: 3.317 (q, *J*= 7.4 Hz, 6H), 1.444 (t, *J*= 7.4 Hz, 9H). ¹³C: 33.80, 9.02. ESI⁺: 119.0999, ESI⁻: 186.9554.

S₂PF₆: S₂OH (1074 mg, 7.89 mmol) was added to aqueous solution of HPF₆ (1346 mg, 9.22 mmol, 15% stoichiometric excess) and stirred under vacuum for 2h. The product was then filtered and washed with acetone. A clear liquid was isolated after drying under vacuum for 2h at 20.2% yield. ¹H: 3.337 (q, *J*= 7.4 Hz, 6H), 1.467 (t, *J*= 7.4 Hz, 9H). ¹³C: 33.75, 9.06. ESI⁺: 119.0910, ESI⁻: 144.9635.

S₂ClO₄: S₂OH (1074 mg, 7.89 mmol) was added to an equimolar aqueous solution of HClO₄ (1132 mg, 7.89 mmol) and stirred under vacuum for 2h. The mixture was allowed to stir for 24h while drying under high vacuum. 82.8% S₂ClO₄ was yielded as a copper colored solid. ¹H: 3.35 (q, *J*= 8 Hz, 6H), 1.47 (t, *J*= 8 Hz, 9H), ¹³C: 33.80, 9.09. ESI⁺: 119.0897, ESI⁻: 98.9519, 100.94890 (large splitting due to ³⁵Cl and ³⁷Cl isotopes).

S₂BETI and S₂TFSI Prepared as per our previous publication⁷⁰ 86.5% was yielded for S₂BETI and 54.0% was yielded for S₂TFSI, both as yellow liquids. S₂BETI: ¹H: 3.43 (q, *J*= 8 Hz, 6H), 1.56 (t, *J*= 8 Hz, 9H), ¹³C: 33.77, 9.03, ESI⁺: 91.0637, 119.0990 ESI⁻:

379.91528. S₂TFSI: ¹H: 3.372 (q, *J*= 7.6 Hz, 6H), 1.516 (t, *J*= 7.4 Hz, 9H), ¹³C: 33.78, 9.06, ESI⁺: 119.0975, ESI⁻: 279.9238.

c. Electrolyte Preparation

All electrolytes were assembled in the molar ratio of 20 PEO : 1 LiX: 1: S₂X, where X is the anion of interest. Low molar ratios are ideal for synthesis of solid thin-film electrolytes; greater concentrations of IL result in poor film properties. The weight percent of IL ranges from 18% to 28% depending on the anion. The electrolyte films of different composition were solution cast from tetrahydrofuran (TFSI, BETI, and BOB), dimethylformamide (PF₆) or acetonitrile (ClO₄) onto Bytac molds in an MBRAUN Labmaster 100 argon glove box. The resultant films were dried for several days at 60 °C, before being placed into CR2032 coin cell enclosures for electrolyte testing.

d. Electrolyte Characterization

Differential scanning calorimetry (DSC) measurements were performed on a TA Instruments Q100 differential scanning calorimeter. Samples were hermetically sealed in Al pans under Ar prior to measurements, which were run using a heat/cool/heat method to erase thermal history at a heating rate of 10 °C/min and a cooling rate of 5 °C/min from -50 °C to 120 °C.

Conductivity measurements for electrolytes were performed in a SS/electrolyte/SS coin cell set up on a Solartron 1287A/1255B platform over the frequency range 1 MHz to 1 Hz. Testing parameters were controlled by the associated CorrWare and ZPlot software, while data analysis was performed using CorrView, ZView and Origins 8. All temperature testing was done in a RevSci IncuFridge with

± 0.5 °C temperature accuracy allowing 45 mins to equilibrate at each temperature. Prior to testing constructed cells were annealed for 3 hrs. at 50 °C.

Transference measurements were performed in a Li/electrolyte/Li coin cell set on the Solartron setup. A potential of 10 mV was applied across each cell until steady state current reached. All tests were run at 40 °C except for ClO₄, which was run at 50 °C after allowing for 1 hour of temperature equilibration. Impedance spectroscopy was conducted before and after steady state to determine resistance of the electrolyte.

Linear sweep voltammetry was performed on Li/electrolyte/SS cells. Cells were stepped at 1 mV/sec from 2.5 V vs. Li/Li⁺ reference to 6.5 V vs. Li/Li⁺ reference, and breakdown was determined by the first change in derivative.

Overvoltage experiments were performed on the Solartron set-up to determine the interfacial stability and reversibility of the electrolyte material. The electrolyte was sandwiched between two lithium electrodes. A current density of 0.1 mA/cm² was applied to the film and was reversed every hour. 25 cycles, each consisting of 1 hr. positive current and 1 hr. negative, were applied to the cell at 55 °C. All cells were annealed for 1 hour at 55 °C prior to testing. Impedance spectroscopy was periodically conducted to monitor development of resistances at the interface during the galvanostatic cycling.

3. Results and Discussion

The effect of the anion on the electrochemical properties of polymer electrolytes has been a source of ongoing research. With this in mind, it was of tantamount importance to characterize the effect of the anion on the observed electrolyte properties. As a comparison to previous work TFSI was used as the baseline to compare ClO₄, BOB,

BETI and PF₆. Given the novel nature of some of the triethyl sulfonium based ILs, DSC was first performed to characterize the thermal properties. Elevated temperatures are crucial for promoting conductivity to threshold values in solid polymer electrolytes. Additionally, the physical state of the IL is important as not all of the anions are liquids at room temperature. The DSC thermograms are also seen to closely mirror the ionic conductivity values determined from AC impedance in the full electrolyte system.

Differential Scanning Calorimetry of Ionic Liquid

The studied pure ILs underwent numerous transitions (Table V-1). The largest peak was taken to be either the melting or freezing point of the neat IL. All other transitions tabulated by whether they occurred during the heating or cooling cycle because of the large hysteresis. S₂TFSI and S₂BETI had the lowest transition temperatures and are both liquids at room temperature. TFSI and BETI are both imide based architectures, which have been promising anions for ionic liquid development. S₂BOB was a low melting point solid; at the slightly elevated temperatures of interest, it is a liquid. It was also the only ionic liquid to undergo a 2nd order phase change. The absence of its freezing point is believed to be the result of the slow kinetics of crystallization. S₂ClO₄ is a solid up to ~100 °C, barely allowing it to be considered an ionic liquid. This ability of S₂ClO₄ to crystallize is strongly believed to be the source of its low ionic conductivity in the solid polymer electrolyte. S₂PF₆ was also isolated as a solid, but with a significantly lower melting point. All of the pure ILs tested had observable hysteresis between the observed transition in the heating and cooling cycle.

Table V-1 DSC peaks of the neat ionic liquids

Anion	First Order Transitions				T _g	
	Freezing	Melting	Cooling	Heating		
BOB		47.19		62.24	-47.41	-34.2
ClO ₄	98.72	104.14	69.90, 49.56	71.26, 79.62		
PF ₆	34.1	69.75	2.16, -6.26			
BETI	-23.55	13.06				
TFSI	-30.79	-34.29		-11.83, -7.18		

Ionic Conductivity

The ionic conductivity of the solid polymer electrolytes during cooling can be seen in Figure V-1. Each anion demonstrates varying ionic conductivity over the measured temperature range. The lower limit of conductivity is approximately physiological temperature for all anions except for ClO₄ which drops from 0.21 mS/cm at 55 °C to 0.017 mS/cm at 45 °C. At 45 °C all five of the solid polymer electrolytes have sufficient conductivity to be functional in a lithium battery system. At 45 °C the ionic conductivity of BOB is 0.229 mS/cm, BETI 0.415 mS/cm, PF₆ 0.210 mS/cm, ClO₄ 0.017 mS/cm, TFSI 0.828 mS/cm. At this slightly elevated temperature all of the anion systems, except ClO₄, show ionic conductivity >0.1 mS/cm, which is necessary for higher current applications. When values drop below this threshold, the polymer electrolytes have been shown ineffective at conducting lithium ions.

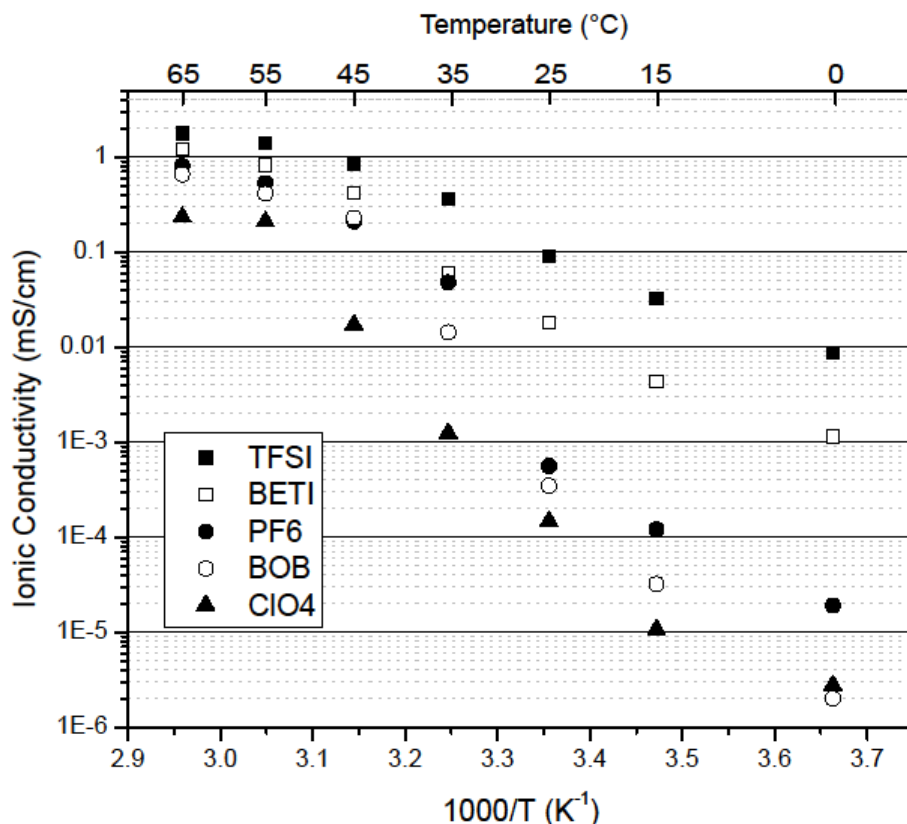


Figure V-1 Ionic conductivity of the solid polymer electrolytes determined by AC impedance spectroscopy upon cooling of the SS/electrolyte/SS cells from 65 °C.

Differential Scanning Calorimetry of the Electrolyte

The conductivity is intimately related to the transition temperature observed during DSC (Table V-2 Figure V-2). The freezing and melting points are tabulated separately because of the large thermal hysteresis observed in the polymer electrolytes. The transition from semicrystalline to amorphous, allows for the PEO chains to move past each other without the inhibition of long range ordering. This ultimately allows PEO to reversibly coordinate to ions, permitting their conduction down electrical and concentration gradients. This phase transition in the electrolyte manifests itself as an endothermic peak. Comparing the relative transition temperatures of all the anions shows

a strong correlation with the relative ordering of each anion's conductivity of the polymer electrolyte. TFSI had the lowest transition at 13.53 °C, and over the studied temperature range maintained the highest conductivity values. BETI had a similar transition temperature of 15.98 °C, and possessed the second highest ionic conductivity values. The DSC values of the other three anions, suggest that BOB should be third, followed by ClO₄, with PF₆ lowest. The conductivity values did not follow this trend as ClO₄ generally demonstrated the lowest conductivity. Between BOB and PF₆, the latter generally maintained a higher conductivity despite having a higher transition temperature. This disagreement with the relationship between DSC and conductivity is hypothesized to be the result of the unfavorable movement of ions in the IL itself. Elevated melting points limit ionic mobility because of the association of microscopic crystalline domains, which ultimately lowers the observed ionic conductivity values. It is also of note that ionic conductivity values are measured not the lithium conductivity. The difference between these numbers could falsely indicate movement of the anion and not the lithium cation.

Table V-2 DSC peaks of the electrolyte

Anion	Cooling	Heating
BOB	24.66	44.18
ClO ₄	30.63	42.9
PF ₆	35.28	48.01
BETI	15.98	39.97
TFSI	13.53	41.87

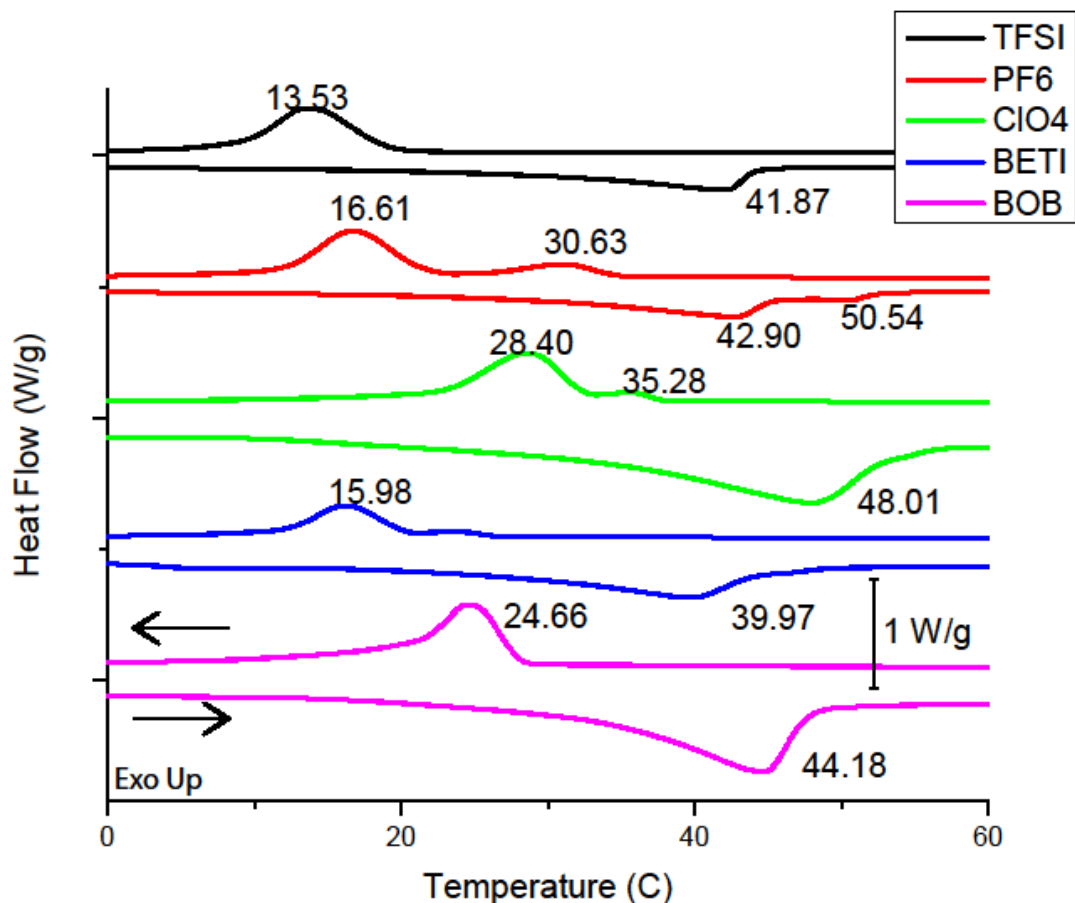


Figure V-2 Selected portion of thermograms from the electrolyte based on the indicated anion. The formulation is the molar ratio 20 PEO: 1 LiX : 1 S₂X, where X is indicated in the legend. The heating rate was 10 °C/min and cooling rate was 5 °C/min in a heat/cool/heat format with endpoints of -50 °C and 120 °C.

All of the trend lines for ionic conductivity show a discontinuity on either side of the transition temperature observed by DSC. At high temperature the gain from increased temperature is minimal. At low temperatures the gain in conductivity over temperature is significant. This region of steeper slopes however, has not shown enough conductivity to be a functional lithium electrolyte. Ordinal ranking of the ionic

conductivities of the anions shows that TFSI and BETI have the best ionic conductivity over the observed temperature range, while ClO₄ possessed the worst ionic conductivity.

Transference

The other important element of conductivity is the determination of which ionic species are the charge carriers. To accomplish this we followed the procedure outlined by Evans et al.⁶⁰, whereby a small voltage is applied until steady state current is attained. Equation 2 is used to calculate the lithium transference number (T_{Li+}), with the resistances in the equation measured by impedance spectroscopy. This value between 0 and 1 is a measure of what fraction of the total current is due to the movement of a given species. T_{Li+} vary widely depending on the electrolyte as well as the testing method but are typically below 0.5.⁷³ Polymer systems range from ~0.1 to 0.5 while ionic liquid systems with a larger number of charged species typically range from ~0.1 to 0.3.^{35,44} The T_{Li+} values for the different anions can be seen in Figure V-3.

$$T_{Li+} = \frac{I_e(\Delta V - I_o R_o)}{I_o(\Delta V - I_e R_e)} \quad (2)$$

The T_{Li+} values for the studied solid polymer electrolytes range from ~0.2 to 0.3. These numbers are on the high end of the range for IL based electrolyte systems. And although the transference numbers are below average for polymer systems with only lithium salts, the researched polymer/IL/Li salt hybrid electrolytes demonstrate significantly higher conductivity. BETI demonstrates the highest T_{Li+} at 0.31. The lowest values are for ClO₄ and PF₆, which are 0.21 and 0.23, respectively. Ranging between these two values were the measured T_{Li+} of BOB and BETI which are 0.29 and

0.27 respectively. It is of note with ClO₄ that due to low ionic conductivity its transference measurements were conducted at 50 °C, while all other anions were run at 40 °C. This can be easily explained from Figure V-3 where the conductivity of ClO₄ based systems lags significantly behind other anion systems at a given temperature.

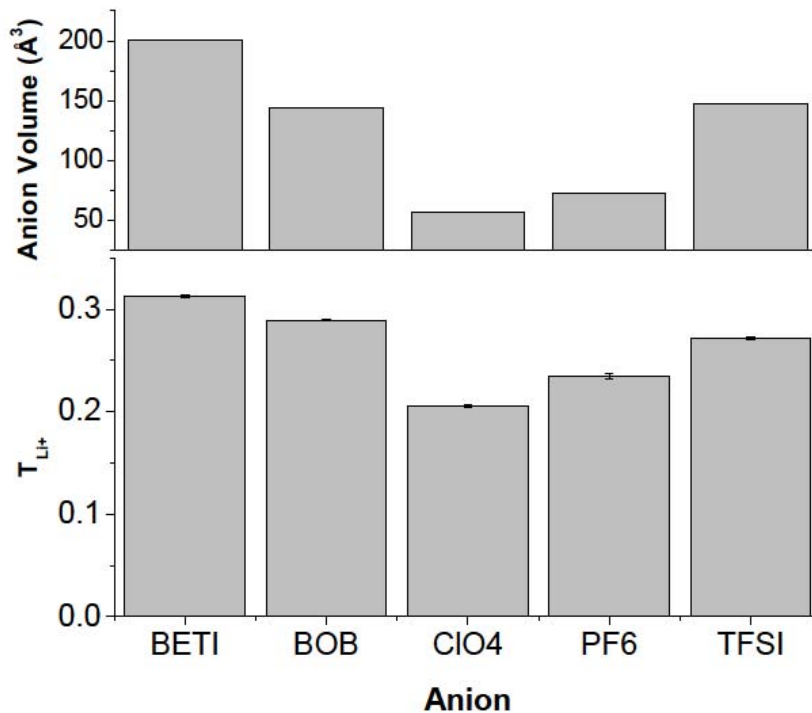


Figure V-3 Lithium transference number of the solid polymer electrolytes. T_{Li+} was determined using the potentiostatic measurement conducted at 40 °C for all anions except ClO₄, which was run at 50 °C. Molar volume from Table V-3 is overlaid to show relationship between volume and T_{Li+}.

Given the interest in having electrolytes which are single Li⁺ conductor, it was of great interest to understand the differences between the anions. Table V-3, which contains the molar volumes of the anions, shows that a trend is readily apparent.⁷⁴ Larger volumes correspond to larger T_{Li+}. Categorically separating the volumes into small (~60-

70 Å³) medium (~145 Å³) and large (~200 Å³) anions matches the observed T_{Li+} (Figure V-3). This relationship between size and ion mobility can be explained in a straightforward manner by the ability of small ions to move with greater ease through the dense polymer matrix. Large molar volumes require more concerted movements of the polymer chains to allow movement of the ions. While this thinking suggests it would be possible to generate a single lithium ion conductor by increasing the size of the counterion, it obfuscates the duality of conductivity in polymer systems. By increasing the volume of the counterion, ultimately the local environment around Li⁺ is significantly altered, such that all ion movement is limited, resulting in a carefully balanced tradeoff between T_{Li+} and conductivity.⁷⁵

Table V-3 Volume of anion as determined by molinspiration program.⁷⁴

Anion	Volume Å ³
BOB	143.665
ClO ₄	56.546
PF ₆	72.615
BETI	200.377
TFSI	147.645

Cathodic Stability

The stability of the electrolyte to the cathode, herein referred to as cathodic stability, is critical for the development of high voltage cells. Some olivine and spinel type cathode systems have voltage plateaus well above 4 V vs. Li/Li⁺, which leads to premature decay with carbonate based electrolyte systems. Solid polymer electrolytes with ILs generally are able to meet these higher stability windows with cathodic stabilities exceeding 5 V vs. Li/Li⁺.⁵¹ The incorporation of ILs is expected to have little impact upon this value, as sulfur based ILs have demonstrated wide ESWs.

To determine the limit for cathodic stability linear sweep voltammetry was undertaken from a voltage well within operational range (2.5 V vs. Li/Li⁺) to one exceeding operational stability (6.5 V vs. Li/Li⁺). Upon the first large change in derivative of current, breakdown of the electrolyte was assumed such that the electrolyte would no longer be able to electrochemically function as a lithium conductor. While other counter electrodes besides stainless steel were investigated they have been unable to yield satisfactory results. However half-cell assemblies with LiFePO₄ and LiCoO₂ have shown stability over cycling.⁷⁶ Thus it is believed that the results are reflective of the breakdown of the electrolyte under operating conditions. Figure V-4, shows the measured breakdown voltage for each electrolyte formulation. All the solid polymer electrolytes displayed sufficient stability to be useful in the currently commercialized cathodes, LiFePO₄ and LiCoO₂. With all cathodes it is necessary to provide a buffer region above the fully charged potential ensuring that all energy is stored reversibly in the electrode. The next generation of high voltage cathodes ranges up to 5 V vs. Li/Li⁺, and thus requires cathodic stability of the electrolyte to exceed this value. The ClO₄ based system demonstrated stability up to 5.37 V, which is promising for future work on high power batteries. The imide based chemistries, BETI and TFSI, demonstrated stabilities of 5.00 and 4.97 V respectively. This figure of merit is promising for most experimental cathode systems, but is tempered by concern for stability to aluminum which is used as the cathode's current collector. BOB and PF₆, which have cathodic stabilities of 4.56 and 4.63 respectively, only offer promise for electrodes that have been already commercialized and other lower voltage experimental cathodes. While LiPF₆ is investigated in high voltage systems, the observed failure is believed to be the result of

testing at elevated temperature, which is necessary for lithium conduction. Given the high stability of several of these anion polymer electrolyte systems there are a number of possibilities to develop high voltage lithium battery systems.

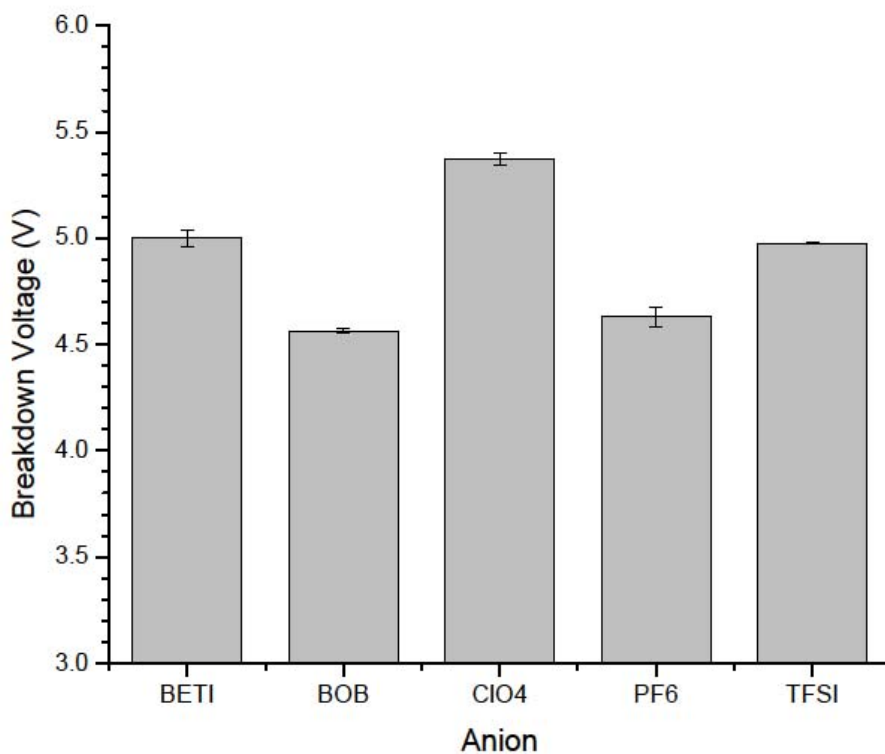


Figure V-4 Cathodic stability of the solid polymer electrolytes. Breakdown was determined by first change in the derivative of the potential upon sweeping a SS/electrolyte/Li cell from 2.5 to 6.5 V vs. Li/Li⁺. Cells were run at 25 °C.

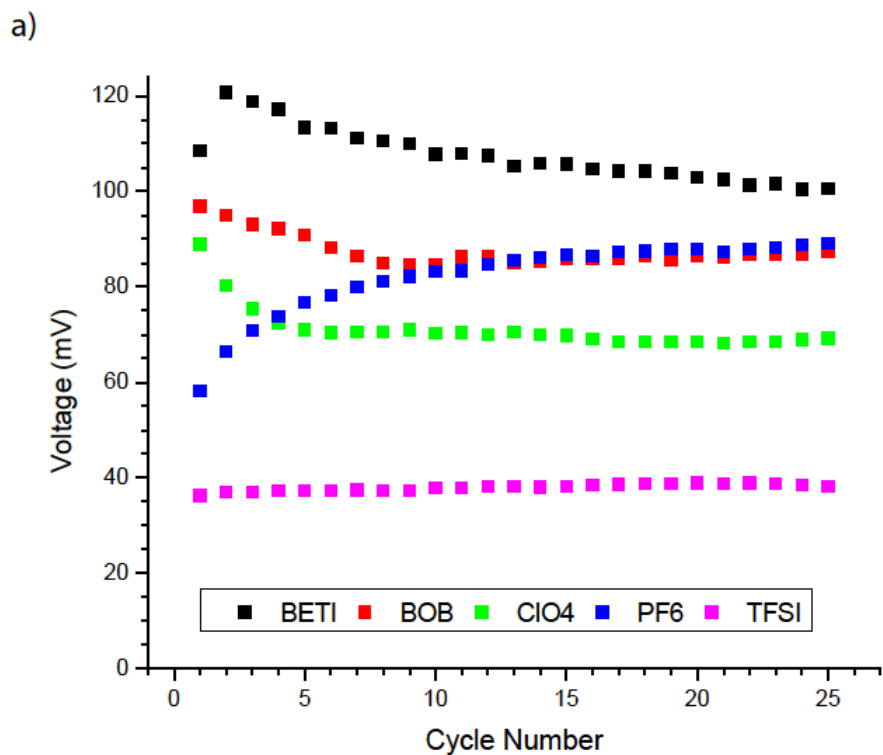
Overvoltage

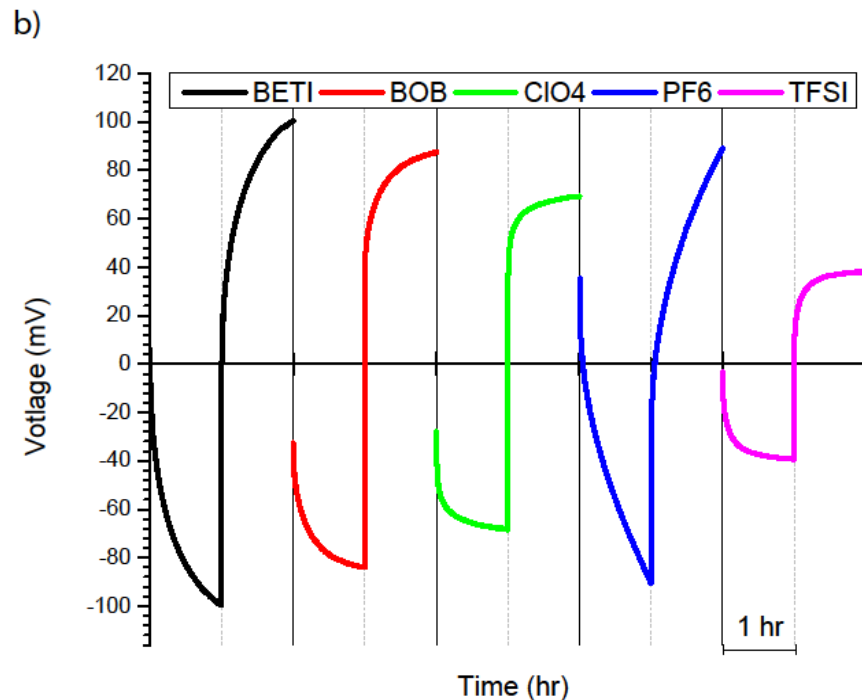
Overvoltage studies measure a cell's stability to lithium and the energy required to move a lithium ion from the bulk electrolyte onto the surface of an electrode. Over extended cycling the energy expended in moving lithium ions should be minimal and

constant. To confirm this aggressive cycling was undertaken to characterize the effect of the different anions on the electrolyte. Testing was conducted at 55 °C to allow for comparison between all of the anions; several were more conductive at lower temperatures.

In Figure V-5a, the end voltage over 25 cycles can be seen for each anion. The most salient observation is the low end voltage and its constant nature for the TFSI anion relative to the other anions. Low absolute overvoltages are critical for the electrolyte as it is a measure of the energy lost in the cell at the interface, which ultimately detracts from the voltage a single cell is able to deliver. This indicates the ideal ability of the TFSI based electrolyte to transport lithium ions effectively through the bulk and across a stable interface. BETI, BOB and ClO₄ all demonstrated decreasing end voltage values over the cycling. This is believed to be the result of the slow kinetics of the solid polymer electrolyte in chain rearrangement to permit bulk and interfacial conductivity. After the initial decline BOB and ClO₄ reach a plateau, this plateau lasts for the duration of the test. Lastly, with PF₆ a sizable increase in the end voltage values can be seen. Given the elevated temperature at which this cycling is conducted it is believed that the PF₆ anion is decaying. Evaluating the end voltages over 25 cycles for the anions and their long term stability, a ranking can be established which indicates that TFSI is the best anion tested, while PF₆ or BETI is the worst.

Figure V-5 Value of overpotential at the end of each 2 h cycle for symmetrical Li/electrolyte/Li cells. b. Overpotential as a function of time during the 25th cycle for the indicated ionic liquid. Each cycle was 1 h negative current followed by 1 h positive current both at 0.1 mA/cm². Testing was conducted at 55 °C.



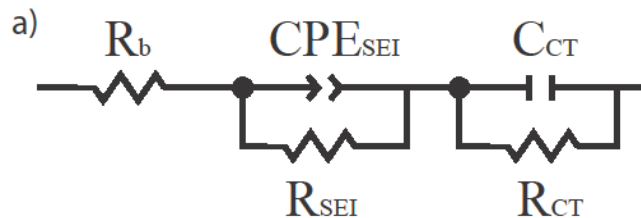


In evaluating the overvoltage it is important that the data for a given cycle demonstrate a plateau, which indicates that no additional resistance is accumulating in the interface as lithium is plated after formation of the concentration gradient. The voltage profile for the 25th cycle of each electrolyte tested at 55 °C is shown in Figure V-5b. To measure the stability of the plateau region over each hour segment the time at which the voltage reached 90% of the end overpotential was recorded. From the overvoltage test it appears that some electrolytes more accurately fit the desired results. BETI and PF₆, which do not demonstrate a stable plateau region, reached the 90% threshold at 64.7% and 85.4% of full time respectively. Conversely, ClO₄ which demonstrated the most stable plateau among tested anions reached the 90% threshold at 21.7% of full time. TFSI which demonstrated the lowest absolute potential reached the 90% threshold at 30.3% of full time. BOB the 3rd most stable reached the 90% threshold at 39.3% of full

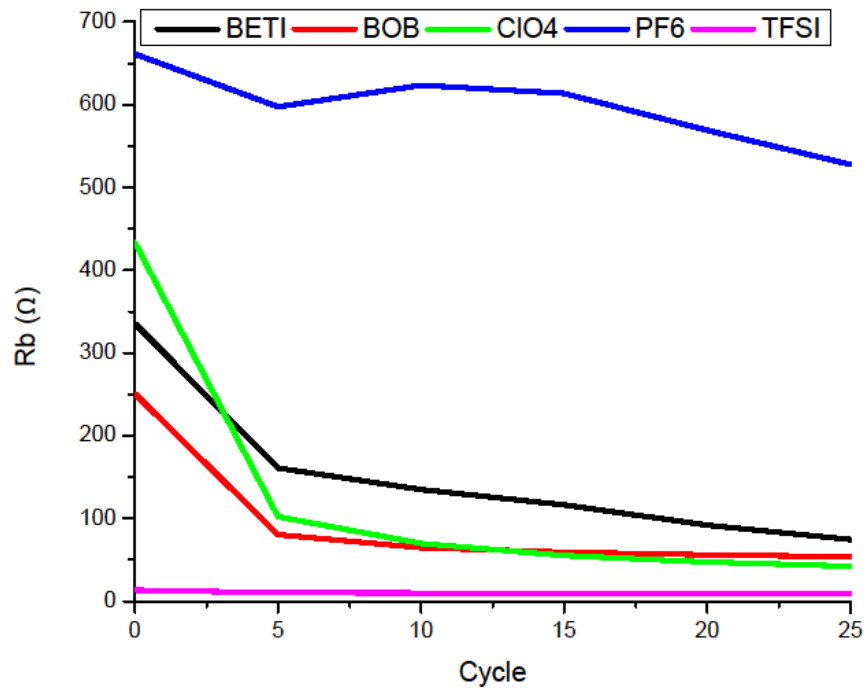
time. Taken in conjunction with the change in voltage over time, TFSI demonstrates the most ideal overvoltage properties of all tested anions in the solid polymer electrolyte.

Interspersed every 5 cycles during the overvoltage cycling, impedance spectroscopy was conducted to monitor the resistance of each electrolyte composition. To model the electrolyte and the corresponding interface with the lithium electrode, a model circuit consisting of three elements was used. The three components: the bulk electrolyte (R_b), the solid-electrolyte interphase (R_{SEI} and CPE_{SEI}), and the charge transfer (R_{CT} and C_{CT}) can be seen in Figure V-6a. The model circuit, while a simplification of the complex electrochemical movement occurring in the electrolyte, fits closely to the Nyquist plots.

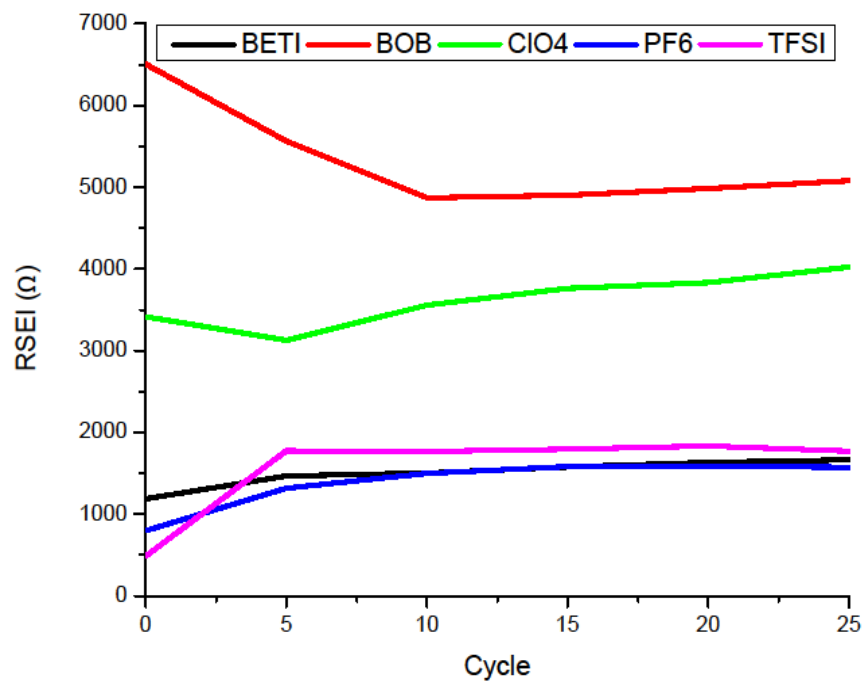
Figure V-6 a. Equivalent circuit used to model the electrolyte during overvoltage cycling b bulk resistance of each anion formulation during the overvoltage cycling c. the resistance of the SEI film d. the resistance due to charge transfer. To highlight the low resistance of the charge transfer there is a gap in the y-axis values. The electrolyte tested had a thickness of 0.0254 cm and a cross sectional area of 0.217 cm².

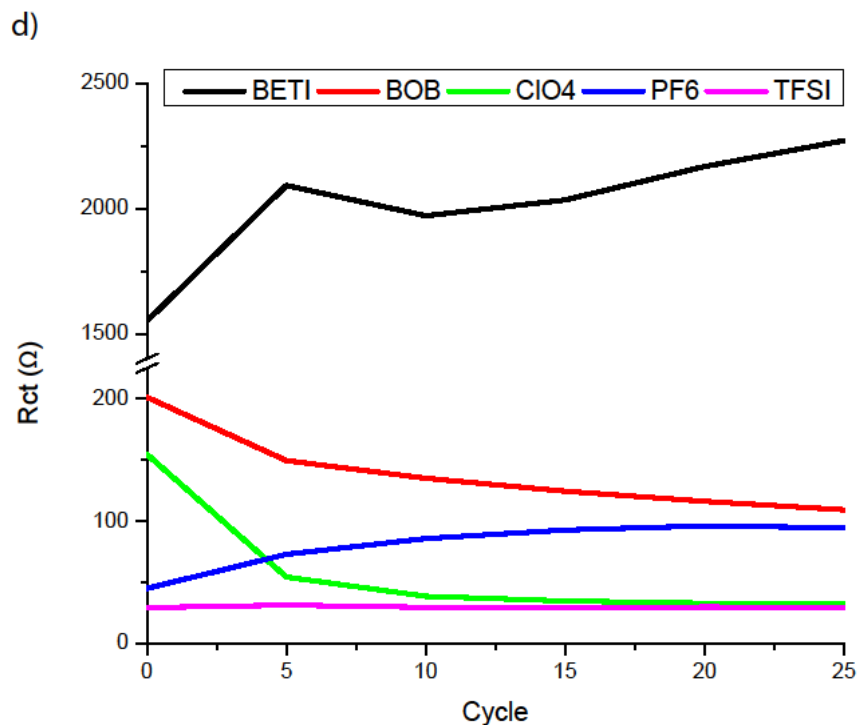


b)



c)





The change in resistance over the cycling is plotted in Figures V-6b-d (b- electrolyte resistance, c- resistance of the SEI, d- charge transfer resistance). The bulk resistance of the electrolyte is generally the lowest value for a given anion. Over the duration of the testing all anion chemistries showed a decrease in R_b . With the systems this initial decrease is believed to be related to the relaxation of the polymer chains, which facilitates ion movement. Only for the PF_6 system did this decrease appear to extend beyond the 1st time point. If as proposed at higher temperatures PF_6 is degrading, there would in fact be additional charge carriers. If correct, this would indicate that a decreasing portion of the ionic conductivity for PF_6 is Li^+ .

The resistance of the SEI develops quickly during the first few cycles and then remains constant for BETI, PF_6 and TFSI. ClO_4 shows a constant increase in resistance over the cycling, which is not exhibited by the end voltages which remain constant over

the cycling. The constant increase in the SEI against lithium electrodes points to instability in the interface; this however must be related to a non-essential component to lithium transport. BOB, which has the most resistive SEI, demonstrates an initial drop in the interface followed by a gradual increase over cycling. Given that BOB is known to form resistive interfaces⁶, its relative position is unsurprising. For the constant resistances the formation of a stable SEI bodes well for their usage in lithium battery systems.

The R_{ct} of the electrolyte systems are generally fairly small relative to the R_{SEI} . For all anion systems except BETI the values are $< 250 \Omega$ and remain largely constant over the testing. BETI however, had markedly high R_{ct} , which is increasing over the cycling. As no other negative charge carriers are present such a large difference between BETI and the other anions can be easily attributed to the difficulty in arranging such a bulky anion at the interface. This difference is especially clear when comparing the two imide based anions; the R_{SEI} appears similar between the two systems, while the R_{ct} are more than an order of magnitude apart. On the whole the TFSI-based solid electrolyte system demonstrated the lowest resistances for any system. All except for BETI were dominated by the R_{SEI} , which points towards needing further work developing and characterizing the interface.

4. Conclusions

The development of solid polymer electrolytes has been hindered by their ability to demonstrate conductivity at close to ambient temperatures without compromising the main benefits of a polymer-based system. Our previous work demonstrated the real possibility of using triethyl sulfonium TFSI as an additive to accomplish this goal.

Concern over the stability of TFSI led to the pursuit of alternative electrolyte formulations that replaced the TFSI anion. In substituting the TFSI anions there was a sizable decrease in ionic conductivity, which became less significant at higher temperatures. All systems, ClO_4 excepted, cross the threshold value of 0.1 mS/cm at $\sim 40^\circ\text{C}$, from lowest to highest temperature: TFSI, BETI, PF_6 and BOB. ClO_4 meets this conductivity threshold above 50°C . Lithium transference for these solid polymer systems ranged from 0.21 to 0.31, and is directly correlated to the size of the anion. The largest anion BETI demonstrated the highest T_{Li^+} while the smallest anions of ClO_4 and PF_6 demonstrated the lowest T_{Li^+} . Solid polymer electrolyte systems generally demonstrate wide electrochemical stability windows, which would ultimately be useful for the next generation of high voltage cathode materials. The tested anion formulations all demonstrated cathodic stability sufficient to be used with the commercial cathodes of LiCoO_2 and LiFePO_4 . BETI, TFSI and ClO_4 demonstrated sufficient stability to be useful in 5 V cathode systems, which would allow for more power and voltage from each lithium battery cell. Anodic stability and low lithium plating voltages was confirmed for the varied anion system. BOB, ClO_4 and TFSI have demonstrated reasonable voltages that are stable over cycling. The voltage that is observed for lithium plating is strongly dependent upon the formation of the SEI of the electrolyte. Herein a series of hybrid solid polymer electrolytes containing sulfur based ILs was characterized that demonstrate potential use for safer high power biomedical applications.

VI. Ionic Liquids in Block Copolymer Electrolytes

1. Introduction

Electrolytes in lithium batteries have become a topic of great interest as scientists and engineers recognize that the electrolyte in lithium batteries limits many of the measured figures of merit in a battery.^{6,8,9} Electrolytes impact performance largely through the stability window, which limits cathode choice and the necessity of solid-electrolyte interphase (SEI) formation that affects the lifetime of a cell. Additionally, the safety issues of the battery are largely a result of the combustible nature of the liquid carbonates. To overcome the safety problems of electrolytes consisting of small volatile organic molecules, there has been much interest in solid polymer electrolytes (SPE). The limiting factor to SPE has been conductivity; many proposed solutions have merely resorted to combining the polymer with the traditional liquid carbonates.

Ionic liquids (ILs) have been used successfully to overcome the limited conductivity of polymer matrices because they possess ideal electrochemical properties namely high conductivity, electrochemical stability, and no volatility. When incorporated into poly(ethylene oxide) (PEO) based polymer matrices they have been shown to elevate the ionic conductivity of the electrolyte several orders of magnitude.^{33,51,66} Shin et al.⁵¹ have shown that adding 1-butyl-1-methyl pyrrolidinium bis(trifluoromethane sulfonyl) imide (TFSI) to PEO leads to a marked increase in ionic conductivity of 2 orders of magnitude for the highest tested concentrations (molar ratio of 20 PEO: 1 LiTFSI: 3.24 IL). This conductivity increase though is accompanied by a decrease in the lithium transference number (T_{Li^+} , the fraction of total current observed

due to movement of lithium ions). A low T_{Li^+} inherently limits the capacity that can be delivered by lithium within each cycle.^{44,45}

The success of IL additives spurred interest in novel sulfur based IL scaffolds that would overcome observed limitations while mimicking the preferred method of Li^+ conduction through the polymer chains.^{2,41,52} Our previous work demonstrated the possibility of using triethylsulfonium TFSI as an additive to accomplish this goal.⁷⁰ A flexible and mechanically stable electrolyte was characterized, with ionic conductivity of 0.120 mS/cm at 25 °C and ~0.70 mS/cm at 40 °C (molar ratio of 20 PEO:1 LiTFSI: 1 IL). This elevated conductivity of the electrolyte was accompanied by reversible stability against both lithium and at voltages exceeding 4.5 V vs. Li/Li^+ .

Lingering concerns about the reactivity of TFSI with aluminum motivated our research to investigate different anions, which possess similar electrochemical properties without reactivity to aluminum.⁶ In substituting the TFSI anions there was a sizable decrease in ionic conductivity, which became less significant at higher temperatures. The tested anion formulations all demonstrated electrochemical stability sufficient for use with commercial electrodes. Among the tested anions TFSI had the best properties, and was closely followed by the bisoxalatoborate (BOB) and ClO_4 based systems. However, the measured lithium transference was inferior to salt in polymer electrolytes and ranged from 0.21 to 0.31.

In previous work we demonstrated the development of a lithiated block copolymer electrolyte (BCP).^{21,22} The system consisted of a diblock of PEO and partially lithiated poly(methacrylic acid) blocks which demonstrated extraordinarily high lithium transference numbers. Most liquid electrolytes have T_{Li^+} values ranging from 0.3-0.5;

this BCP system had T_{Li^+} values ranging from 0.7-0.9.² High T_{Li^+} values are ideal because it means that there is less parasitic current and less build-up of charge at the interface. Given its wide electrochemical stability this block copolymer system was only limited by its low ionic conductivity values.

Combining the high conductivity and low transference values for the PEO-IL system and the low conductivity and high transference values for the BCP system into one hybrid electrolyte system was of great interest. This novel system should it contain the ideal properties of each system would be a successful SPE for use in lithium batteries. Herein, we report on the thermal, mechanical and electrochemical properties of a novel hybrid block copolymer-ionic liquid solid polymer electrolyte.

2. Experimental

a. Materials

Lithium foil and $AgNO_3$ were used as received from Aldrich. Triethyl sulfonium iodide (97%) (S_2I), boric acid (99%), and oxalic acid (10% aqueous solution) were used as received from Alfa-Aesar. LiBOB was used as received from Chemetall. Poly(ethylene oxide-*b*-methacrylic acid) (27k-*b*-3k), which is synthesized by hydrolyzing the *t*-butyl acrylate block of a poly(ethylene oxide-*b*-butylacrylate) precursor, was used as received from Polymer Source.

b. Materials Synthesis

As per our previous work⁷⁷ S_2BOB was synthesized. 80.9% of a white solid was yielded. 1H : 3.317 (q, $J= 7.4$ Hz, 6H), 1.444 (t, $J= 7.4$ Hz, 9H). ^{13}C : 33.80, 9.02. ESI⁺: 119.0999, ESI: 186.9554.

The lithiated block copolymer was adapted from Ghosh et al.⁵⁷ The starting polymer is slightly different as we started with the acrylic acid as opposed to the methacrylate. This eliminated the need to hydrolyze the ester group, and allowed for complete lithiation of the minor block. Equimolar LiOH in water to methacrylic acid moiety was used. The polymer was then extensively dried to have quantitative yield.

c. Electrolyte Preparation

All electrolytes were assembled in the molar ratio of x PEO : y LiBOB : z S₂BOB (Figure VI-1), where the reported ratio of PEO refers to only the PEO block not the whole polymer. The electrolyte films of different composition were solution cast from dimethylformamide onto Bytac molds in an MBRAUN Labmaster 100 argon glove box. The resultant films were dried for several days at 80 °C, before being placed into CR2032 coin cell enclosures for electrolyte testing.

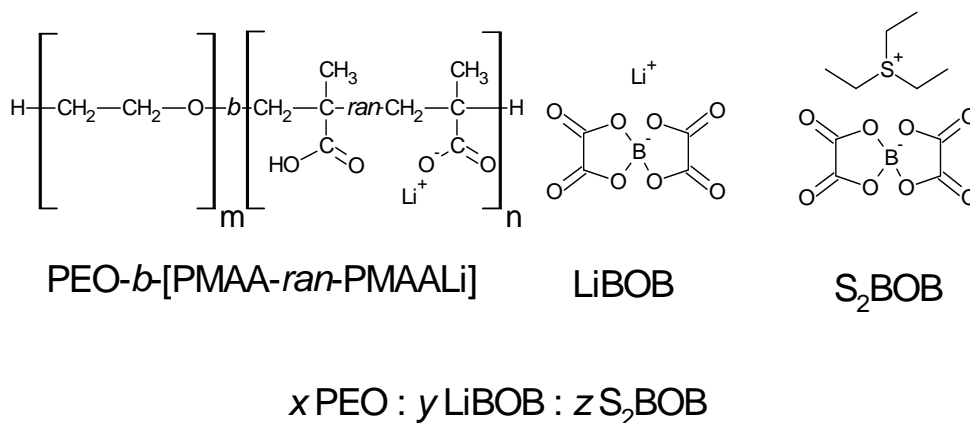


Figure VI-1 Compounds used to make the solid polymer electrolyte. All ratios cited in this paper are of the molar formula x PEO : y LiBOB : z S₂BOB.

d. Electrolyte Characterization

Differential scanning calorimetry (DSC) measurements were performed on a TA Instruments Q100 differential scanning calorimeter. Samples were hermetically sealed in Al pans under Ar prior to measurements, which were run using a heat/cool/heat method to erase thermal history at a heating rate of 10 °C min⁻¹ and a cooling rate of 5 °C min⁻¹ from -50 °C to 120 °C. Transmission electron microscopy was carried out on a JEM 2100 LaB₆ TEM with an accelerating voltage of 200 kV on as-cast films on a Cu grid.

Conductivity measurements for electrolytes were performed in a stainless steel (SS)/electrolyte/SS coin cell set up on a Solartron 1287A/1255B platform and scanned over the frequency range 1 MHz-1 Hz. Testing parameters were controlled by the associated CorrWare and ZPlot software, while data was processed using CorrView, ZView and Origins 8. All temperature testing was completed in a RevSci IncuFridge with ±0.5 °C temperature accuracy allowing 45 mins to equilibrate at each temperature. Prior to testing constructed cells were annealed for 3 hrs. at 70 °C.

Transference measurements were performed on a Li/electrolyte/Li coin cell set on the Solartron setup. A potential of 10 mV was applied across each cell until steady state current was reached. All tests were run at the indicated temperature after allowing for 1 hour of temperature equilibration. Impedance spectroscopy was conducted before and after steady state to determine resistance of the electrolyte. Using the change in resistance and current from initial to steady state we calculated the T_{Li^+} as in Evans et al.⁶⁰

Linear sweep voltammetry was performed on Li/electrolyte/Pt cells. Cells were stepped at 1 mV/sec from 2.5 V vs. Li/Li⁺ reference to 6.0 V vs. Li/Li⁺ reference, and breakdown was determined by the first change in derivative.

As per the work of Newman⁶², current interrupt tests were performed by first applying a current density of 0.1 mA/cm² for 15 minutes. The current to the cell was turned off and the potential of the cell was monitored as it returned to open circuit. The diffusion coefficient was then determined by fitting a line to this curve.

Overvoltage experiments were run on the Solartron set-up to determine the interfacial stability and reversibility of lithium deposition in the electrolyte material. The electrolyte was sandwiched between two lithium electrodes. A current density of 0.1 mA/cm² was applied to the film and was reversed every hour. 100 cycles, each consisting of 1 hr. positive current and 1 hr. negative, were applied to the cell at 40 °C. All cells were annealed for 1 hour at 40 °C prior to testing. Impedance spectroscopy was periodically conducted to monitor development of resistances during the galvanostatic cycling.

3. Results and Discussion

The BCP-IL electrolyte as cast is shown in Figure VI-2. It is a transparent film that is both strong and flexible. The current drop casting method results in film thickness on the order of hundreds of microns. Work with other desired anions, such as TFSI, did not result in films because their plasticizing effect was too great. TEM imaging of the BCP-IL system was then performed, and is shown in Figure VI-3. Previous work on a similar BCP without IL showed high contrast domains of lithium aggregates that precipitate out of the BCP matrix. The natural contrast of the lithium rich domains is due to the breakdown of BOB in the presence of moisture during transfer to the TEM, as per the work of Yang et al.⁷⁸ These spherical domains ranged in size from ~2-4 nm. This BCP-IL system showed lithium rich domains of the same size, but fewer in number

density. This is expected as in the previous non-IL containing BCP system the concentration of lithium salt was over six-fold times greater.²²



Figure VI-2 Visual image of the solid block copolymer showing the flexible transparent nature of the as-cast film. The film ratio is 20 PEO of the BCP : 1 LiBOB : 0.1 S₂BOB.

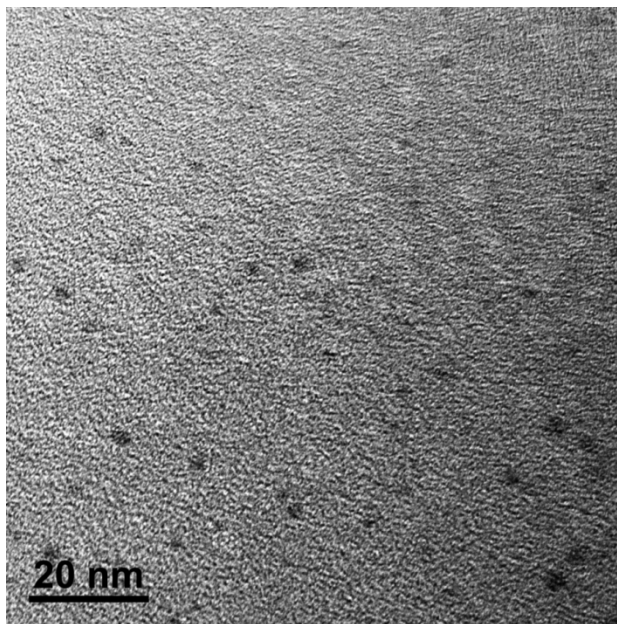


Figure VI-3 TEM of the as-cast 20 PEO : 1 LiBOB : 0.1 S₂BOB BCP-IL electrolyte. Dark regions are lithium aggregates that have precipitated from the polymer matrix.

Differential Scanning Calorimetry

Given the inverse relationship between the crystallinity of the PEO domains and its conduction mechanism, all of the electrolytes were characterized by DSC.⁷⁹ Hermetically sealed pans were prepared under argon to ensure no moisture would interfere with the test results. Because all of the heating cycles showed an endothermic peak at 33.5 °C, and all of the cooling cycles showed a exothermic peak at 32.5 °C only the exemplar DSC curve of 20:1:0.5 is shown in Figure VI-4. The slight difference in peak shape between the heating and cooling is due to the differences in the temperature ramp rates. The transition of the neat IL (47.2 °C) and the lithium salt is well above the observed peak. Thus, the observed peaks are due solely to the melting transition of the polymer electrolyte whose crystallinity has already been reduced due to the presence of

the IL. The depressed nature of the transition temperature bodes well for the utility of this electrolyte in biomedical devices because it occurs below physiological temperature.

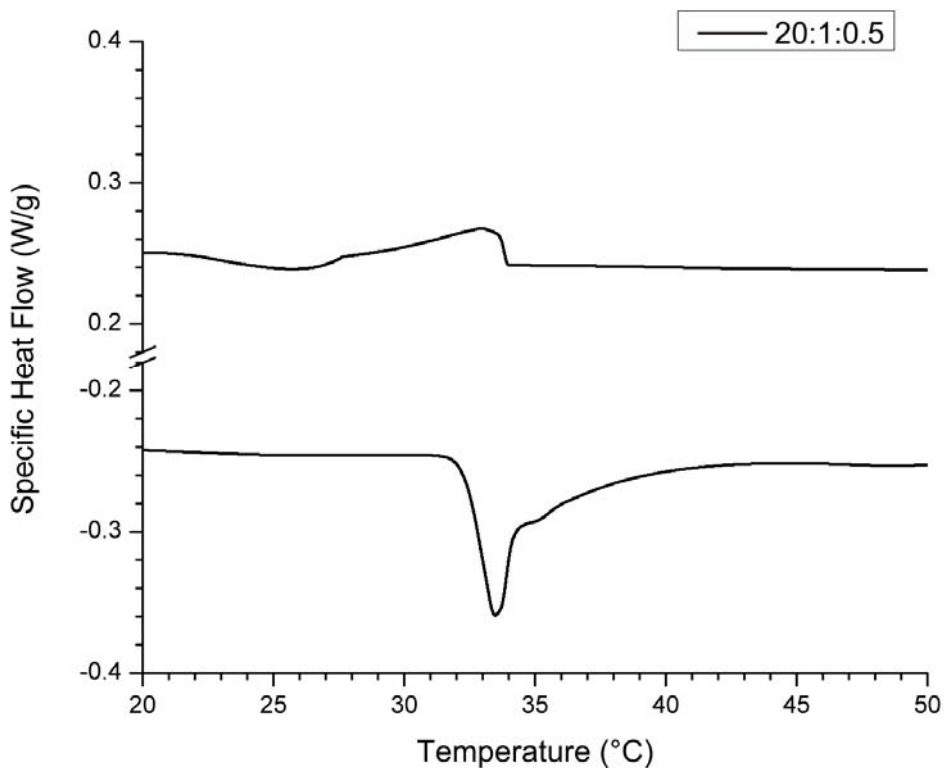


Figure VI-4 DSC of the 20 PEO : 1 LiBOB :0.5 S₂BOB system. A heat/cool/heat cycle was followed between -50 and 120 °C with a cooling rate of 5°C/min and a heating rate of 10°C/min. There were no peaks outside of this range.

Ionic Conductivity

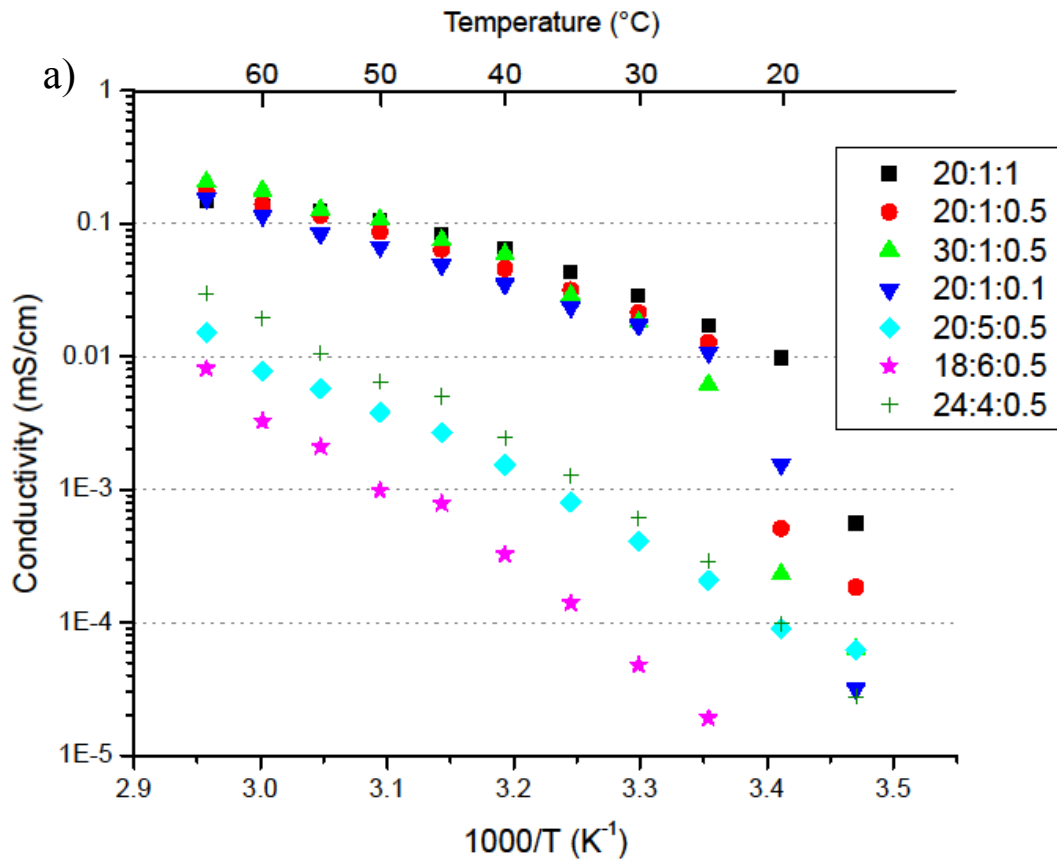
The ionic conductivity values of the electrolyte were taken using impedance spectroscopy. The low frequency intercept was taken to be the resistance and from this value ionic conductivity values were determined. Selected ratios can be seen in Figure VI-5a, with an expanded view of the higher conductivity electrolytes in Figure VI-5b.

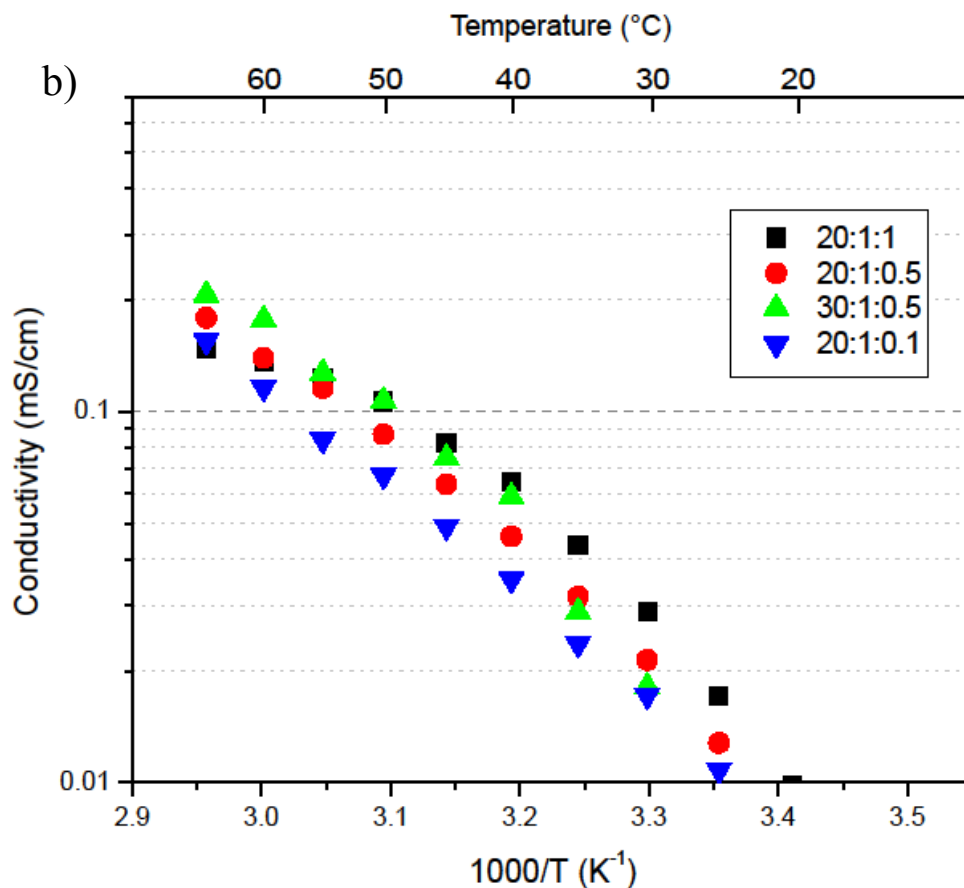
The maximum conductivity values at each temperature for the optimal ratio is as follows
 25 °C: 0.017 mS/cm , 37 °C: 0.048 mS/cm, 50 °C: 0.107 mS/cm and 65 °C: 0.206 mS/cm

Figure VI-5 (a) Ionic conductivity of the solid polymer electrolytes determined by AC impedance spectroscopy upon cooling of the SS/electrolyte/SS cells from 65 °C.

(b) Enlargement of the previous graph showing the region of high conductivity.

Molar ratios are x PEO : y LiBOB : z S2BOB.





Given that all electrolytes exhibited similar transition temperatures in DSC, only a small variation in conductivity values was expected.⁷⁰ This trend was not observed, instead wide variability in the conductivity values was observed. The electrolytes can visually be grouped into two groups: one of elevated conductivity and one of lower conductivity. The group with elevated conductivity consists of electrolyte with low concentration of LiBOB salt. The group with depressed conductivity consists of electrolyte with more concentrated salt. This latter high salt concentration BCP-IL was originally of great interest because the optimal formulation of the BCP containing no IL tended towards high salt concentrations.²² The conductivity values for this group was lower than the BCP system containing no IL. Additionally worse mechanical properties

were observed in these systems relative to the both the previous formulations and those with lower salt concentrations.

The high conductivity BCP-IL electrolytes with lower salt concentrations exhibited elevated ionic conductivity, in addition to pliability and transparency (Figure VI-2). At temperatures below 40 °C these more dilute electrolytes exhibited superior conductivity relative to the previous BCP containing no IL system, with larger differences at lower temperatures. These ionic conductivity values indicate success in continuing to improve movement of ions in solid polymer systems. At 50 °C the minimum threshold for ionic conductivity of 0.1 mS/cm is met, however experimentally useful Li^+ conductivity has been attained at 35 °C. While not ideal, the slight elevation in temperature required for useful conductivity is readily obtained in medically implanted systems and other specialized applications.

The conductivity plots were fit to the Arrhenius equation to compare this BCP-IL electrolyte system with its two predecessor systems, the pure BCP and the homopolymer PEO-IL electrolyte systems. The parameters are tabulated in Table VI-1 from fitting the temperature regime above the phase transition to the Arrhenius equation. The BCP-IL had activation energies between 51.6 kJ/mol and 58.7 kJ/mol. This is much closer to the PEO-IL system value of 47.0 kJ/mol than the BCP containing no IL systems which had activation energies of 71.2 kJ/mol and 86.1 kJ/mol. This lower value indicates less temperature dependence for ionic conduction. Additionally, the IL appears to have an advantageous effect on ion mobility promoting movement by decreasing the energy threshold. Overall the large change in activation energy between electrolyte with and without IL points to differing methods of ionic conduction.

Table VI-1. Fitting parameters to the Arrhenius for the high temperature region.

BCP-IL data is from this paper, the BCP containing no IL data is from Ghosh and Kofinas²² and the PEO-IL data is from Fisher et al.⁷⁷ E_a is the activation energy and A is the pre-exponential factor.

Ratio	E_a (kJ/mol)	A ($\times 10^{-4}$ S/cm)
20:1:1	54.56	4.95
20:1:0.5	51.59	1.80
20:1:0.1	53.35	2.74
30:1:0.5	58.68	28.6
3:1:0 ²²	71.23	451
2:1:0 ²²	86.11	38100
PEO 20:1:1 ⁷⁷	47.04	1.24

Transference

Given the high transference of the BCP containing no IL electrolyte, elevated T_{Li^+} values were expected.²² The values for the concentrations of 30:1:0.5, 20:1:0.5 and 20:1:0.1 at 40 °C and 60 °C are plotted in Figure VI-6. The minimal IL concentrations (20:1:0.1) resulted in measured T_{Li^+} values of 0.40 at 40 °C and 0.30 at 60 °C. Higher IL concentrations resulted in T_{Li^+} values that ranged from 0.15 to 0.22. For a given concentration T_{Li^+} decreased with increasing temperature. The observed phenomenon is the result of increased ionic mobility of the larger ions in the system due to increased chain mobility with higher temperatures. The system with increased T_{Li^+} (20:1:0.1) is significant because it exceeded the values attained for the PEO-IL based electrolyte, while the higher concentrations all measured similar to the PEO-IL systems.⁷⁷ The attained values were depressed relative to the BCP containing no IL, due to the deleterious presence of other small ion species. The positively charged lithium based aggregates in the minor block of the BCP entrap free anions thereby increasing the

fraction of free Li^+ relative to all free ions. In the BCP without IL system the only cation present was Li^+ which results in higher T_{Li^+} values relative to the BCP-IL system because it contains triethylsulfonium cations, which are not attracted to the aggregates. Given the different slopes (activation energies) of the conductivity plots for both the BCP-IL and the BCP containing no IL electrolytes, the inverse relationship between ion concentration and T_{Li^+} can be attributed to the presence of an additional ionic conduction pathway involving the IL. The improvement in T_{Li^+} while still maintaining high ionic conductivity shows that the BCP-IL system has promise as a solid electrolyte for lithium batteries.

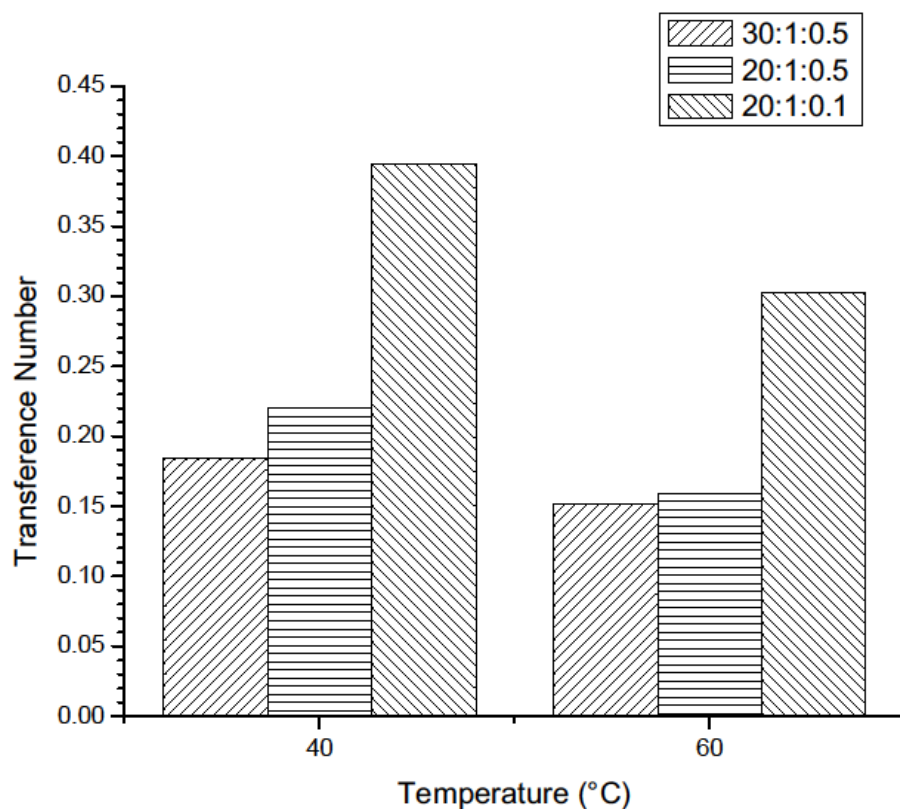


Figure VI-6 Measured lithium transference values for the BCP-IL system run at the indicated temperature. Molar ratios are x PEO : y LiBOB : z S₂BOB.

Diffusion

The salt diffusion coefficient (D_s) is indicative of the ability of ions to move through the polymer electrolyte system. The relationship between diffusion and transference number has been shown by Edman⁸⁰ to be intimately intertwined with the lithium concentration, higher concentrations result in greater T_{Li^+} values. The D_s values from the current interrupt experiments are shown in Table VI-2. The measured D_s values are all on the order of 10^{-7} cm²/s. Comparing the determined values to literature shows that the BCP-IL system possesses elevated diffusion coefficients relative to PEO salt systems, ($\sim 10^{-8}$ cm²/s).^{81,82} Given the addition of IL these numbers indicate increased ease of ionic conduction, which is seen from the AC impedance of the BCP-IL electrolyte. With increased temperature there is a marginal increase in diffusion coefficients of the solid polymer electrolyte.

Table VI-2 Measured salt diffusion coefficients by the current interrupt method.^{62,80}

Ratio	40 °C ($\times 10^7$ cm²/s)	60 °C ($\times 10^7$ cm²/s)
20:1:0.5	1.62±0.05	2.79±0.02
30:1:0.5	1.80±0.10	2.83±0.26

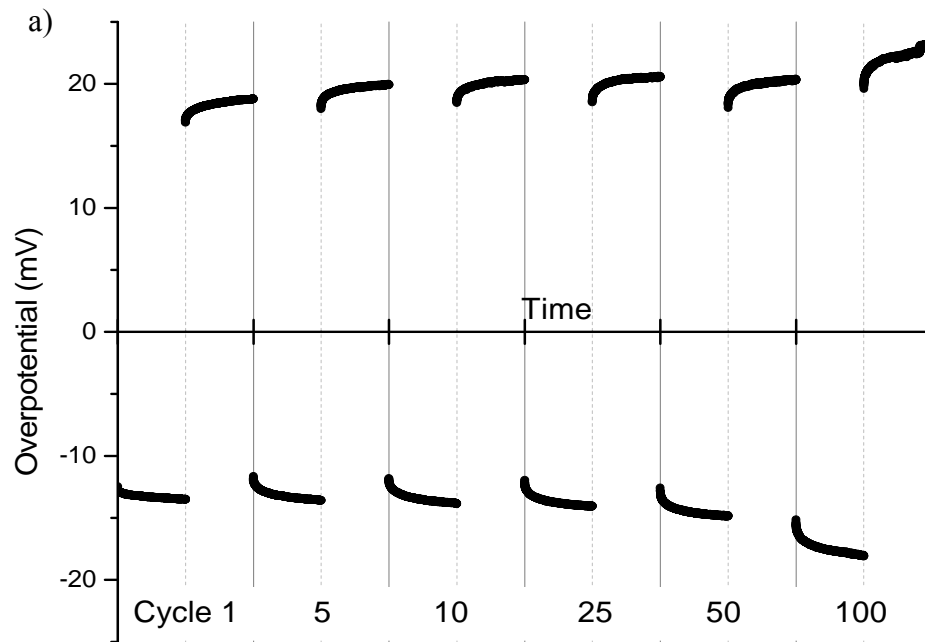
Electrochemical Stability

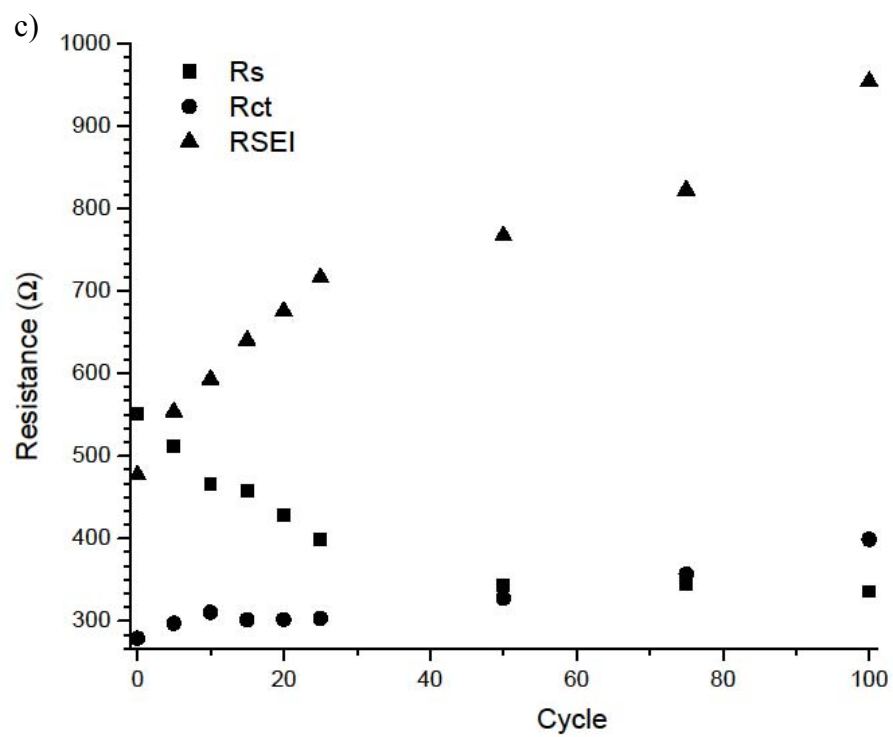
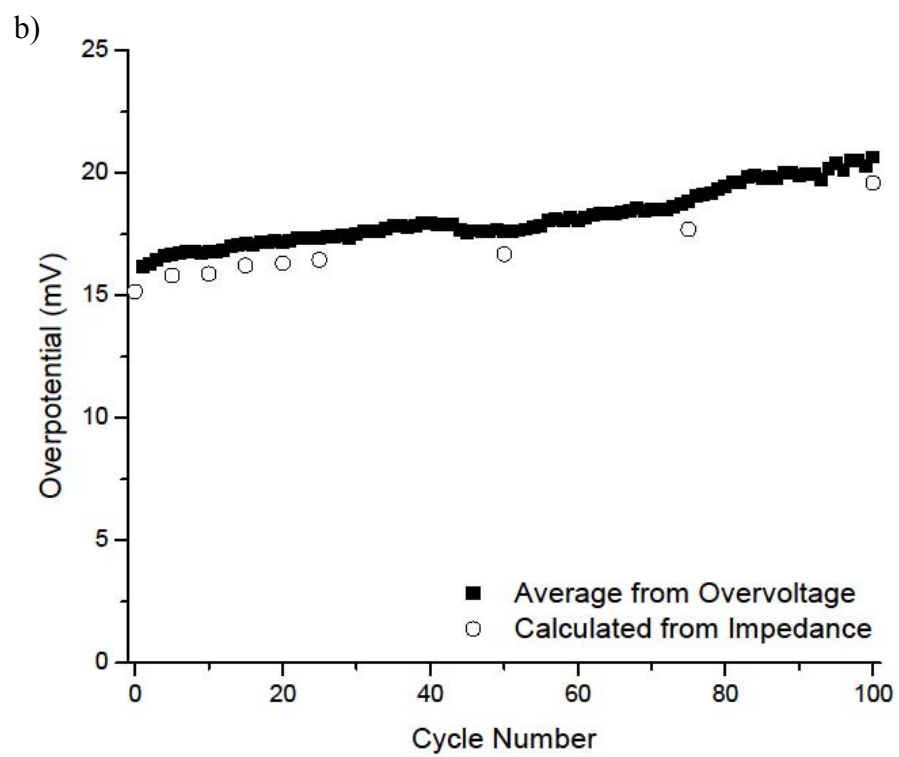
The polymer electrolyte was also investigated as to its stability at high voltages vs. Li/Li⁺. A sweep of the voltage from 2.5 to 6.0 V was conducted with a lithium reference and a platinum counter electrode. The cathodic stability (resistance to reduction) was measured to be 4.44 ± 0.07 V vs. Li/Li⁺. This value is comparable to carbonate based liquid electrolytes, but being a polymer based system it is thermally safer. For comparison to previous work the counter electrode was changed to stainless

steel, which is not stable at high voltages. The values returned were significantly higher, around 4.7 V. The BCP containing no IL electrolyte showed stability against SS of 5 V, while the system using the homopolymer PEO-IL electrolyte showed stability of ~4.5 V against SS. This indicates that the decreased stability is likely the result of the ionic liquid. It does appear that the block copolymer matrix does add stability to the IL containing electrolytes because the comparable value has marginally more stability. The constructed hybrid system possesses sufficient stability to be useful for all commercialized cathode materials.

Electrolyte stability at low potentials towards metallic lithium is critical in an electrolyte for lithium batteries. To measure this, galvanostatic cycling was undertaken on a symmetrical lithium cell with the 20:1:0.1 electrolyte at 40 °C. Ideally a constant potential would be measured indicating stability at the interface. In Figure VI-7a the profiles of selected overvoltage cycles can be seen. Upon initial visual inspection the profiles demonstrate a stable plateau that is reached quickly. However, with continued cycling the profile does start to deviate more from ideal, which given further electrolyte optimization could be reduced. Though, when compared to previous cycling^{21,77} the potentials of this hybrid block copolymer system is lower than either of the two previous systems. Simply, this test demonstrates good mobility of lithium ions through the BCP-IL bulk and across the interface to the electrode where they are reduced back to lithium.

Figure VI-7 (a) Overpotential as a function of time for selected cycles of the 20 PEO : 1 LiBOB : 0.1 S₂BOB BCP-IL system. Each cycle consisted of 1 hour of positive and negative current at a rate of 0.1 mA/cm² while at 40 °C. (b) ■ final values of the average overpotential as plotted against cycle. ○ are calculated from the resistance determined by the intermittent AC impedance scans. (c) The resistances as plotted against cycle were determined from fitting the AC impedance scans to a 3 element equivalent circuit. R_S- bulk or series resistance, R_{CT}-charge transfer resistance, R_{SEI}- resistance of the SEI.





To provide numerical insight into the overvoltage analysis the percent of time it takes to reach the defined percentage of the final overpotential value is tabulated in Table VI-3. Throughout the testing, the cell reached the 90% threshold, early and in some cases instantaneously. This indicates that the increase in overpotential within a given cycle is minimal. This observation shows stability of the interface towards single direction ion movement on a short timescale. Using the higher threshold values of 95% and 99% it becomes clear that the stability could be improved within a given cycle. The time to the threshold value decreases to a minimum over the first 10 cycles, before steadily increasing until the 100th cycle. The initial decrease in the time taken to reach the thresholds is likely the result of more energetically favored arrangements of the polymer at the interface. The shift over extended cycling towards longer times to reach the threshold indicates the disappearance of the ideal plateau, which is clearly observable when comparing the 100th cycle to earlier cycles. This BCP-IL electrolyte formulation possess superior properties for lithium stripping and plating, which upon further optimization is expected to show greater long term stability.

Table VI-3 Fraction of full time it took for the overpotential value to reach the specified % of the final overpotential value. For example, during the 100th cycle with negative polarity to the current it took 3.36% of the hour for the measured overpotential to reach 90% of the final overpotential.

Cycle	90%		95%		99%	
	-	+	-	+	-	+
1	0.00%	0.00%	1.09%	10.90%	56.71%	66.40%
5	0.00%	0.00%	19.11%	2.34%	65.92%	27.39%
10	0.62%	0.00%	10.22%	0.92%	38.56%	16.64%
25	1.31%	0.00%	15.42%	6.18%	62.80%	44.44%
50	1.67%	0.00%	15.32%	7.58%	62.79%	54.73%
100	3.36%	3.61%	21.33%	31.46%	82.24%	83.30%

In Figure VI-7b the final overpotential value is plotted against the cycle number. There is a small initial increase, but the final value stays fairly constant below 17 mV until around the 60th cycle. From this point until the 100th cycle a small rise of ~3 mV can be seen in the final overpotential value. This indicates a slow, gradual decay of the electrolyte at the interface with lithium. While not ideal, the wide potential ranges in which a lithium electrolyte operates leads to observable decay over long periods of time and aggressive cycling. The overall small increase from the beginning of the test indicates long-term stability without the potential for cell failure due to lithium dendrite growth.

AC impedance scans were intermittently conducted during the overvoltage testing to monitor the development of resistance in the electrolyte. The plots were then fit to an equivalent circuit consisting of a bulk resistance, a charge transfer element (resistor and capacitor in parallel) and the SEI (resistor and constant phase element in parallel). The

resistances are plotted against cycle number in Figure VI-7c. Initially the bulk resistance and the SEI resistance are the highest. As cycling progressed though the bulk resistance of the electrolyte decreased. This is likely the result of more favorable arrangement of the polymer chains to promote ionic movement. Conversely, the SEI and charge transfer resistances increase over the cycling period. By the 100th cycle, the SEI dominates the other two values and is the largest factor in the aforementioned increase in the final overpotential values. For comparison, all of the resistances were summed and then plugged into Ohm's law to get a voltage to compare to the end values from Figure VI-7b (○). These values matched the trend of the final values, but were systemically off by 3%. Upon cell disassembly the area was found to be slightly enlarged, which resulted in smaller than actual resistances accounting for the difference. The AC impedance data indicates that further annealing at the outset of cycling would likely improve initial overvoltage, and the SEI remains the largest impediment to stable long term cycling of lithium batteries.

4. Conclusions

The development of a solid polymer electrolyte holds great promise for increasing the safety of lithium batteries. Building upon earlier work we combined our triethylsulfonium BOB ionic liquid with our PEO-PMAALi block copolymer in the hopes of creating a superior polymer electrolyte. The conductivity of the BCP-IL system was marginally higher than the original BCP containing no IL below 40 °C. At 40 °C the conductivity was 0.059 mS/cm and at 65 °C the conductivity was 0.206 mS/cm. The BCP-IL electrolyte demonstrated superior T_{Li^+} values to the homopolymer PEO-IL system of ~ 0.40 , and had D_s of $\sim 2 \times 10^{-7}$ cm²/s. The increase in lithium mobility with the

BCP matrix holds great promise for the development of a solid polymer electrolyte. The cathodic stability was found to be slightly depressed but still high enough for utility with all commercial cathodes. The ability of this electrolyte to reversibly strip and plate lithium was confirmed. Over 100 cycles it showed only a marginal increase in plating potential, from 16.2 mV to 20.6 mV.

VII. Zwitterionic Liquid

1. Introduction

Electrolytes for lithium batteries must possess a number of ideal characteristics.^{6,7} However, since no single chemical has all the ideal properties additives are generally used to get at these ideal electrochemical properties. In liquid electrolytes additives are predominantly chosen to aid in formation of the solid electrolyte interphase (SEI), to confer stability at high voltages or to suppress flammability and thermal issues.⁶ Polymer electrolytes though are chosen as a starting point because many of these aforementioned issues are resolved by switching to a polymer. However, in polymer electrolytes additives are chosen to increase conductivity. Without involving combustible liquids, research on these additives has predominantly focused on ionic liquids and ceramics.^{28,33} While both additives result in improved properties, none makes the polymer electrolyte sufficient for use in a lithium battery system.

IL additives have improved the ionic conductivity values of polymer systems, however they have decreased the lithium transference (fraction of total observed current due to lithium).⁵¹ ILs were selected because of their versatility of structure resulting in widely varying electrochemical properties. Our previous work has shown greatly increased conductivity with triethyl sulfonium based ILs.^{70,77} This cation scaffold was selected for because of its similarity to PEO and its oxyethylene units which are lithium conductors. However, this system was similarly accompanied by diminished lithium transference. Given the possibilities with ILs the development of future additives need not be limited. This designer additive would serve a two-fold purpose in a solid polymer

electrolyte helping to not only increase conductivity, but lithium conductivity as well without compromising the benefits of using a polymer based system.

The inclusion of additional Li^+ results in higher transference numbers.⁸⁰ In previous work in our group we synthesized a block copolymer with a lithiated block that resulted in elevated lithium transference.^{21,22} This however did not have sufficient ionic conductivity to be useful as an electrolyte at 40°C. Further increasing lithium concentration to having an ionomer further pushes the transference closer to unity whilst further lowering the ionic conductivity.⁷⁵ A research thrust for additives needs to encompass the need for higher lithium concentrations without compromising the structural integrity of the solid polymer film.

Zwitterions are molecules that contain atoms with both a positive and a negative charge. They have been investigated for electrochemical cells because they contain both positive and negative charges meaning they do not move in an applied electrical field.⁸³⁻⁸⁵ These systems, when used in conjunction with lithium salts, have shown increased lithium diffusion and peak current while decreasing the effect of the SEI. These results are postulated to be the result of either shielding of the ion-ion pairs or the availability of an additional conductivity pathway. Given the improvements of zwitterionic liquids used as electrolyte additives this provides a template for future development.

With this in mind we set out to synthesize an IL that combined the ideal conductivity with the presence of increased Li^+ . This zwitterionic liquid could simultaneously plasticize the polymer matrix for increased ionic conductivity and increase lithium ion concentration resulting in higher transference values. In this article, we report on the synthesis of the novel diethylsulfonium carboxylate based zwitterionic

liquid. It is incorporated into a polymer electrolyte and its electrochemical properties as an additive for a lithium battery are evaluated.

2. Experimental

a. Materials

LiTFSI ($\text{LiN}(\text{SO}_2\text{CF}_3)_2$), diethyl sulfide, iodoacetic acid and lithium foil were used as received from Aldrich. Poly(ethylene oxide) (Mw 300k) was used as received from Alfa-Aesar. LiBOB was used as received from Chemetall. Characterization was performed by NMR on a Bruker AV-400 high resolution NMR. ^1H and ^{13}C were performed in deuterated methanol. Mass spectroscopy measurements were performed on a JEOL AccuTOF-CS ESI-TOF mass spectrometer. ESI+/ESI- modes were looked at over the m/z range of 80-500.

b. RTIL preparation

Carboxymethyl diethyl sulfonium cation synthesis: Equimolar amounts of diethyl sulfide (4.900 g, 53.24 mmol) and iodoacetic acid (10 g, 53.24 mmol) were mixed in 20 mL of dry acetone and allowed to stir for 3 days before being dried. A viscous dark red product was returned in 86.9% yield, which was then partitioned before being carried through to the next step.

Lithiation: $\text{S}_{22}(\text{CH}_2\text{COOH})\text{I}$ (6.476 g, 23.45 mmol) was stirred with equimolar LiOH (0.573 g, 23.45 mmol) and LiTFSI (6.732 g, 23.45 mmol) in water for 2 hours. The aqueous solution was first washed with DCM and only the aqueous solution was kept. The solution was then dried and dissolved into acetone then washed with DCM again. A purple viscous liquid was isolated after drying the acetone phase resulting in a recovered

yield of 6.30 g corresponding to 61.7% yield. ^1H : 4.085 (s, 2 H), 3.384 (q, $J=7.4$ Hz, 4H), 1.465 (t, $J=7.4$ Hz, 6H). ^{13}C : 168.09, 44.79, 34.75, 9.35. ESI^+ : 149.08252, ESI^- : 279.91005. Elemental analysis results as conducted by Galbraith Laboratories: C: 25.5%, H: 4.29%, O: 11.34%, Li: 2.46%, S- 11.37%, I- 44.99% (sample contained H_2O and LiOH impurities).

c. Electrolyte Preparation

All electrolytes were assembled in the molar ratio of x PEO : y LiBOB : z $\text{S}_{22}(\text{CH}_2\text{COOLi})\text{TFSI}$ (Figure VII-1). The electrolyte films of different composition were solution cast from dimethylformamide onto Bytac molds in an MBRAUN Labmaster 100 argon glove box. The resultant films were dried for several days at 80 °C, before being placed into CR2032 coin cell enclosures for electrolyte testing.

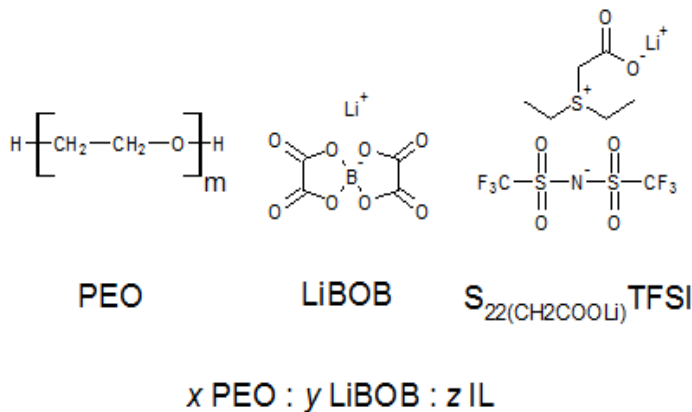


Figure VII-1 Compounds used to make the solid polymer electrolyte. All ratios cited in this paper are of the molar formula x PEO : y LiBOB : z IL.

d. Electrolyte Characterization

Conductivity measurements for electrolytes were performed in a stainless steel (SS)/electrolyte/SS coin cell set up on a Solartron 1287A/1255B platform over the

frequency range 1 MHz to 1 Hz. Testing parameters were controlled by the associated CorrWare and ZPlot software, while data was processed using CorrView, ZView and Origins 8. All temperature testing was completed in a RevSci IncuFridge with ± 0.5 °C temperature accuracy allowing 45 mins to equilibrate at each temperature. Prior to testing constructed cells were annealed for 3 hrs. at 70 °C.

3. Results and Discussion

The zwitterionic liquid was solution cast resulting in a thin polymer film similar in characteristics to previous work on the PEO-based systems.^{70,77} Given the novel nature of these additives the first characterization test was to see the effects of the zwitterionic liquid on ionic conductivity. Ionic conductivity of the electrolytes during the cooling process is plotted in Figure VII-2, where the ratio is x PEO: y LiBOB: z IL. Among the ratios, the formulations with higher ionic concentrations generally exhibited higher conductivities. The best system over nearly the entire measured temperature range was 20:0.5:1, even beating the more ionically rich 20:1:1 system. The higher lithium salt concentration of this latter system depressed the overall conductivity at temperatures above 25 °C. The conductivity values of 20:0.5:1 are as follows: at 65°C: 0.67 mS/cm, at 40°C: 0.15 mS/cm and at 25°C: 0.017 mS/cm. Remarkably, the systems with only the zwitterionic liquids also showed high conductivity. The 20:0:1.0 system exceeded 0.1 mS/cm conductivity at 43°C which means it could be useful for biomedical applications.

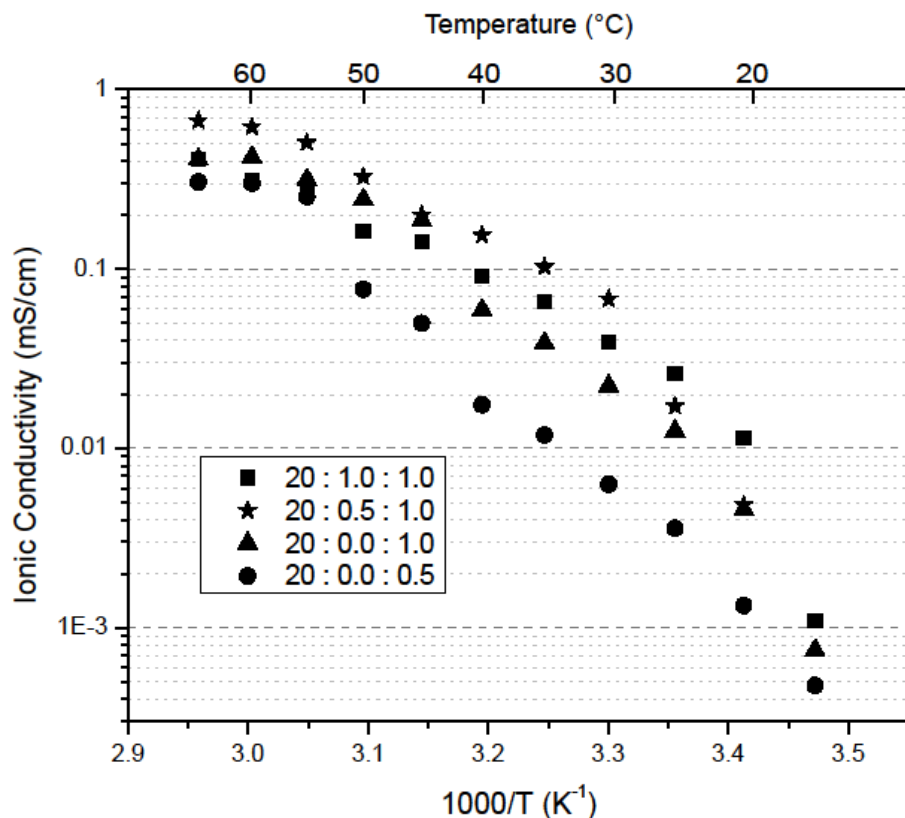


Figure VII-2 Ionic conductivity of the solid polymer electrolytes determined by AC impedance spectroscopy upon cooling of the SS/electrolyte/SS cells from 65 °C.

Ratios are x PEO : y LiBOB : z S₂₂(CH₂COO-Li⁺) TFSI

The effect of the zwitterionic system (20:0.5:1.0) was benchmarked against the penultimate PEO-IL system of 20 PEO: 1 LiTFSI: 1.5 S₂TFSI.⁷⁰ At 25 °C the PEO-IL was 0.12 mS/cm compared with 0.017 mS/cm for the zwitterionic liquid. The difference is nearly tenfold between the two systems; however, at this temperature neither ionic liquid was able to sufficiently enable the movement of lithium ions. At 40 °C the PEO-IL system is ~0.7 mS/cm, whereas the zwitterionic liquid was 0.15 mS/cm. This decrease to between a four- and five-fold difference is likely due to the increased reliance of ionic conduction on PEO segmental motion. This pathway becomes available because of the

plasticizing effect of the additive. The difference multiple decreases further between the two systems at 65 °C; PEO-IL is 2.25 mS/cm compared with 0.67 mS/cm for the zwitterionic liquid. Given the difference in ionic conductivity values between the two systems, the plasticizing effect of the zwitterionic liquid is inferior to S₂TFSI. The plasticization is important because this is what enables PEO chain movement and ultimately lithium ion conduction through the electrolyte.

When comparing the electrolyte systems it is important to look at the trend lines when fit to the curves using the Arrhenius equation. All of the tested ratios have distinct slopes of the trend lines below 50°C indicating differing activation energies and likely slightly differing molecular interactions leading to ionic transport. The linear relationship in this temperature range shows that for each marginal increase in temperature more ions become available to be moved. Given the differences in electrolyte composition there is a clear impact of the IL and the salt controlling not only the number of ions but by which pathway as well. Above 50°C each line shows a clear change in slope indicating the presence of an alternative conductivity mechanism. Comparing different composition, the slopes at this high temperature are more parallel to one another indicating that the conductivity mechanism is similar; the absolute values of conductivity differs through because of differing ionic concentrations. When contrasted to the PEO-IL system⁷⁰ there is similar slope in the high temperature regime, but a steeper slope in the low temperature regime. As previously discussed the similarity in slope in the high temperature regime likely indicates the predominance of conduction via PEO segmental motion. For the low temperature regime, the varying slopes likely points to the different effect on plasticization of the zwitterionic liquid when compared to triethyl sulfonium. The higher

charge density of the zwitterion likely inhibits the favorable plasticizing behavior witnessed with triethyl sulfonium based ionic liquids.

4. Conclusion

Zwitterionic liquids are a unique opportunity where an IL can serve two purposes in a solid polymer electrolyte system. In this set-up it serves to both plasticize the polymer chains and acts as a source of lithium. When combined with PEO pliable thin films are formed that can be tested as lithium electrolytes. The ionic conductivities were measured showing appreciable conductivity for selected systems above 35 °C. The highest conductivities were returned for the 20:0.5:1.0 system above room temperature. This preliminary data shows a marginal increase in conductivity. However, many more tests are needed to see the suitability of the zwitterionic liquid as an electrolyte additive. Given its inactivity in an applied electrical field strong preference for lithium ion conduction is expected. The complex chemistry of this additive though may adversely affect stability at high potentials. Continued characterization work is expected though to confirm these hypotheses and possibly provide insight into future novel electrolyte additive development.

VIII. Future Directions

Through the four generations of electrolyte systems, the plausibility of a lithium battery system using a solid electrolyte has been shown. The increased safety realized by switching away from organic carbonates is the real driver behind this work. The next step in the development of this electrolyte is to scale up electrolyte production. This larger quantity of electrolyte would enable cell cycling and cell safety testing which would validate many of the claims of increased safety without compromising performance. Furthermore, construction of numerous pouch cells would easily showcase the increased flexibility and pliability. Upon validation of the energy density deliverable from a battery no change is expected over lithium batteries with liquid electrolytes because of a fairly equal replacement between the separator and the hybrid solid polymer electrolyte film. However, because elemental lithium will be used in place of graphite a large increase in volumetric and gravimetric energy density per unit of active material will occur. Power density though is expected to decrease as a function of lower currents. Additionally, the energy and power densities of a full battery will be increased because the steel casing of these safer batteries can be replaced with a thin laminating film. Because these components do not scale when miniaturizing the battery and thus much greater benefits will be seen with smaller cells. The difficulty in this step though lies in acquiring the necessary pieces of equipment and more than likely a dry room. The capital investment is the barrier at this stage to the further development of the electrolyte for lithium batteries.

From an academic perspective there are a number of avenues to pursue that could improve the properties of the electrolyte. At the outset of the research a whole family of

sulfur based ionic liquids was synthesized, but ultimately never tested. It would be interesting to evaluate the diethyl sulfonium and tetrahydrothiophene based ionic liquids. Properties within a class of ionic liquids are interesting and sometimes unexpected, as with the ideal carbon chain lengths for pyrrolidinium of one and four.⁸⁶ There is also some work that can be done on the MW of the polymer as well as each block and its effect on the electrochemical properties. I do not believe though that there is much more room to investigate different polymer matrices, as this area is largely limited by the difficulty in working with lithium ions. Lastly some work can be done to increase mechanical strength at higher temperatures. It may be possible to increase mechanical strength by blocking a third polymer, by blending another polymer, or by incorporating hard ceramic particles. Inert polymers with high temperature stability such as polystyrene or polydimethylsiloxane may be the solution.

Given the success of the electrolyte it is important to optimize all components of the lithium battery. The electrodes used to do preliminary testing were limited to simplistic translations of formulations used with liquid carbonate based electrolytes. Future work would likely increase the ratio of polymer used as binder or use the polymer electrolyte as binder. Given the limited conductivity of polymers relative to liquids increasing the ratio from 10% towards 30% would likely increase the energy per unit weight of the active material. Additionally, the use of non-commercial cathode systems, such as sulfur, would show improvement of the polymer battery relative to liquids. Sulfur is limited because of the dissolution of polysulfides into the electrolyte; a polymer already containing sulfur IL might inhibit this process demonstrating actual capacity much closer to theoretical than previously achieved.

Lastly I believe there is further room to investigate the molecular interactions in the electrolyte. Using more in depth NMR and other analytical techniques would yield further information about how the ions move and interact with the polymer matrix. Magic angle spinning is able to directly determine each ion species diffusion and conductivity. This information would result in greater detail on not only the current system but also insight into the design of future electrolytes that more strongly favor lithium conduction. Additionally, work on femtosecond laser pulses as done in Robert Kostecki's lab at Lawrence Berkeley Lab would be useful in probing the SEI.⁸⁷ This research would allow for precise depth profiling of the SEI leading to a better understanding of the interpenetration of the polymer into the electrode and possibly lead to ways to continue to improve this limiting factor in deployment of a solid polymer electrolyte. On the whole knowledge of polymer electrolytes and the electrochemical interfaces they form is lacking. These insights could lead to further optimization of not only our hybrid polymer electrolyte system, but others as well.

IX. Contributions

Over the past four years my research focused on the development of polymer electrolytes has to this point led to 4 publications, 1 patent, 1 invention disclosure, 7 conference talks and 4 poster presentations. Chapter IV is jointly published in the *Journal of Power Sources*⁷⁰ and the half-cell cycling is published as a conference proceeding in *Electrochemical Transactions*⁷⁶. The full article was selected among the “25 Hottest Articles” in the journal for the 4th quarter of 2011. Chapter V and VI are published as two separate papers in the *Journal of the Electrochemical Society* in 2012^{77,88}. The early work from Chapter IV and V has resulted in a provisional patent, while the more recent work in Chapter VI has resulted in an invention disclosure through the University of Maryland - Office of Technology Commercialization.

Since 2009 I have been a John and Maureen Hendricks Energy Fellow recipient. This annual award supports students engaged in research that advances the frontiers of energy science and technology. Presentations on the research discussed in this dissertation have been given at a number of prestigious national and international conferences. Talks have been given at The Materials Research Society Meeting, The Electrochemical Society Meeting, The International Society of Electrochemistry Meeting and The American Chemical Society National and Mid-Atlantic Regional Meeting. For the 2012 ECS conference I was selected for a student travel grant from both the national battery division, and the University of Maryland ECS student chapter. Conference posters have been presented at the International Meeting on Lithium Batteries, the Conference on Ionic Liquids, the Fischell Festival, and the Royal Society of Chemistry International Symposia on Challenges in Renewable Energy.

The research has also led to the formation of a small company called SafeLiCell LLC. SafeLiCell has been entered into several business plan competitions and awarded money. I took second place in the \$100k ACC Clean Energy Challenge winning \$15k and a presentation led by Mian Khalid took second place at the ACS Green Chemistry and Engineering Business Plan Competition winning \$10k. The company also was selected as a finalist and semi-finalist in 2010 and 2012 respectively in the UMD \$75k Business Plan Competition.

X. References

- (1) Moore, G. E. "Cramming more components onto integrated circuits" *Electronics* **1965**, 38.
- (2) Tarascon, J. M.; Armand, M. "Issues and challenges facing rechargeable lithium batteries" *Nature* **2001**, 414, 359-367.
- (3) Bensinger, G. In *Wall Street Journal* New York City, 2012.
- (4) *World Battery Materials: Industry Study with Forecasts for 2012 & 2017*, The Fredonia Group, 2009.
- (5) Lide, D. *CRC Handbook of Chemistry and Physics, 88th Edition (CRC Handbook of Chemistry and Physics)*; CRC, 2007.
- (6) Xu, K. "Nonaqueous liquid electrolytes for lithium-based rechargeable batteries" *Chemical Reviews* **2004**, 104, 4303-4417.
- (7) Goodenough, J. B.; Kim, Y. "Challenges for Rechargeable Li Batteries" *Chemistry of Materials* **2009**, 22, 587-603.
- (8) Armand, M. "Charge Transfer of Polymer Electrolytes" *Faraday Discussions of the Chemical Society* **1989**, 65-76.
- (9) Gray, F. M. *Solid Polymer Electrolytes*; VCH Publishers: New York, 1991.
- (10) Tatsuma, T.; Taguchi, M.; Iwaku, M.; Sotomura, T.; Oyama, N. "Inhibition effects of polyacrylonitrile gel electrolytes on lithium dendrite formation" *Journal of Electroanalytical Chemistry* **1999**, 472, 142-146.
- (11) Yamada, A.; Chung, S. C.; Hinokuma, K. "Optimized LiFePO₄ for Lithium Battery Cathodes" *Journal of the Electrochemical Society* **2001**, 148, A224-A229.

- (12) Wang, X.; Yasukawa, E.; Kasuya, S. "Nonflammable Trimethyl Phosphate Solvent-Containing Electrolytes for Lithium-Ion Batteries: I. Fundamental Properties" *Journal of the Electrochemical Society* **2001**, *148*, A1058-A1065.
- (13) Goodenough, J. B. "Fast Ionic-Conduction in Solids" *Proceedings of the Royal Society of London Series a-Mathematical Physical and Engineering Sciences* **1984**, *393*, 215-234.
- (14) Dias, F. B.; Plomp, L.; Veldhuis, J. B. J. "Trends in polymer electrolytes for secondary lithium batteries" *Journal of Power Sources* **2000**, *88*, 169-191.
- (15) MacCallum, J. R.; Smith, M. J.; Vincent, C. A. *Solid State Ionics* **1984**, *11*, 307.
- (16) Gray, F. M. *Polymer Electrolytes*; Royal Society of Chemistry: Cambridge, 1997.
- (17) Blomgren, G. E. In *Lithium Batteries*; Gabano, J.-P., Ed.; Academic Press: New York, 1983.
- (18) Capuano, F.; Croce, F.; Scrosati, B. "Composite Polymer Electrolytes" *Journal of the Electrochemical Society* **1991**, *138*, 1918-1922.
- (19) *Lithium Polymer Batteries Proceedings*; Raghavan, S. R.; Khan., S. A., Eds.; The Electrochemical Society: NJ, 1997.
- (20) Borghini, M. C.; Mastragostino, M.; Passerini, S.; Scrosati, B. "Electrochemical Properties of Polyethylene Oxide-Li[(CF₃SO₂)₂N]-Gamma-LiAlO₂ Composite Polymer Electrolytes" *Journal of the Electrochemical Society* **1995**, *142*, 2118-2121.
- (21) Ghosh, A.; Wang, C.; Kofinas, P. "Block Copolymer Solid Battery Electrolyte with High Li-Ion Transference Number" *Journal of the Electrochemical Society* **2010**, *157*, A846-A849.
- (22) Ghosh, A.; Kofinas, P. "Nanostructured Block Copolymer Dry Electrolyte" *Journal of the Electrochemical Society* **2008**, *155*, A428-A431.

- (23) Sadoway, D. R.; Huang, B.; Trapa, P. E.; Soo, P. P.; Bannerjee, P.; Mayes, A. M. "Self-doped block copolymer electrolytes for solid-state, rechargeable lithium batteries" *Journal of Power Sources* **2001**, 97-98, 621-623.
- (24) Singh, M.; Odusanya, O.; Wilmes, G. M.; Eitouni, H. B.; Gomez, E. D.; Patel, A. J.; Chen, V. L.; Park, M. J.; Fragouli, P.; Iatrou, H.; Hadjichristidis, N.; Cookson, D.; Balsara, N. P. "Effect of Molecular Weight on the Mechanical and Electrical Properties of Block Copolymer Electrolytes" *Macromolecules* **2007**, 40, 4578-4585.
- (25) Blonsky, P. M.; Shriver, D. F.; Austin, P.; Allcock, H. R. "Polyphosphazene solid electrolytes" *Journal of the American Chemical Society* **1984**, 106, 6854-6855.
- (26) Abraham, K. M.; Alamgir, M. "Dimensionally stable MEEP-based polymer electrolytes and solid-state lithium batteries" *Chemistry of Materials* **1991**, 3, 339-348.
- (27) Song, J. Y.; Wang, Y. Y.; Wan, C. C. "Conductivity study of porous plasticized polymer electrolytes based on poly(vinylidene fluoride) - A comparison with polypropylene separators" *Journal of the Electrochemical Society* **2000**, 147, 3219-3225.
- (28) Stephan, A. M.; Nahm, K. S. "Review on composite polymer electrolytes for lithium batteries" *Polymer* **2006**, 47, 5952-5964.
- (29) Minami, T.; Hayashi, A.; Tatsumisago, M. "Recent progress of glass and glass-ceramics as solid electrolytes for lithium secondary batteries" *Solid State Ionics* **2006**, 177, 2715-2720.
- (30) Neudecker, B. J.; Dudney, N. J.; Bates, J. B. "Lithium-Free" Thin-Film Battery with In Situ Plated Li Anode" *Journal of the Electrochemical Society* **2000**, 147, 517-523.
- (31) Quartarone, E.; Mustarelli, P. "Electrolytes for solid-state lithium rechargeable batteries: recent advances and perspectives" *Chemical Society Reviews* **2011**, 40, 2525-2540.

- (32) Howlett, P. C.; MacFarlane, D. R.; Hollenkamp, A. F. "High lithium metal cycling efficiency in a room-temperature ionic liquid" *Electrochemical and Solid State Letters* **2004**, *7*, A97-A101.
- (33) Shin, J. H.; Henderson, W. A.; Passerini, S. "Ionic liquids to the rescue? Overcoming the ionic conductivity limitations of polymer electrolytes" *Electrochemistry Communications* **2003**, *5*, 1016-1020.
- (34) Galinski, M.; Lewandowski, A.; Stepniak, I. "Ionic liquids as electrolytes" *Electrochimica Acta* **2006**, *51*, 5567-5580.
- (35) Lewandowski, A.; Swiderska-Mocek, A. "Ionic liquids as electrolytes for Li-ion batteries--An overview of electrochemical studies" *Journal of Power Sources* **2009**, *194*, 601-609.
- (36) Garcia, B.; Lavallée, S.; Perron, G.; Michot, C.; Armand, M. "Room temperature molten salts as lithium battery electrolyte" *Electrochimica Acta* **2004**, *49*, 4583-4588.
- (37) Paillard, E.; Zhou, Q.; Henderson, W. A.; Appetecchi, G. B.; Montanino, M.; Passerini, S. "Electrochemical and Physicochemical Properties of PY₁₄FSI-Based Electrolytes with LiFSI" *Journal of the Electrochemical Society* **2009**, *156*, A891-A895.
- (38) Chariclea, S.-K.; Richard, T. C. "Stability and Electrochemistry of Lithium in Room Temperature Chloroaluminate Molten Salts" *Journal of the Electrochemical Society* **1994**, *141*, 873-875.
- (39) Nakagawa, H.; Izuchi, S.; Kuwana, K.; Nukuda, T.; Aihara, Y. "Liquid and Polymer Gel Electrolytes for Lithium Batteries Composed of Room-Temperature Molten Salt Doped by Lithium Salt" *Journal of the Electrochemical Society* **2003**, *150*, A695-A700.
- (40) Holzapfel, M.; Jost, C.; Prodi-Schwab, A.; Krumeich, F.; Würsig, A.; Buqa, H.; Novák, P. "Stabilisation of lithiated graphite in an electrolyte based on ionic liquids: an electrochemical and scanning electron microscopy study" *Carbon* **2005**, *43*, 1488-1498.

- (41) Matsumoto, H.; Sakaebe, H.; Tatsumi, K. "Preparation of room temperature ionic liquids based on aliphatic onium cations and asymmetric amide anions and their electrochemical properties as a lithium battery electrolyte" *Journal of Power Sources* **2005**, *146*, 45-50.
- (42) Ishikawa, M.; Sugimoto, T.; Kikuta, M.; Ishiko, E.; Kono, M. "Pure ionic liquid electrolytes compatible with a graphitized carbon negative electrode in rechargeable lithium-ion batteries" *Journal of Power Sources* **2006**, *162*, 658-662.
- (43) Noda, A.; Hayamizu, K.; Watanabe, M. "Pulsed-Gradient Spin Echo 1H and 19F NMR Ionic Diffusion Coefficient, Viscosity, and Ionic Conductivity of Non-Chloroaluminate Room-Temperature Ionic Liquids" *The Journal of Physical Chemistry B* **2001**, *105*, 4603-4610.
- (44) Cheng, H.; Zhu, C.; Huang, B.; Lu, M.; Yang, Y. "Synthesis and electrochemical characterization of PEO-based polymer electrolytes with room temperature ionic liquids" *Electrochimica Acta* **2007**, *52*, 5789-5794.
- (45) Sun, J.; MacFarlane, D. R.; Forsyth, M. "Lithium polyelectrolyte-ionic liquid systems" *Solid State Ionics* **2002**, *147*, 333-339.
- (46) Zhang, S.; Sun, N.; He, X.; Lu, X.; Zhang, X. "Physical Properties of Ionic Liquids: Database and Evaluation" *Journal of Physical and Chemical Reference Data* **2006**, *35*, 1475-1517.
- (47) Tsunashima, K.; Sugiya, M. "Physical and electrochemical properties of low-viscosity phosphonium ionic liquids as potential electrolytes" *Electrochemistry Communications* **2007**, *9*, 2353-2358.
- (48) Tsunashima, K.; Yonekawa, F.; Sugiya, M. "A Lithium Battery Electrolyte Based on a Room-temperature Phosphonium Ionic Liquid" *Chemistry Letters* **2008**, *37*, 314-315.

- (49) Matsumoto, H.; Matsuda, T.; Miyazaki, Y. "Room Temperature Molten Salts Based on Trialkylsulfonium Cations and Bis(trifluoromethylsulfonyl)imide" *Chemistry Letters* **2000**, *29*, 1430-1431.
- (50) Qinghua, Z.; Shimin, L.; Zuopeng, L.; Jian, L.; Zhengjian, C.; Ruifeng, W.; Liu Jin, L.; Youquan, D. "Novel Cyclic Sulfonium-Based Ionic Liquids: Synthesis, Characterization, and Physicochemical Properties" *Chemistry - A European Journal* **2009**, *15*, 765-778.
- (51) Shin, J. H.; Henderson, W. A.; Passerini, S. "PEO-based polymer electrolytes with ionic liquids and their use in lithium metal-polymer electrolyte batteries" *Journal of the Electrochemical Society* **2005**, *152*, A978-A983.
- (52) Stallworth, P. E.; Fontanella, J. J.; Wintersgill, M. C.; Scheidler, C. D.; Immel, J. J.; Greenbaum, S. G.; Gozdz, A. S. "NMR, DSC and high pressure electrical conductivity studies of liquid and hybrid electrolytes" *Journal of Power Sources* **1999**, *81-82*, 739-747.
- (53) Olsen, I.; Koksang, R.; Skou, E. "Transference Number Measurements on a Hybrid Polymer Electrolyte" *Electrochimica Acta* **1995**, *40*, 1701-1706.
- (54) Fu, R.; Ma, Z.; Zheng, J. P.; Au, G.; Plichta, E. J.; Ye, C. "High-Resolution ⁷Li Solid-State NMR Study of Li_xV₂O₅ Cathode Electrodes for Li-Rechargeable Batteries" *The Journal of Physical Chemistry B* **2003**, *107*, 9730-9735.
- (55) Smith, G. D. In *COIL- 3* Cairns, Australia, 2009.
- (56) Bruce, P. G. "Energy storage beyond the horizon: Rechargeable lithium batteries" *Solid State Ionics* **2008**, *179*, 752-760.
- (57) Ghosh, A.; Kofinas, P. "PEO based Block Copolymer as Solid State Lithium Battery Electrolyte" *ECS Transactions* **2008**, *11*, 131-137.

- (58) Niedzicki, L.; Kasprzyk, M.; Kuziak, K.; Zukowska, G. Z.; Marcinek, M.; Wieczorek, W.; Armand, M. "Liquid electrolytes based on new lithium conductive imidazole salts" *Journal of Power Sources* **2011**, *196*, 1386-1391.
- (59) Fergus, J. W. "Ceramic and polymeric solid electrolytes for lithium-ion batteries" *Journal of Power Sources* **2010**, *195*, 4554-4569.
- (60) Evans, J.; Vincent, C. A.; Bruce, P. G. "Electrochemical Measurement of Transference Numbers in Polymer Electrolytes" *Polymer* **1987**, *28*, 2324-2328.
- (61) Doyle, M.; Fuller, T. F.; Newman, J. "The importance of the lithium ion transference number in lithium/polymer cells" *Electrochimica Acta* **1994**, *39*, 2073-2081.
- (62) Ma, Y.; Doyle, M.; Fuller, T. F.; Doeff, M. M.; Jonghe, L. C. D.; Newman, J. "The Measurement of a Complete Set of Transport Properties for a Concentrated Solid Polymer Electrolyte Solution" *Journal of the Electrochemical Society* **1995**, *142*, 1859-1868.
- (63) Uno, T.; Kawaguchi, S.; Kubo, M.; Itoh, T. "Ionic conductivity and thermal property of solid hybrid polymer electrolyte composed of oligo(ethylene oxide) unit and butyrolactone unit" *Journal of Power Sources* **2008**, *178*, 716-722.
- (64) Pitawala, H.; Dissanayake, M.; Seneviratne, V.; Mellander, B. E.; Albinson, I. "Effect of plasticizers (EC or PC) on the ionic conductivity and thermal properties of the (PEO)₉LiTf: Al₂O₃ nanocomposite polymer electrolyte system" *Journal of Solid State Electrochemistry* **2008**, *12*, 783-789.
- (65) Chen-Yang, Y. W.; Wang, Y. L.; Chen, Y. T.; Li, Y. K.; Chen, H. C.; Chiu, H. Y. "Influence of silica aerogel on the properties of polyethylene oxide-based nanocomposite polymer electrolytes for lithium battery" *Journal of Power Sources* **2008**, *182*, 340-348.

- (66) Shin, J. H.; Henderson, W. A.; Passerini, S. "An elegant fix for polymer electrolytes" *Electrochemical and Solid State Letters* **2005**, *8*, A125-A127.
- (67) Fang, S.; Yang, L.; Wei, C.; Peng, C.; Tachibana, K.; Kamijima, K. "Low-viscosity and low-melting point asymmetric trialkylsulfonium based ionic liquids as potential electrolytes" *Electrochemistry Communications* **2007**, *9*, 2696-2702.
- (68) Meyer, W. H. "Polymer Electrolytes for Lithium-Ion Batteries" *Advanced Materials* **1998**, *10*, 439-448.
- (69) Krause, L. J.; Lamanna, W.; Summerfield, J.; Engle, M.; Korba, G.; Loch, R.; Atanasoski, R. "Corrosion of aluminum at high voltages in non-aqueous electrolytes containing perfluoroalkylsulfonfyl imides; new lithium salts for lithium-ion cells" *Journal of Power Sources* **1997**, *68*, 320-325.
- (70) Fisher, A. S.; Khalid, M. B.; Widstrom, M.; Kofinas, P. "Solid polymer electrolytes with sulfur based ionic liquid for lithium batteries" *Journal of Power Sources* **2011**, *196*, 9767-9773.
- (71) Golding, J.; Forsyth, S.; MacFarlane, D. R.; Forsyth, M.; Deacon, G. B. "Methanesulfonate and p-toluenesulfonate salts of the N-methyl-N-alkylpyrrolidinium and quaternary ammonium cations: novel low cost ionic liquids" *Green Chemistry* **2002**, *4*, 223-229.
- (72) Vijayaraghavan, R.; MacFarlane, D. R. "Organoborate Acids as Initiators for Cationic Polymerization of Styrene in an Ionic Liquid Medium" *Macromolecules* **2007**, *40*, 6515-6520.
- (73) Fauteux, D.; Massucco, A.; McLin, M.; Van Buren, M.; Shi, J. "Lithium polymer electrolyte rechargeable battery" *Electrochimica Acta* **1995**, *40*, 2185-2190.
- (74) Molinspiration; Molinspiration Property Calculation Service; Vol. 2011.

- (75) Pont, A.-L.; Marcilla, R.; De Meaza, I.; Grande, H.; Mecerreyes, D. "Pyrrolidinium-based polymeric ionic liquids as mechanically and electrochemically stable polymer electrolytes" *Journal of Power Sources* **2009**, *188*, 558-563.
- (76) Fisher, A. S.; Khalid, M. B.; Kofinas, P. "Dry Polymer/Sulfur-Based Ionic Liquid Hybrid Electrolytes for Lithium Batteries" *ECS Transactions* **2012**, *41*, 77-83.
- (77) Fisher, A. S.; Khalid, M. B.; Widstrom, M.; Kofinas, P. "Anion Effects on Solid Polymer Electrolytes Containing Sulfur Based Ionic Liquid for Lithium Batteries" *Journal of the Electrochemical Society* **2012**, *159*, A592-A597.
- (78) Yang, L.; Furczon, M. M.; Xiao, A.; Lucht, B. L.; Zhang, Z.; Abraham, D. P. "Effect of impurities and moisture on lithium bisoxalatoborate (LiBOB) electrolyte performance in lithium-ion cells" *Journal of Power Sources* **2010**, *195*, 1698-1705.
- (79) Johansson, P.; Tegenfeldt, J.; Lindgren, J. "Modelling amorphous lithium salt-PEO polymer electrolytes: ab initio calculations of lithium ion-tetra-, penta- and hexaglyme complexes" *Polymer* **1999**, *40*, 4399-4406.
- (80) Edman, L.; Doeff, M. M.; Ferry, A.; Kerr, J.; De Jonghe, L. C. "Transport Properties of the Solid Polymer Electrolyte System P(EO)_nLiTFSI" *The Journal of Physical Chemistry B* **2000**, *104*, 3476-3480.
- (81) Gorecki, W.; Jeannin, M.; Belorizky, E.; Roux, C.; Armand, M. "Physical properties of solid polymer electrolyte PEO(LiTFSI) complexes" *Journal of Physics: Condensed Matter* **1995**, *7*, 6823.
- (82) Vincent, C. A. "Ion transport in polymer electrolytes" *Electrochimica Acta* **1995**, *40*, 2035-2040.
- (83) Yoshizawa, M.; Narita, A.; Ohno, H. "Design of Ionic Liquids for Electrochemical Applications" *Australian Journal of Chemistry* **2004**, *57*, 139-144.

(84) Byrne, N.; Howlett, P. C.; MacFarlane, D. R.; Forsyth, M. "The Zwitterion Effect in Ionic Liquids: Towards Practical Rechargeable Lithium-Metal Batteries" *Advanced Materials* **2005**, *17*, 2497-2501.

(85) Tiyaipiboonchaiya, C.; Pringle, J. M.; Sun, J.; Byrne, N.; Howlett, P. C.; MacFarlane, D. R.; Forsyth, M. "The zwitterion effect in high-conductivity polyelectrolyte materials" *Nat Mater* **2004**, *3*, 29-32.

(86) MacFarlane, D. R.; Meakin, P.; Sun, J.; Amini, N.; Forsyth, M. "Pyrrolidinium Imides: A New Family of Molten Salts and Conductive Plastic Crystal Phases" *The Journal of Physical Chemistry B* **1999**, *103*, 4164-4170.

(87) Zorba, V.; Syzdek, J.; Mao, X.; Russo, R. E.; Kostecki, R. "Ultrafast laser induced breakdown spectroscopy of electrode/electrolyte interfaces" *Applied Physics Letters* **2012**, *100*, 234101-5.

(88) Fisher, A. S.; Khalid, M. B.; Kofinas, P. "Block Copolymer Electrolyte with Sulfur Based Ionic Liquid for Lithium Batteries" *Journal of the Electrochemical Society* **2012**, *159*.